Molecular Characterization of Inositol Monophosphatase Like Enzymes in *Arabidopsis thaliana*

Aida Nourbakhsh

Dissertation submitted to the faculty of the Virginia Polytechnic Institute and State University in partial fulfillment of the requirements for the degree of

Doctor of Philosophy
In
Biochemistry

Glenda E. Gillaspy, Chair
Eric P. Beers
Michael Klemba
Pablo Sobrado

June 11, 2012
Blacksburg, VA

Keywords: inositol, inositol monophosphatase, L-histidine, L-histidinol, L-histidinol 1-phosphate, L-histidinol 1-phosphate phosphatase, *Arabidopsis thaliana*

Molecular Characterization of Inositol Monophosphatase Like Enzymes in *Arabidopsis thaliana*

Aida Nourbakhsh

ABSTRACT

myo-Inositol synthesis and catabolism are crucial in many multicellular eukaryotes for production of phosphatidylinositol and inositol phosphate signaling molecules. *myo*-inositol monophosphatase (IMP) is a major enzyme required for the synthesis of *myo*-inositol and breakdown of inositol (1,4,5)-trisphosphate ($InsP_3$), a potent second messenger involved in many biological activities. Arabidopsis contains a single canonical IMP gene, which was previously shown in our lab to encode a bifuntional enzyme with both IMP and L-galactose 1-phosphatase activity. Analysis of metabolite levels in *imp* mutants showed only slight modifications with less *myo*-inositol and ascorbate accumulation in these mutants. This result suggests the presence of other functional IMP enzymes in plants. Two other genes in Arabidopsis encode chloroplast proteins, which we have classified as IMP-like (IMPL), because of their greater homology to the prokaryotic IMPs such as the SuhB, and CysQ proteins. Prokaryotic IMP enzymes are known to dephosphorylate D-Inositol 1-P (D-Ins 1-P) and other substrates *in vitro,* however their *in vivo* substrates are not characterized. A recent study revealed the ability of IMPL2 to complement a bacterial histidinol 1-phosphate phosphatase mutant defective in histidine synthesis, which suggested an important role for IMPL2 in amino acid synthesis. The research presented here focuses on the characterization of IMPL functional roles in plant growth and development. To accomplish this I performed kinetic comparisons of the Arabidopsis recombinant IMPL1 and IMPL2 enzymes with various inositol phosphate substrates and with L-histidinol 1-phosphate, respectively. The data supports that IMPL2 gene encodes an active histidinol 1-phosphate phosphatase enzyme in contrast to the IMPL1 enzyme which has the ability to hydrolyze D-Ins 1-P substrate and may be involved in the recycling of inositol from the second messenger, $InsP_3$. Analysis of metabolite levels in *impl2* mutant plants

reveals that *impl2* mutant growth is impacted by alterations in the histidine biosynthesis pathway. Together these data solidify the catalytic role of IMPL2 in histidine synthesis in plants and highlight its importance in plant growth and development.

ACKNOWLEDGEMENTS

I would like to acknowledge my advisor Glenda Gillaspy for giving me the opportunity to work with her on this project and for mentoring me to become an independent scientist, for being there for me when I needed help, and for encouraging me during very difficult times. I also would like to acknowledge my committee members, Dr. Michael Klemba, Dr. Pablo Sobrado and Dr. Eric Beers for their help and advice in this project. I would like to acknowledge Dr. Robert White for synthesizing histidinol 1-phosphate, this project would have not been possible without his assistance. I would also like to thank Kim Harich and Keith Ray for helping with the LC-MS/MS work and Eva Collakova for helping me with GC/MS and extraction procedures.

I would like to also acknowledge Janet Donahue, our lab technician, for teaching me many techniques and helping me with trouble shooting experiments, my lab mates, Jenna Hess, Phoebe Williams, Padma Rangarajan, Mihir Mandal, Juin Yen, for creating a fun and productive work environment. I especially want to thank Phoebe and Padma for spending a lot of time editing my dissertation and Mihir for helping me with drawing the molecules.

Finally, I want to thank my family, especially my mother, Fattaneh Kosary, for spending a lot of time in Blacksburg with me and my father, Mohammadreza Nourbakhsh, for being very supportive all these years.

TABLE OF CONTENTS

TABLE OF FIGURES

TABLE OF TABLES

LIST OF ABBREVIATIONS

Ins/inositol	*myo*-inositol
Gal	galactose
InsPs	inositol phosphates
PtdIns	phosphatidylinositol
PtdInsPs	phosphatidylinositol phosphates
IPPase	inositol polyphosphate 1-phosphatases
PAP	3'-phosphoadenosine 5'-phosphate
PAPase	3'-phosphoadenosine 5'-phosphate phosphatase
FBPase	fructose-1,6-bisphosphate 1-phosphatases
His	histidine
histidinol-P	L-histidinol 1-phosphate
HPP	histidinol-phosphate phosphatase
GUS	β-glucuronidase
CaMV	cauliflower mosaic virus
MS	Murashige & Skoog (plant culture salts)
HPA	histidinol-phosphate aminotransferase
SnRK	sucrose nonfermenting-1-related kinase
PLC	phospholipase C
Ins(1,4,5)P_3	*myo*-inositol-(1,4,5)-trisphosphate
$InsP_6$	inositol hexakisphosphate
IMP	inositol monophosphatase
IMPL	inositol monophosphatase-like
BBMII	N'-[(5'-phosphoribosyl)formimino]-5-aminoimidazole-4-carboxamide) ribonucleotide

AICAR	5’-phosphoribosyl-formimino]-4-carboximide-5-imidazole
IGPS	imidazole glycerol-phosphate synthase
HDH	histidinol dehydrogenase

CHAPTER I

OBJECTIVES

myo-Inositol (inositol) is a polyol, which plays an important role in plant growth and development. Inositol on its own is an important plant growth factor and can also act as a scaffold for building inositol phosphate signaling molecules (Gillaspy, 2011). Given the importance of inositol synthesis in growth and development of plants, the genes encoding the enzymes involved in inositol synthesis have been of interest. In the past decade, multigene families encoding *myo*-inositol monophosphate synthase (MIPS) and inositol monophosphatase (IMP) enzymes have been identified in Arabidopsis and microarray data and preliminary expression studies have shown the possibility of specialized roles for individual enzyme isoforms. Arabidopsis has one canonical IMP gene (At3g02870) and two IMP-like (IMPL) genes (IMPL1, At1g31190 and IMPL2, At4g39120) that are the most closely related genes to Arabidopsis IMP (29-34% amino acid sequence identity, respectively). It is important to understand whether these genes encode biochemically distinct enzyme isoforms and if they are spatially/temporally regulated at the transcriptional level. Phylogenetic analysis was done using the three IMP gene products in Arabidopsis along with other plant, microbial and animal proteins which all contain the conserved Inositol P domain, the amino acid sequence or domain that conveys Li^+ sensitivity (Torabinejad and Gillaspy, 2006). The tree predicts that Arabidopsis IMP is most related to other plant IMPs, many of which have been characterized biochemically. In contrast, IMPL1 and IMPL2 are contained on distinct branches showing a closer relationship with the prokaryotic IMPs or SuhB proteins (Chang et al., 1991).

Considering the sequence homology of IMPL enzymes to the various functioning prokaryotic IMPs and the extensive demand of plant cells for inositol phosphate metabolites, I hypothesized that IMPL enzymes have specific roles in regulation or synthesis of inositol phosphate molecules that may be similar or different from their prokaryotic homologues. The principal goal of my research is to identify the functional role of IMPL proteins in inositol synthesis and study the impact of these enzymes on the overall homeostasis of inositol-containing metabolites.

Objective 1. Understand the isoform-specific expression patterns of the IMP gene family.
Objective 2. Identify the subcellular location of IMP and IMP Like proteins.
Objective 3. Characterize the IMP Like proteins and determine their substrate preferences.
Objective 4. Identify and characterize loss- and gain-of-function mutants in both IMP Like genes.

INTRODUCTION

I. Overview of Inositol Synthesis Pathway

myo-Inositol is synthesized by both eukaryotes and prokaryotes by what is unofficially known as the Loewus pathway (Loewus and Murthy, 2000). At a glance, the single documented biosynthetic route begins with the conversion of glucose-6-phosphate to D-*myo*-inositol 3-phosphate catalyzed by *myo*-inositol phosphate synthase (MIPS) and ends with dephosphorylation by *myo*-inositol monophosphatase (IMP) to generate free inositol (Figure 1) (Loewus and Murthy, 2000). By studying MIPS and IMP enzymes, we can gain a better understanding of the role of inositol synthesis in plant growth and survival. As seen in Figure 1, the plant cell has a diverse demand for the free inositol pool to synthesize essential molecules. In yeast and animal cells, inositol is primarily incorporated into phosphatidylinositol (PtdIns), phosphatidylinositol phosphates (PtdInsP), and inositol phosphates that function in signal transduction pathways (Odorizzi et al., 2000; Payrastre et al., 2001; Tolias and Cantley, 1999). Synthesis of other important cellular components such as glycerophosphoinositide anchors and sphingolipids utilize the inositol carbon skeleton (Dunn et al., 2004; Loertscher and Lavery, 2002; Sims et al., 2004). In addition to these molecules, plants utilize free inositol to synthesize crucial cellular compounds including those involved in hormone regulation (indole acetic acid-inositol conjugates), stress tolerance (ononitol, pinitol), and oligosaccharide synthesis (galactinol) (Loewus and Murthy, 2000). Plants also produce large amounts of phosphorus-storing inositol hexakisphosphate ($InsP_6$) which is synthesized in other organisms as well. $InsP_6$ has been shown to modulate the activities of several chromatin-remodeling complexes *in vitro* that can alter gene expression (Shen et al., 2003). In addition, it has been shown that $InsP_6$ plays a role in regulation of telomere length (Saiardi et al., 2005). $InsP_6$ kinase antagonizes the

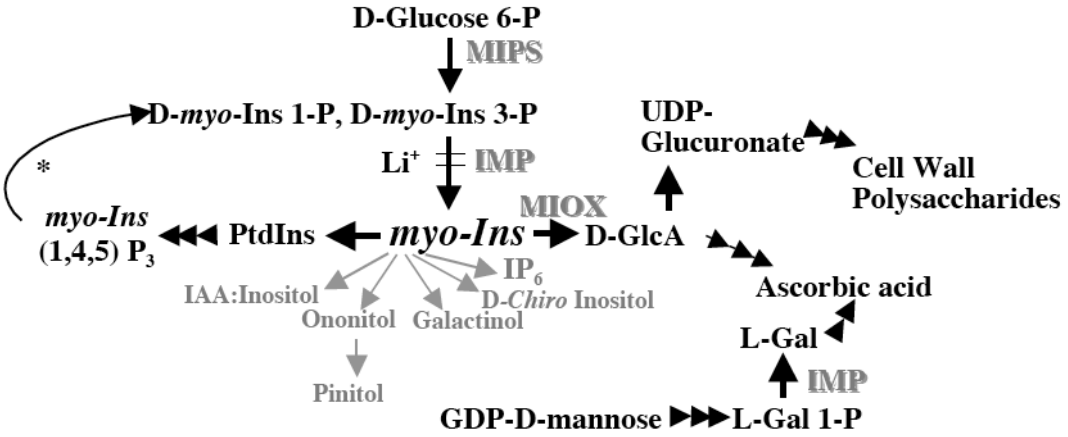

Figure 1. Inositol Synthesis and Metabolism Pathway.

De novo inositol synthesis (i.e. the Loewus pathway) utilizes the *myo*-inositol phosphate synthase (MIPS) and *myo*-inositol monophosphatase (IMP) enzymes. The substrate for IMP is D-Ins 3-P = L-Ins 1-P. Oxidation of inositol by *myo*-inositol oxygenase (MIOX) produces D-glucuronic acid (D-GlcA) that is a possible entry point into ascorbic acid synthesis. The major route to ascorbic acid in plants is via the Smirnoff-Wheeler pathway and utilizes GDP-D-mannose. Note that IMP also catalyzes the conversion of L-Gal 1-P to L-Gal in the Smirnoff-Wheeler pathway, and recycles D-Ins 1-P obtained from second messenger D-Ins (1,4,5)P_3 into inositol. Inositol is also used for the synthesis of several compounds indicated in gray. The * indicates the inositol signaling pathway. Adapted from Torabinejad and Gillaspy (2006).

actions of Tel1 and Mec1 kinases, which are known regulators of telomere length and mutant yeast with elevated or reduced levels of inositol pyrophosphates contain shorter and longer telomeres, respectively. Interestingly, $InsP_6$ was identified as a specific functional co-factor in the crystal structure of the Arabidopsis TIR1-ASK1 complex that regulates auxin signaling (Tan et al., 2007). The TIR1 receptor is from a small family of F-box proteins that regulates gene expression by promoting SCF ubiquitin-ligase degradation of auxin transcription repressors upon auxin perception. $InsP_5$ was found in association with the jasmonic acid (JA) receptor, another F box protein that controls JA perception in plants (Sheard et al., 2010; Tan et al., 2007).

II. Signaling and Metabolic Pathway of Ins(1,4,5)P_3 in Plants

The inositol signaling pathway represents an intricate ensemble of cellular switches that regulate a number of processes through $InsP_3$-mediated calcium release (Figure 2). In this pathway, extracellular signals first activate membrane-bound receptors (Berridge, 1993). Activation of receptor stimulates the cleavage of $PtdInsP_2$ substrates by phospholipase C (PLC) to produce $InsP_3$ and diacylglycerol (DAG). The second messenger, $InsP_3$ binds to intracellular receptors to increase release of calcium into the cytosol. Calcium binds to downstream targets such as calmodulin which will in turn activate other molecules, resulting in biological responses such as stimulation of gene expression, secretion, cell enlargement, and cell division (Trewavas and Gilroy, 1991). To act as a second messenger for creating a specific response within the cell, intracellular levels of $InsP_3$ must be regulated during production and degradation. $InsP_3$ levels are altered by phosphorylation and dephosphorylation, creating series of inositol polyphosphates. In plants and animal cells, several inositol polyphosphate kinases act upon $InsP_3$ to create $InsP_5$ and $InsP_6$ molecules (Seeds and York, 2007; Valluru and Van den Ende, 2011). Meanwhile, three specific phosphatases are required for the complete breakdown of $InsP_3$ molecule, recycling inositol back to the cellular free inositol pool. The first step in second messenger breakdown utilizes the inositol polyphosophate 5-phosphatase enzymes (5PTase). These enzymes remove the 5-position phosphate from the inositol ring (Astle et al., 2007; Erneux et al., 1998). The bifunctional FRY1/SAL1 enzyme then hydrolyzes $InsP_2$ to yield Ins(1)P, the substrate for IMP enzyme (Xiong et al., 2001). SAL1 was initially identified as a gene that confers salt tolerance when expressed in yeast and has both bisphosphate nucleotidase and inositol polyphosophate 1-phosphatase activities (Quintero et al., 1996). IMP enzyme is used in

the last step of second messenger catabolism; therefore it is able to regulate the amount of inositol produced through *de novo* synthesis and $InsP_3$ signal recycling (Loewus and Murthy, 2000; Maslanski et al., 1992; Moore et al., 1999).

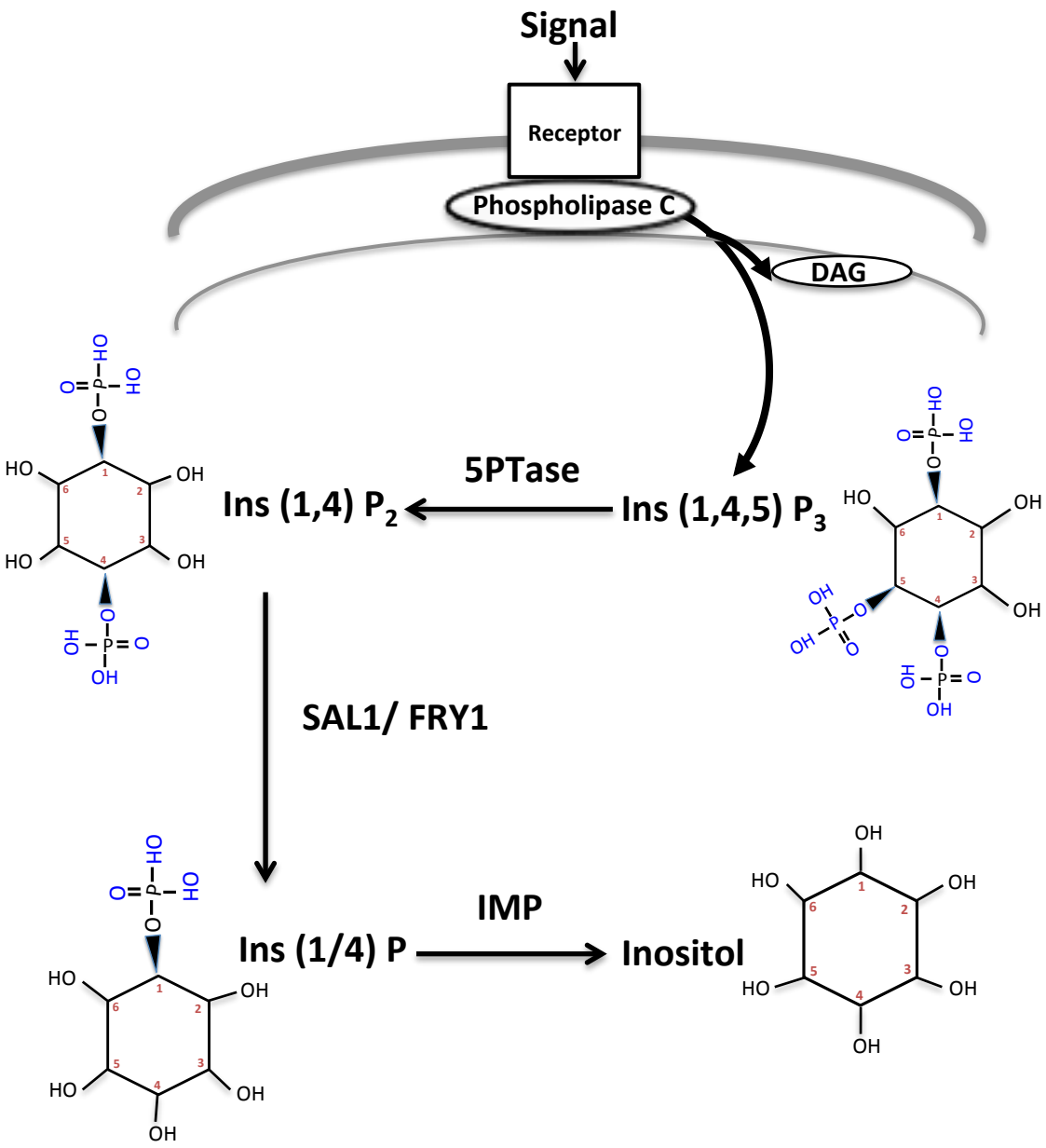

Figure 2. Degradation of Second Messenger $InsP_3$.

Signals are perceived by membrane bound receptors that upon activation stimulate phospholipase C (PLC) to convert the substrate $PtdInsP_2$ into the second messenger $InsP_3$. To terminate the signal transduction, $InsP_3$ is broken down to $InsP_2$ by 5PTase enzymes. SAL1 and IMP, to produce free inositol, subsequently hydrolyze $InsP_2$.

III. Functional Genomics of Inositol Monophosphatases

The IMP gene was first cloned from bovine brain tissue and there have been excellent studies on the IMP enzyme from several plant and animal tissues (Chen and Charalampous, 1966; Eisenberg, 1967; Hallcher and Sherman, 1980; Majerus et al., 1999). The incentive to identify IMP activity in brain tissue centers on the unique role of IMP in both *de novo* inositol synthesis and PtdIns signaling. As mentioned earlier, InsP signaling requires IMP to dephosphorylate the last product of $InsP_3$ second messenger during its catabolism. This dual requirement in both pathways may allow for coordination of inositol synthesis and $InsP_3$ recycling. The best evidence for this comes from the use of LiCl, as an inhibitory molecule, in both biochemical and physiological studies. In some animal tissues and yeast, the application of LiCl alters development and also causes a reduction in the free inositol levels (Moore et al., 1999; Shaldubina et al., 2002; Vaden et al., 2001). For example, when *Xenopus laevis* embryos are exposed to Li^+, dorsalization occurs (Kao et al., 1986) which is accompanied by a decrease in both free inositol and $InsP_3$ levels (Maslanski et al., 1992). This is thought to happen when PtdIns signaling is inhibited on the ventral side of the embryo and causing the dorsal formation to be recapitulated throughout the embryo. The dorsalization phenotype can be "rescued" by co-introduction of inositol with Li^+ (Busa and Gimlich, 1989), thus implicating that the action of IMP is targeted by Li^+.

The amino acid sequence or domain that conveys Li^+ sensitivity is known (Neuwald et al., 1991; York et al., 1995). The Inositol P domain (as defined by the Pfam protein domain database: www.pfm.wustl.edu) is a 155 amino acid residue domain found in some prokaryotic and eukaryotic proteins. The phylogenetic analysis of 73 proteins with Inositol P domain, coming from various organisms, indicates that there are four different types of proteins containing this domain: fructose-1,6-bisphosphate 1-phosphatases (FBPases), IMP enzymes, IMP-like enzymes and inositol polyphosphate 1-phosphatases (IPPases). Most of the FBPases however, were removed from the phylogenetic analysis in Figure 3 because these proteins are more distantly related compared to the other three types. Most of the IMP enzymes on branch 1a and 1b have been previously characterized. The multigene family of three *Lycopersicon esculentum* (tomato) IMP (Gillaspy et al., 1995) is found on a separate clade along with single *Dictyostelium*

discoideum (slime mold) IMP (Van Dijken et al., 1996), single *Mesembryanthemum crystallium* (iceplant) IMP (Nelson et al., 1998) and *Arabidopsis thaliana* IMP (Torabinejad et al., 2009).

The three tomato IMPs are highly conserved enzymes that act specifically on monophosphorylated substrates and were found to be sensitive to LiCl similar to animal IMP proteins (Berdy et al., 2001; Gillaspy et al., 1995); however the effects of Li^+ on development and inositol levels are more complex than in animal embryos or yeast. LiCl treatment disrupts the development of tomato seedlings and this phenotype cannot be reversed by co-introduction of inositol. It has been speculated that inositol is not able to reverse the effects of Li^+ treatment because the spatial distribution of inositol and complexity of inositol metabolic events in the seedling limit the ability for added inositol to reach areas affected by Li^+ application (Torabinejad and Gillaspy, 2006). The tomato IMP genes are differentially and developmentally regulated and protein accumulation is controlled by light. Maximal levels of IMP proteins are present in tomato tissues undergoing rapid cell division such as seedlings and developing anthers (Gillaspy et al., 1995; Suzuki et al., 2007). Considering the increased complexity of inositol utilization in plants, explicit regulation of IMP gene family is not unexpected.

The IPPases (EC 3.1.3.57) catalyze the removal of 1-phosphate from Ins(1,4)P_2 substrates which is a required step in $InsP_3$ catabolism (York et al., 1995). The human and animal IPPases are located on branch 3b and some of these proteins have been characterized to function as both IPPase and 3'-phosphoadenosine 5'-phosphate (PAP) phosphatase (PAPase) proteins (Spiegelberg et al., 1999). The last part of branch 3 (3c) contains a group of plant and fungal proteins that are predicted to have dual PAPase/IPPase functions. The yeast Hal2 protein was isolated under conditions that impart improvement of growth under salt stress (Murguia et al., 1996). It was shown that the PAPase activity of ScHal2 was required for achieving salt tolerance. The Arabidopsis Fry1 enzyme mentioned earlier is also an enzyme that exhibits PAPase activity, yet it possesses a less efficient IPPase activity (Quintero et al., 1996). It is of interest that the IMPL2 (At4g39120) protein is located on the third clade (3c) indicating a potential phylogenetic relationship to the CysQ or IPPase/PAPase homologs. Interestingly, it has been shown that Arabidopsis Fry1 acts as a suppressor of posttranscriptional silencing, a defense mechanism used in plants, by de-

repressing exoribonucleases, XRN2, XRN3 and XRN4 (Gy et al., 2007). Fry1 maintains the activity of XRN by converting the XRN inhibitor, PAP to AMP.

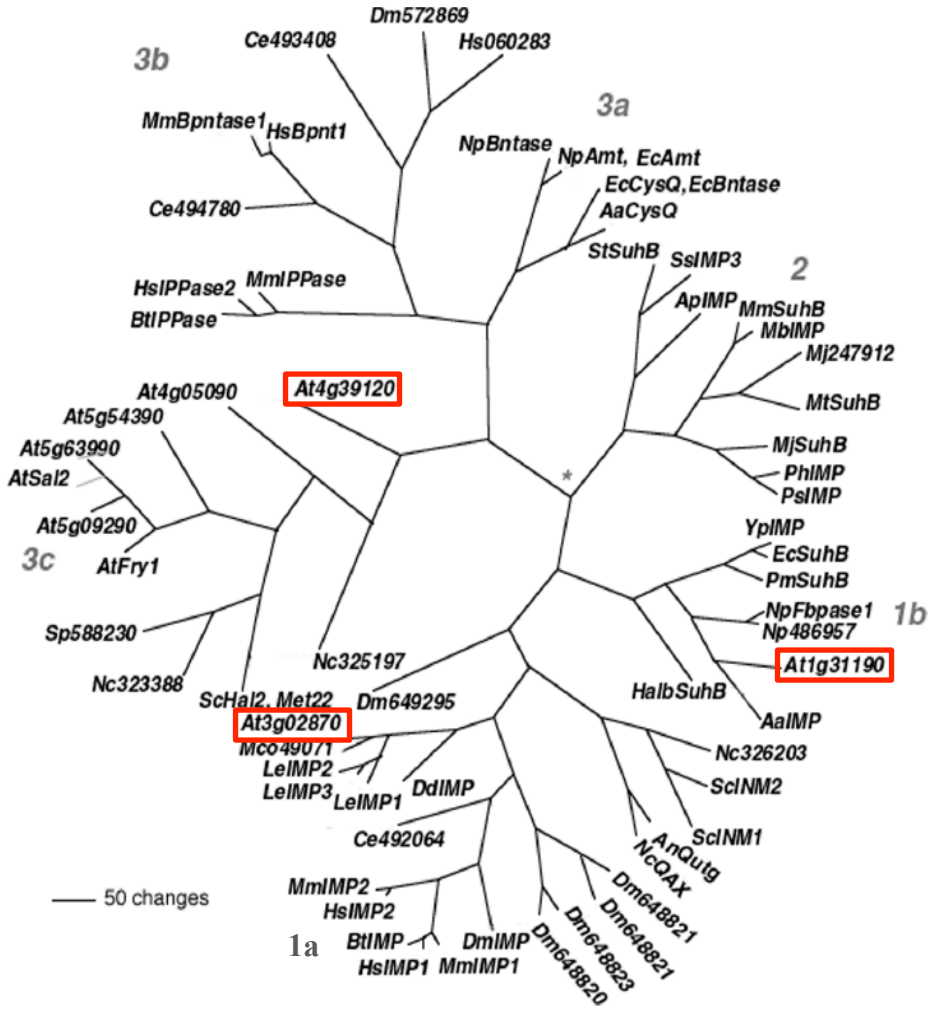

Figure 3. Phylogenetic Analysis of IMPL Proteins.

Phylogenetic analysis of proteins containing the Inositol P Domain. ClustalX and PAUP4.0b were used to create amino acid alignments and an unrooted bootstrapped phylogenetic tree. Assignment of branch categories are indicated by numbers. The asterisk denotes a possible placement for a common ancestor protein. The first two initials of each protein name represent the genus and species. Numbers that follow are from Genbank protein accession numbers or in the case of Arabidopsis, the gene number. IMP, IMPL1 and IMPL2 are indicated by red boxes (see Abbreviations). Adapted from Torabinejad and Gillaspy (2006).

Abbreviations: Ap, *Aeropyrum pernix*; Aa, *Aquifex aeolicus*; An, *Aspergillis nidulans*; Bt, *Bos taurus*; Ce, *C. elegans*; Dm, *D. melanogaster*; Dd, *Dictyostelium discoideum*; Ec, *E. coli*, Hal, *Halobacterium* sp. NRC-1; Hs, *Homo sapiens*; Le, *Lycopersicon esculentum*; Mc, *Mesembryanthemum crystallium*; Mj, *Methanococcus jannaschii*; Mb, *Methanosarcina barkeri*; Mm, *Methanosarcina mazei*; Mt; *Methanothermobacter thermautotrophicus*; Mm, *Mus musculus*; Nc, *Neurospora crassa*; Np, *Nostoc punctiforme*; Ns, *Nostoc* sp. PCC 7120; Pm, *Pasteurella multocida*; Pa, *Pyrococcus abyssi*; Pf, *Pyrococcus furiosus*; Ph, *Pyrococcus horikoshii*; Ps, *Pirellula* sp.; Rn, *Rattus norvegicus*; Sc, *S. cerevisiae*; Ss, *Sulfolobus solfataricus*; St, *Sulfolobus tokodaii*; Sp, *Schizosaccharomyces pombe*; Yp, *Yersinia pestis.* At1g31190 (IMPL1), At3g02870 (IMP), At4g39120 (IMPL2).

Prokaryotic Inositol Monophosphatases

Of special interest to my work is the presence of Arabidopsis IMPL1 gene (At1g31190) on branch 1b. No other multicellular eukaryote contains both an IMP and a SuhB or prokaryotic homolog, which suggests that plants differ in the IMP enzymatic needs as compared to animals. Several genes located adjacent to the IMPLs on the tree could be informative as to function, and here a description of what is known about the functions of SuhB and CysQ will be presented. EcSuhB was first identified in a suppressor screen of several temperature-sensitive mutants such as *rpoH* or *dnaB (Matsuhisa et al., 1995)*. However, an *E. coli* mutant with an inactivated SuhB is cold-sensitive and has defects in protein synthesis (Chang et al., 1991). Cold-resistant suppressors with an RNase III mutation restore the phenotypes of *suhB* mutants. Two known RNase III mutations, both defective in RNA cleavage activity, restored growth of *suhB* mutants. These mutations did not alter the level of SuhB expression, which suggests that RNase III and SuhB proteins bind to one another and are antagonistic (Inada and Nakamura, 1995). These results together indicate that SuhB/IMP protein in *E. coli* is involved in regulation of a number of genes at the transcriptional level. It is also possible that SuhB maintains mRNA stability by interacting and inactivating RNase III from degrading mRNA molecules (Inada and Nakamura, 1996). Although SuhB shows IMP kinetic characteristics with a substrate preference for Ins 1-P, the genetics data mentioned above strongly suggest a distinct role for SuhB/IMP proteins in prokaryotes.

In Figure 3, there is a distinct branch (3a) relating to prokaryotic enzymes that most likely have PAPase activity as deduced from studies of *E. coli* CysQ protein, which is required for cysteine biosynthesis. PAP is an intermediate in the sulfate assimilation pathway and it has been speculated that excess PAP or one of its derivatives, 3'-phosphoadenosine 5'-phosphosulfate (PAPS), is toxic to the cell (Neuwald et al., 1992). The amino acid sequence homology between CysQ and inositol monophosphatases supports a role for some prokaryotic IMPs in regulating levels of phosphorylated nucleotides such as PAP allowing it to provide its biosynthetic task without causing toxicity to the cell.

Arabidopsis Inositol Monophosphatase

A recent publication from our lab describes extensive biochemistry work on the Arabidopsis recombinant IMP protein, which shows that this enzyme is bifunctional. Interestingly, in addition to InsP hydrolysis, IMP also catalyzes the conversion of L-Gal 1-P to L-Gal in the Smirnoff-Wheeler pathway resulting in ascorbic acid synthesis (Conklin et al., 2000; Laing et al., 2004; Torabinejad et al., 2009). Due to the L-galactose 1-phosphatase activity this enzyme has been renamed as VTC4 to indicate its role in Vitamin C synthesis. Metabolite levels were measured in two independent *vtc4* mutant lines and the data indicates that a loss-of-function in IMP/VTC4 results in 22-34% reduction in inositol levels. A reduction in inositol synthesis may affect inositol phosphate signaling as shown by the physiological responses of the mutant plants to ABA, salt and cold stress. Data indicates that *vtc4* mutants are slightly hypersensitive to ABA and NaCl during seed germination as there is a reduction in seed germination over a period of 60 hours. The *vtc4* mutant seedlings also show lower germination and root growth as compared to wild-type seedlings when grown at 4°C. These data indicate that a loss-of-function in *vtc4* results in increased sensitivity to abiotic stresses which are known to be controlled by inositol signaling. These same mutants also show an increase in D,L-Gal product levels and a significant decrease in ascorbic acid levels. One possibility to explain these results is that L-Gal 1-P accumulates in *vtc4* mutants and breaks down during derivatization for gas chromatography, thus we see an increase in the product levels. Overall, this work shows that a loss-of-function in VTC4 impacts inositol and ascorbic acid levels. However, *vtc4* mutants retain 66% to 78% of wild-type inositol contents, suggesting that other redundant enzymes function during inositol synthesis. The two IMPL proteins that are the main focus of this proposal were hypothesized to be good candidates for such enzymes.

Role of IMPL2 in Plant Histidine Biosynthesis

Genes encoding seven of the eight enzymes involved in the histidine (His) biosynthetic pathway have been identified in plants (Petersen et al., 2010) and single genes in the Arabidopsis genome encode most of these enzymes (Stepansky and Leustek, 2006). The missing step in the pathway is HISN7, histidinol-phosphate phosphatase (HPP) (EC 3.1.3.15) and neither the Arabidopsis nor rice genomes contain any genes with significant sequence identity to previously identified microbial members of HPP enzymes. Recently, a novel HPP protein, showing no sequence

similarity to members of HPP superfamily was identified in *Corynebacterium glutamicum* (Mormann et al., 2006) and *Actinobacteria*, including *Streptomyces coelicolor* (Marineo et al., 2008). This new family of HPP proteins show significant sequence similarity to known IMP enzymes (Mormann et al., 2006). Bioinformatic analysis shows that IMPL2 may be a suitable candidate for HPP enzyme in Arabidopsis and that the glycine residue required for HPP activity in the *S. coelicolor* enzyme is conserved in IMPL2 but not IMPL1 where it is replaced by glutamine (Petersen et al., 2010). Petersen et al. (2010) used heterologous expression of IMPL2 to complement the His auxotrophy of the *S. coelicolor* HPP mutant hisN. Expression of IMPL2 allowed the mutant to grow on minimal media without added His while IMPL1 was not able to rescue the His auxotrophy phenotype of hisN. Also, when the glycine residue in IMPL2 was mutated to an arginine, the hisN mutant strain was no longer able to grow on minimal media. These data suggest that IMPL2 may possess HPP activity while IMPL1 does not.

IV. Histidine Biosynthesis Pathway

His is an essential amino acid and it is utilized for protein synthesis in all organisms (Ingle, 2011). The chemical properties of imidazole allow histidine (α-amino-4-imidazole propionile) function in general acid-base reactions catalyzed by enzymes (Figure 4) (Alifano et al., 1996). The biosynthetic pathway of histidine in prokaryotes and lower eukaryotes has been studied extensively for over 40 years and the research has provided a foundation and groundwork for many concepts of cell biology. For example, genetic and biochemical studies on thousands of mutations in the *his* operon of *Salmonella typhimurium*, done in the Ames and Hartman laboratories in the 1950s and 60s contributed vastly to our understanding of operon structure and function (Ames et al., 1960). Although the phenomenon of polarity was first described in the lactose operon, the existence of polarity gradient in operons was studied thoroughly in the *his* system by using a large collection of polar mutations in different *his* genes (Alifano et al., 1996; Roth et al., 1966). The mechanism of attenuation was studied in both *his* and *trp* operons, where the sequence of attenuators and the sequences of structural hairpins have been defined (Jackson and Yanofsky, 1973; Roth and Ames, 1966).

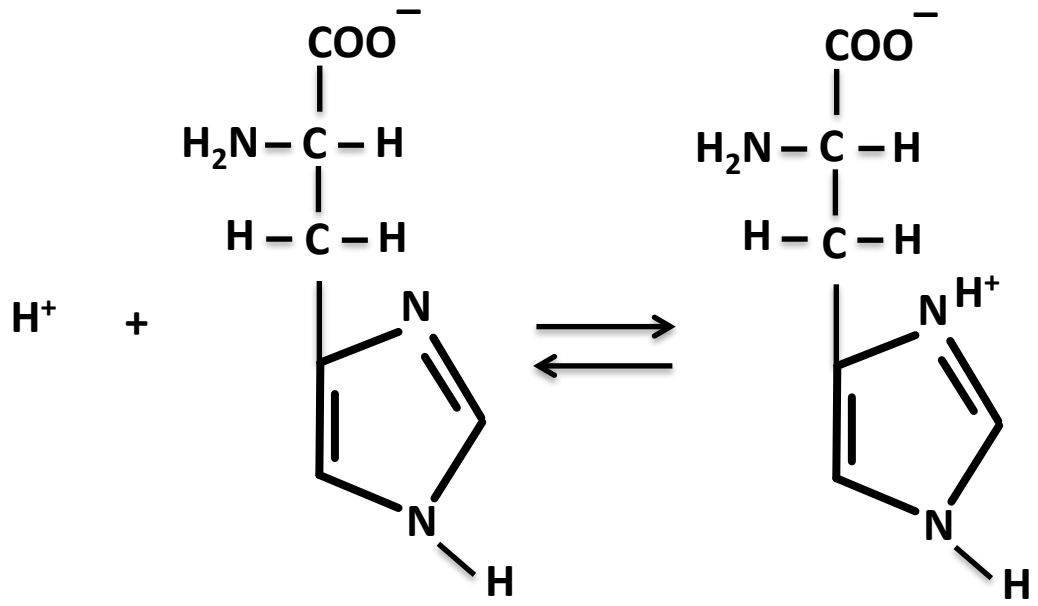

Figure 4. Structure of L-histidine.

The imidazole ring can switch between the protonated and unprotonated states under physiological conditions.

Works done in *S. typhimurium* and *E. coli* has elucidated all the necessary genes in the biosynthetic pathway of histidine (Alifano et al., 1996; Ames et al., 1960; Ames et al., 1961). After the availability of modern DNA sequencing techniques and cloning, data on *his* genes became available for other model organisms providing information for an additional 14 prokaryotes (including *Archea*), 5 fungal, and 3 plant species (Alifano et al., 1996; Ames et al., 1961). The organization of genes in operons and clusters across different species is variable throughout evolution indicating that *his* genes were separated or linked without strict constraints (Alifano et al., 1996). In *S. typhimurium* and *E. coli*, genes are tightly linked in a single operon that encodes all the enzymes required for His synthesis. The order of the genes does not match the order of the enzymes in the pathway; it is possible that this order in the *his* operon resulted from regulatory and metabolic restraints (Alifano et al., 1996).

A single operon is also present in the gram-positive bacterium *Lactococcus lactis* (gram-positive bacteria) with 4 extra open reading frames that code for unidentified proteins with unknown functions (Delorme et al., 1992). The other 8 open reading frames are homologous to the *E. coli* genes for the exception of the *hisB* gene. In *E.coli*, the *hisB* gene encodes a bifunctional enzyme that carries out the 6^{th} and 8^{th} step of the pathway (Alifano et al., 1996). The carboxyl-terminal domain has a dehydratase activity that converts imidazole glycerol-phosphate to imidazole acetol-phosphate in the 6^{th} step and the amino-terminus has a phosphatase activity that converts histidinol 1-phosphate (histidinol-P) to L-histidinol in the 8^{th} step. In *L. lactis* and also other organisms such as *Streptomyces coelicolor*, *Mycobacterium smegmatis* and *B. subtilis*, the *hisB* gene only encodes the dehydratase domain while the phosphatase domain is absent (Alifano et al., 1996; Hinshelwood and Stoker, 1992; Limauro et al., 1990; Marineo et al., 2008). This finding showed that distinct phosphatases carried out the amino-terminal catalysis of HisB enzyme.

Except for histidinol-phosphate phosphatase, genes for all the other enzymes of the His biosynthetic pathway have been identified in plants (Noutoshi et al., 2005b). In *Arabidopsis thaliana*, 10 putative genes have been shown to be related to the enzymes involved in the His biosynthesis pathway.

Several studies have established that His biosynthesis is essential for plant survival (Mo et al., 2006a; Noutoshi et al., 2005b). In physiological studies using triazole herbicides that inhibit imidazoleglycerol-phosphate dehydratase (IGPD), a complete blockage of His production caused lethality (Guyer et al., 1995a; Mori et al., 1995). His is also known to play some role in cross-pathway regulation of other amino acids. For example, inhibiting His biosynthesis in Arabidopsis by treating with triazole led to an elevated expression of genes in other amino acid biosynthetic pathways and the accumulation of a number of amino acids (Guyer et al., 1995a).

However, very little is known about the role of His in plant development and physiology. This is partly due to the difficulty in experimentally separating the metabolic and regulatory function of this essential amino acid and the lack of nonlethal His deficient mutants (Mo et al., 2006a). Our current understanding of the role of His in plants largely comes from studies of plants under severe His starvation conditions that are usually lethal and can cause a wide range of nonspecific responses. As a result, there is little understanding about the role of this amino acid in plant growth and development (Ingle, 2011).

Histidine Biosynthesis in Plants

Through comparative genetic analysis of histidine biosynthesis pathway with microbes and lower eukaryotes it has become evident that plants share the same biosynthetic pathway with other microbial organisms. There are 11 reactions that are catalyzed by 8 enzymes (Figure 5) (Stepansky and Leustek, 2006). The His genes are named as HisN followed by the number corresponding to the enzymatic step catalyzed by the gene product. The pathway starts with the condensation of ATP and phosphoribosyl pyrophosphate (PRPP) to form N'-5'-phosphoribosyl-ATP (PRATP) catalyzed by N'-5'-phosphoribosyl-ATP transferase (ATP-PRT). PRATP is converted to N'-5'-phosphoribosyl-AMP followed by a hydrolytic reaction to open up the purine ring to create the imidazole intermediate, N'-5'-phosphoribosyl-formimino-5-aminoimidazole-4-carboxamide-ribonucleotide (also known as 5'-ProFAR or BBMII). The two reactions just described are catalyzed by phosphoribosyl ATP pyrophosphohydrolase (PRA-PH) and phosphoribosyl-AMP cyclohydrolase (PRA-CH), respectively, encoded by the same gene. Next, BBMII isomerase produces an aminoketose called N'-5'- phosphoribulosyl)-formimino-5-aminoimidazole-4-carboxamide-ribonucleotide (5'-PRFAR or BBMIII). BBMIII is converted to

imidazole glycerol phosphate and 5'-amino-4-carboxamide ribonucleotide (AICAR) by the bifunctional enzyme imidazoleglycerol-phosphate synthase (IGP synthase) in the presence of glutamine. There are two catalytic reactions that occur at this step, including a transfer of an amide from glutamine followed by a cyclization reaction. IGP is dehydrated to imidazoleacetol phosphate (IAP) catalyzed by imidazoleglycerol-phosphate dehydratase (IGPD). The next step is a transamination reaction where IAP and glutamate are converted to histidinol-P and α–ketoglutarate; this reaction is catalyzed by pyridoxal-phosphate-dependent IAP aminotransferase (HPA). Histidinol-P is dephosphorylated to L-histidinol by histidinol phosphate phosphatase. In the final reaction, L-histidinol dehydrogenase (HDH) carries out two oxidation reactions in which histidinol is converted to L-histidine through the production of the unstable intermediate L-histidinal.

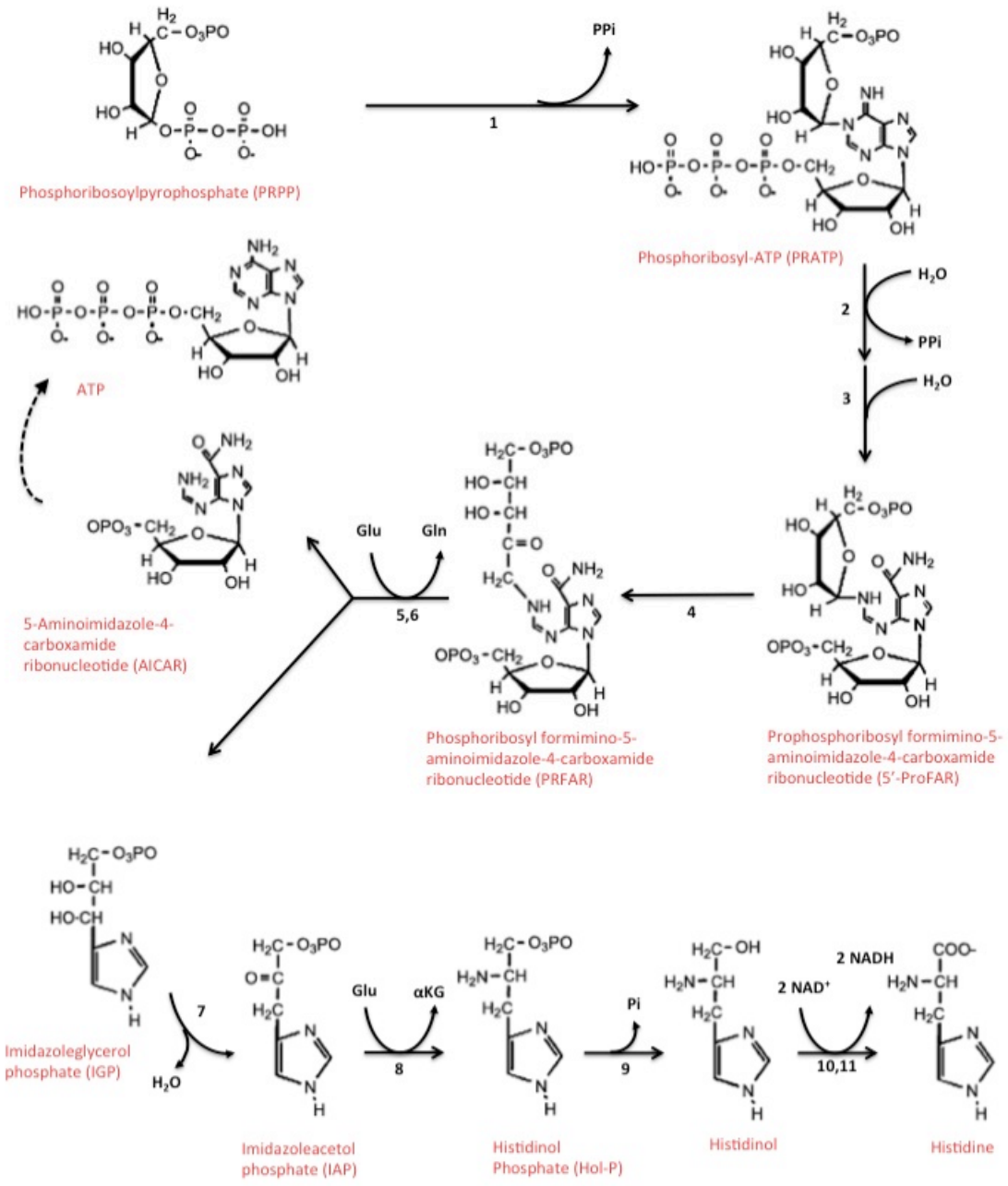

Figure 5. Histidine Biosynthesis Pathway.

The reactions are catalyzed by (1) N'-5'-phosphoribosyl-ATP transferase, (2) phosphoribosyl ATP pyrophosphohydrolase, (3) phosphoribosyl-AMP cyclohydrolase, (4) BBMII isomerase, (5,6) imidazoleglycerol-phosphate synthase, (7) imidazoleglycerol-phosphate dehydratase, (8) IAP aminotransferase, (9) histidinol phosphate phosphatase, (10,11) histidinol dehydrogenase. The dotted arrow shows the entry of AICAR into purine synthesis and ATP recycling pathway. Molecular structures adapted from Stepansky and Leustek (2005).

Regulation of the Histidine Biosynthesis Pathway

Experimental studies on microorganisms have suggested that the His pathway is integrated with other key metabolic pathways (Alifano et al., 1996). Extensive work in bacterial and lower eukaryote model organisms has been done in order to understand the regulatory mechanisms that control His synthesis at both gene expression and enzyme regulation levels (Alifano et al., 1996; Natarajan et al., 1999; Stepansky and Leustek, 2006). ATP-PRT is feedback inhibited by L-histidine in bacteria and yeast and the same mechanism applies to plants (Ohta et al., 2000; Wiater et al., 1971). Kinetic studies done on pea and Arabidopsis ATP-PRT showed that all isoenzymes were inhibited by L-histidine. The substrates PRPP and ATP, which most likely signal for the energetic state of the cell, positively stimulate the activity of bacterial ATP-PRT and the K_m values for Arabidopsis enzymes indicate similar regulation (Alifano et al., 1996; Ohta et al., 2000).

There are few studies that have examined the RNA levels of plant His genes and no indication of developmental or organ-specific expression has been made (Fujimori and Ohta, 1998; Tada et al., 1994). In order to look at spatial and temporal regulation of tobacco HISN6 (codes for IAP aminotransferase), northern blot analysis was performed on several tissues of *N. tobacum* (El Malki et al., 1998). The results suggest that HisN6 is expressed throughout the plant at all stages of development.

The steady state levels of free His most likely correlate with the level of HISN1 gene expression, which codes for the first enzyme in the pathway (Ingle et al., 2005). The overexpression of the *A. lesbiacum* HISN1B gene in Arabidopsis plants showed an increase in the pool of free His up to 15-fold, providing evidence for correlation between HISN1 expression and free His levels (Ingle et al., 2005).

Inhibition of the His biosynthesis pathway leads to alterations in expression of genes required for His synthesis and also genes involved in interconnected metabolic pathway such as *de novo* purine synthesis and some unrelated amino acid synthesis pathways (Guyer et al., 1995a). Inhibition of IGPD in Arabidopsis treated with herbicide IRL 1803 resulted in increase of expression of several genes in the lysine, tyrosine and phenylalanine biosynthetic pathways. In

addition, the free pool of some amino acids such as alanine, aspartate, glutamate, phenylalanine, proline, threonine, tryptophan, tyrosine and valine were increased about 2-fold in response to herbicide treatment (Guyer et al., 1995a). In contrast to histidine starvation, overexpression of HISN1 gene created little or no change in the concentrations of other amino acids (Ingle et al., 2005). These results indicate that there is a correlation between histidine starvation and gene expression in other amino acid synthesis pathways, however the mechanism for this regulation in plants is currently unknown (Stepansky and Leustek, 2006).

In *S. cerevisiae*, a general control (GCN) response governs the amino acid biosynthesis pathways through a B-ZIP transcription factor known as GCN4 (Natarajan et al., 2001). Promoter analysis of HISN1, HISN2, HISN3, HISN4, HISN5, and HISN6A genes in Arabidopsis using the PlantCARE database showed that all these genes contain a putative GCN4 responsive elements in their 5' untranslated regions (Lescot et al., 2002). The presence of a GCN4 promoter element in all the genes involved in His biosynthesis in Arabidopsis indicates a possible regulatory mechanism resembling the general control response in yeast (Stepansky and Leustek, 2006).

Role of Histidine in Plant Growth and Development

Several studies on null *his* mutant plants demonstrated that histidine is required for embryo development. A T-DNA insertion in *At*HISN3, HISN6 and HISN7, that code for BBMII isomerase, IAP aminotransferase and histdinol-P phosphatase respectively, results in embryo lethality and the phenotype can be rescued with addition of His (Mo et al., 2006a; Noutoshi et al., 2005b; Petersen et al., 2010). The heterozygous parent plants show no phenotype and produce viable seeds, and contain wild-type levels of His. In contrast to other amino acids which are known to be transported to the embryo, His may not be provided to the embryo by the parent plants (Stepansky and Leustek, 2006).

Noutoshi et al. (2005) isolated a nonlethal Arabidopsis *albino and pale green 10 (apg10)* mutant plant that exhibited defects in shoot tissues. A mutation from valine to leucine in the active site of BBMII isomerase produced partial elimination of histidine in these plants that exhibited pale green cotyledons and leaves at early stages of development. Measurement of free amino acids in *apg10* mutant plants grown for one week showed a 17% reduction in His, which recovered back

to wild-type levels after growth for two weeks. The recovery of His levels reversed the shoot phenotypes in later stages of development. The *apg10* mutation is in the single copy His4 gene that codes for BBMII isomerase that catalyzes the fourth step in the pathway. Complete loss-of-function *his4* mutants are embryo lethal suggesting that His4 is vital for Arabidopsis development.

In 2005, a novel histidine mutant line (*hpa1*) was characterized in Arabidopsis that carried a base substitution in one of the two HPA genes (Mo et al., 2006a). These plants have a 30% reduction in free His content (but not the total His content) and displayed a specific developmental defect in root meristem maintenance resulting in a very short root system. Interestingly, the *hpa1* mutants did not have any of the previously defined phenotypes of His starvation such as the shoot defects of *apg10* plants and the increase in biosynthesis of other amino acids. However, the levels of several amino acids such as Asp, Lys, Arg, and Glu were reduced in these plants. The authors also showed that the histidine supply is necessary for early stages of development as evidenced by the finding that when mutant plants grown on histidine for 15 days were transferred to histidine-free media, the defective root meristem was rescued. It is also important to note that a complete loss of function in HPA1 caused embryo lethality. A nonfunctional HPP protein that is coded by the IMPL2 gene also leads to embryo lethality suggesting that there is no genetic redundancy in the production of histidinol in Arabidopsis (Petersen et al., 2010).

Structural Analysis of the IMPL2 Enzyme

It has been reported that a conserved Gly residue is required for HPP function in *S. coelicolor (Marineo et al., 2008)*. As mentioned previously the replacement of Gly by Arg in IMPL2 caused a dysfunctional protein that no longer rescued a *S. coelicolor* HPP mutant strain (Petersen et al., 2010). The authors utilized homology modeling to demonstrate the importance of this residue in maintaining the structure of the active site. For this analysis, two structures from *E. coli* and *Bos Taurus* IMP proteins were used as models. IMPL2 has sequence identities of 24.8% and 20.4% to *E.coli* and *Bos Taurus* IMPs, respectively. Superimposition of IMPL2 and *Bos Taurus* IMP (A-chain) in the homology model shows that the location of most of the structural elements is conserved in the IMP protein family. The model demonstrates that the protein has a αβαβα structure with three Mg^{2+} ions in the active site held in position by the carboxylate groups

of Glu and Asp located on the loops and the central helices. Changing Gly-195 which is located on the third β–strand would cause a separation between key active site residues, Asp and Glu, that are located on the adjacent α sheets, disrupting the active site.

Evolutionary Categorization of Histidinol Phosphate Phosphatase Enzymes

The HPP proteins in microorganism are characterized into three superfamilies- the DDDD (contain four invariant Asp residues), PHP (polymerase and histidinol phosphatase) and IMPs (Lee et al., 2008a; Petersen et al., 2010). The DDDD family contains the bifunctional enzymes coded by HisB, mentioned previously. The N-terminal domain contains the HPP activity while the C-terminal is responsible for the IGPD activity (Fani et al., 2007). The PHP family embodies the monofunctional HPPs that were identified in some gram-positive bacteria and yeast (le Coq et al., 1999; Millay and Houston, 1973). The HPP orthologues that are part of the IMP superfamily have been identified in the Actinobacteria, *Corynebacterium glutamicum* and *Streptomyces coelicolor* (Marineo et al., 2008; Mormann et al., 2006). Neither Arabidopsis nor rice genomes contain sequences that have sequence identities that belong to the first two subcategories (Alifano et al., 1996). All the recent data suggests that at least in Arabidopsis, IMPL2 is the sole HPP enzyme with no genetic redundancy present in the genome.

To understand the evolutionarily divergent of the IMPL2 clade from IMP and IMPL1 in plants and green alga, Petersen et al. (2010) constructed a phylogenetic tree that contained alignment of IMP cDNA sequences from several monocot and dicot plants as well as the green alga *Chlamydomonas reinhardtii*. The analysis suggests that two gene duplication events occurred, first giving rise to the IMPL2 clade and the second to the IMPL1 and IMP clades. These gene duplications must have happened prior to the divergence of plants and green algae from the last common ancestor, which has been dated at 1,000 million years ago (Heckman et al., 2001; Petersen et al., 2010).

By comparing the exon-intron structure of the IMP, IMPL1 and IMPL2 genes, it is evident that IMPL1 and IMPL2 have similar gene structures and both contain a signal transit peptide in their first exon (Figure 6). In respect to the evolutionary changes in the active site of the IMP and IMPL2 enzymes, the structure of histidinol 1-P and inositol 1-P are shown in Figure 7. The

IMPL2 active site is able to accommodate a phosphorylated substrate with an imidazole ring that differs in structure from inositol 1-P.

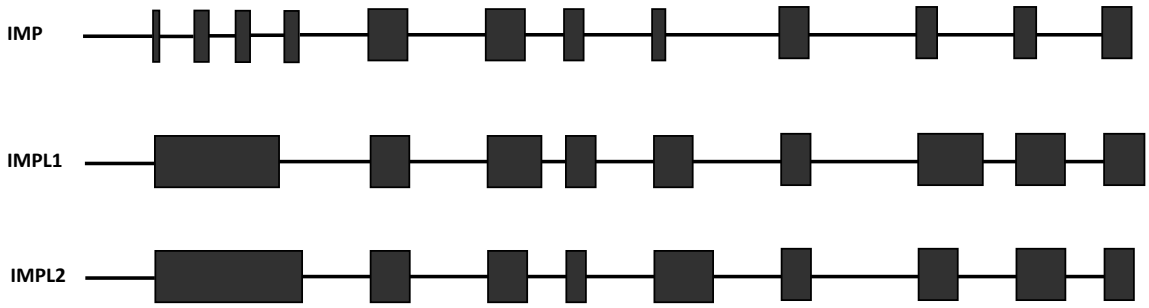

Figure 6. Schematic Gene Structure of IMP, IMPL1 and IMPL2.

The length and number of exons in the IMP gene are different in relation to IMPL1 and IMPL2. The putative signal peptide for chloroplast localization is located in exon one for both IMPL1 and IMPL2. The dark gray boxes indicate exons while the lines represent 5'-UTR and introns.

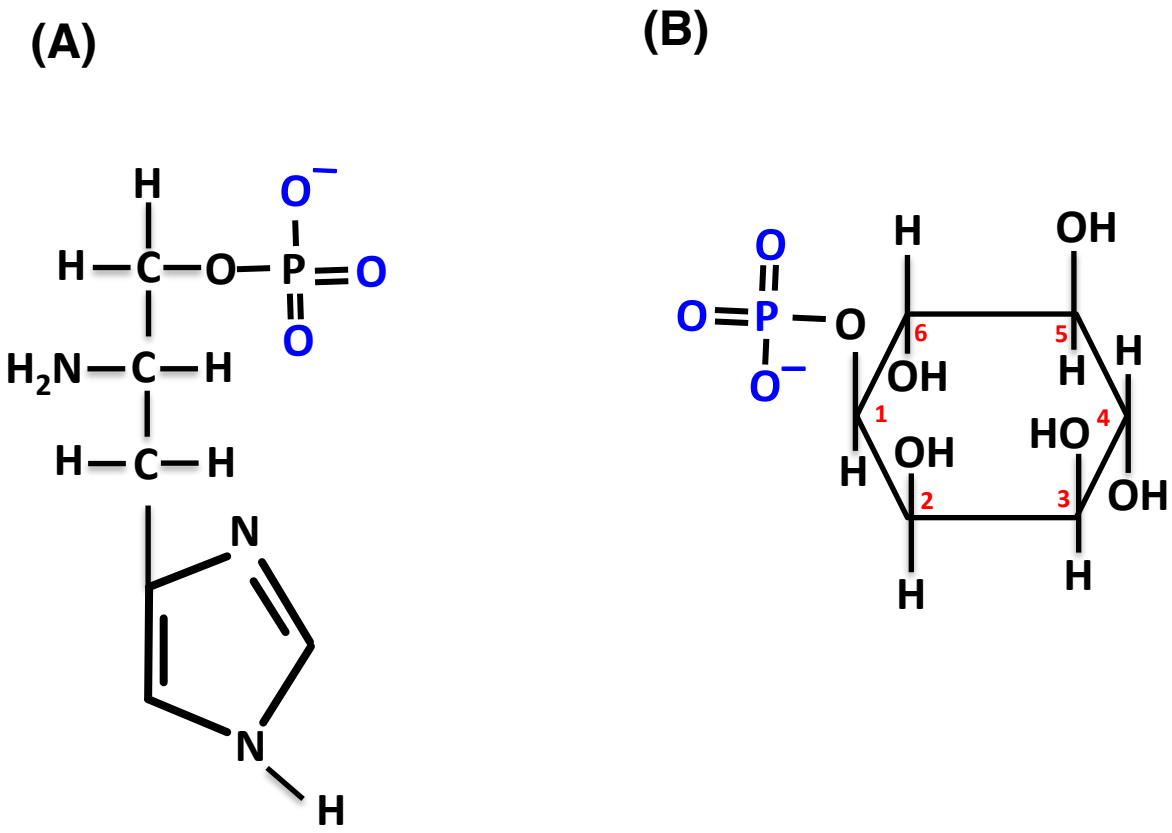

Figure 7. Structural Comparison Between L-histidinol 1-phosphate and D-inositol 1-phosphate.

IMPL2 has substrate specificity for L-histidinol 1-phosphate (A) while IMP and IMPL1 are able to accommodate D-inositol 1-phosphate (B) in their active site.

CHAPTER II

ABSTRACT

myo-inositol synthesis and catabolism are crucial in many multicellular eukaryotes for production of phosphatidylinositol and inositol phosphate signaling molecules. *myo*-inositol monophosphatase (IMP) is a major enzyme required for the synthesis of *myo*-inositol and breakdown of inositol (1,4,5)-triphosphate ($InsP_3$), a potent second messenger involved in many biological activities. Arabidopsis contains a single canonical IMP gene, which was previously shown in our lab to encode a bifunctional enzyme with both IMP and L-galactose 1-phosphatase (L-Gal 1-P) activity. Analysis of metabolite levels in *imp* mutants showed only slight modifications with less *myo*-inositol and ascorbate accumulation in these mutants. This result suggests the presence of other functional IMP enzymes in plants. Two other genes in Arabidopsis encode chloroplast proteins, which we have classified as IMP-like (IMPL), because of their greater homology to the prokaryotic IMPs such as the SuhB and CysQ proteins. Prokaryotic IMPL enzymes are known to dephosphorylate D-Inositol 1-P (D-Ins 1-P) and other substrates *in vitro,* however, their *in vivo* substrates are not characterized. A recent study revealed the ability of IMPL2 to complement a bacterial histidinol 1-phosphate phosphatase mutant defective in histidine synthesis, which suggested an important role for IMPL2 in amino acid synthesis. I describe here the kinetic comparison of the Arabidopsis recombinant IMPL1 and IMPL2 enzymes with various inositol phosphate substrates and with L-histidinol 1-phosphate, respectively. The data shows that the IMPL2 gene encodes an active L-histidinol 1-phosphate phosphatase enzyme in contrast to the IMPL1 enzyme which has the ability to hydrolyze D-Ins 1-P substrate and may be involved in the recycling of inositol from the second messenger $InsP_3$. To delineate the physiological impact of IMPL2, we isolated T-DNA knockout lines of IMPL2 that were severely compromised in growth. These *impl2* mutants can be rescued with exogenous histidine or by complementation with an IMPL2 transgene. Analyses of metabolite levels in *impl2* mutants and complemented plants reveals *impl2* mutant growth is impacted by alterations in the histidine biosynthesis pathway. Together these data solidify the catalytic role of IMPL2 in histidine synthesis in plants.

INTRODUCTION

Histidine (His) is an essential amino acid and it is utilized for protein synthesis in all organisms. Several studies have established that His biosynthesis is essential for plant survival. In physiological studies using triazole herbicides that inhibit imidazoleglycerol-phosphate dehydratase (IGPD), a complete blockage of His production causes lethality (Guyer et al., 1995b; Mori et al., 1995). His is also known to play a role in cross-pathway regulation of other amino acids (Guyer et al., 1995b). For example, inhibiting His biosynthesis in Arabidopsis by treating with triazole led to an elevated expression of genes in other amino acid biosynthetic pathways suggesting a role for His in signaling metabolic status (Guyer et al., 1995b).

However, very little is known about the role of His in plant development and physiology. This is partly due to the difficulty in experimentally separating the metabolic and regulatory functions of this essential amino acid and the embryo lethality that results from loss-of-function mutants of the majority of the genes in the pathway (Mo et al., 2006b). Our current understanding of the role of His in plants largely comes from studies of plants under severe His starvation conditions created by herbicides (Mori et al., 1995) and the *hpa1* and *apg10* mutant plants that have partial histidinol-phosphate aminotransferase and N'-5'-phosphoribosyl-formimino-5-aminoimidazole-4-carboxamide-ribonucleotide (BBMII) isomerase activity, respectively (Mo et al., 2006b; Noutoshi et al., 2005a). As a result, there is little understanding about the role of this amino acid in plant growth and development.

In *Arabidopsis thaliana*, 10 putative genes have been shown to be related to the enzymes involved in the His biosynthetic pathway (Noutoshi et al., 2005a). Until recently, this list included all required enzymes for His biosynthesis except for the histidinol 1-phosphate phosphatase enzyme (Noutoshi et al., 2005a), which catalyzes the next to last step in the pathway. Clues to the nature of the histidinol 1-phosphate phosphatase gene became available with the characterization of a novel histidinol 1-phosphate phosphatase protein family in prokaryotes (Marineo et al., 2008; Mormann et al., 2006), which displays significant amino acid sequence homology to known IMPs that catalyze the hydrolysis of D-*myo*-inositol 1(or 3)-phosphate (D-Ins 1-P, D-Ins 3-P) (Leech et al., 1993). Recently, it was shown that heterologous

expression of Arabidopsis inositol monophosphatase-like 2 gene (IMPL2, At4g39120) but not IMPL1 (At1g31190) gene was sufficient to rescue the His auxotrophy of a *Streptomyces coelicolor* hisN mutant, which is defective in histidinol 1-phosphate phosphatase activity (Petersen et al., 2010). This genetic test thus revealed the identity of the plant histidinol 1-phosphate phosphatase and therefore, all the genes functioning in the Arabidopsis His synthesis pathway are now known (Figure 8).

Arabidopsis contains one canonical IMP enzyme, encoded by the IMP/VTC4 gene (At3g02870). The VTC4 gene encodes an active, bifunctional IMP and L-Gal 1-phosphatase enzyme, however the function of IMPL enzymes, which are closer in amino acid sequence identity to the prokaryote IMPs, has not been elucidated (Torabinejad et al., 2009; Torabinejad and Gillaspy, 2006), although both IMPL1 and IMPL2 have been localized to the chloroplast (Petersen et al., 2010; Sun et al., 2009). Analyses of metabolite levels in *imp* mutants revealed a 30% reduction in *myo*-inositol content indicating the likely presence of other plant IMP enzymes (Torabinejad et al., 2009). Since both Arabidopsis IMPL1 and IMPL2 genes are possible candidates for a redundant IMP function, I sought to purify and characterize these enzymes. Further, given the bifunctionality of the IMP enzyme, I wanted to examine the impact of a loss-of-function in these genes on both the inositol and His synthetic pathways.

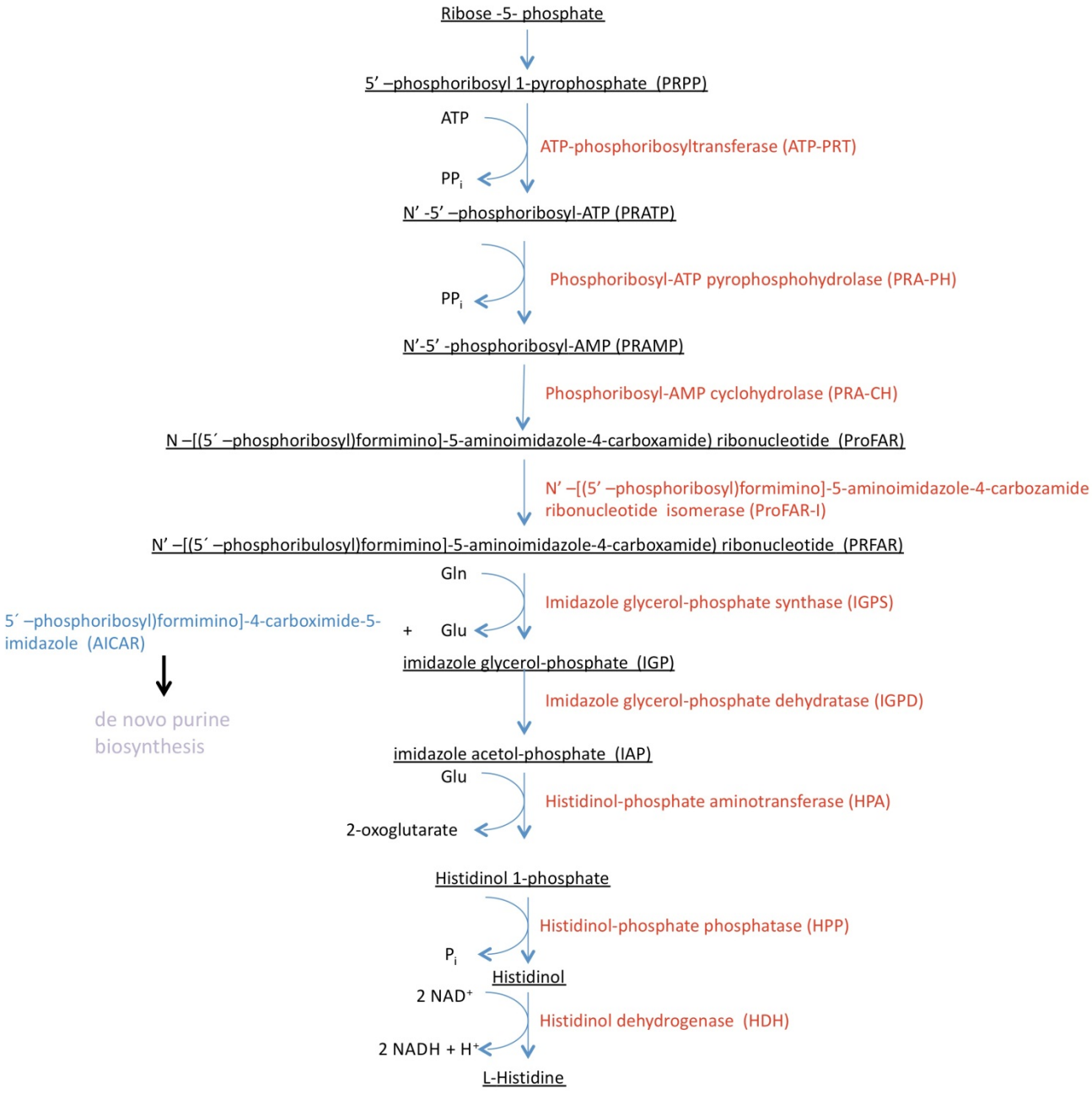

Figure 8. The Histidine Biosynthesis Pathway in Arabidopsis.

The first enzyme in the pathway ATP-PRT is subjected to allosteric inhibition by L-histidine. Abbreviations used for intermediates and enzyme names are indicated in parentheses, and the corresponding Arabidopsis gene names and AGI codes are: At1g58080 (HISN1A), At1g09795 (HISN1B), At1g31860 (HISN2), At2g36230 (HISN3), At4g26900 (HISN4), At3g22425 (HISN5A), At4g14910 (HISN5B), At5g10330 (HISN6A), At1g71920 (HISN6B), At4g39120 (HISN7), At5g63890 (HISN8).

Here, I demonstrate kinetic analysis of recombinant AtIMPL1 and AtIMPL2 proteins and show that AtIMPL2 is able to hydrolyze L-histidinol 1-P *in vitro*. I also show that AtIMPL1 does not hydrolyze L-histidinol 1-P *in vitro* and speculate on possible substrates for this enzyme. Key to my characterization of AtIMPL2 function is an *impl2* mutant. This mutant carries a T-DNA insertion in IMPL2 gene, and my analysis of this "knock-out" mutant verifies that IMPL2 encodes an enzyme which catalyzes the dephosphorylation of L-histidinol 1-P to L-histidinol. The *impl2* mutant exhibits slight elevation in levels of free His content in comparison to wild-type. Interestingly, the mutant shows all the described symptoms of previously reported His mutants such as the pale-green leaf phenotype of *agp10* (Noutoshi et al., 2005a) and the root meristem defect of *hpa1* mutants (Mo et al., 2006b). I demonstrate that the growth and developmental defect of the mutant is directly linked to alteration in His biosynthesis which is most likely caused by the accumulation of the enzyme's substrate, L-histidinol 1-P.

RESULTS

Expression of Recombinant Inositol Monophosphatase Like (IMPL1 and IMPL2) Proteins

To examine the functional roles of IMPL1 and IMPL2 enzymes, I designed a strategy to express and purify recombinant IMPL1 and IMPL2 proteins. Both genes encode putative chloroplast transit peptides, as predicted by the Wolf P-Sort program (http://wolfpsort.org/), which function in the transport of these proteins into the chloroplast. The transit peptides were determined by alignment of IMPL amino acid sequences with those of non-chloroplastic IMPs. To construct plasmids capable of expressing recombinant IMPL1 and IMPL2 enzymes, the open reading frame minus the putative chloroplastic transit peptide of the IMPL1 gene (At1g31190) and the IMPL2 gene (At4g39120) were cloned in a plasmid containing the *tac* promoter, and sequences encoding a thrombin cleavage site, and a C-terminal glutathione s-transferase. Overexpression of soluble IMPL protein in *Escherichia coli* strain pREP4/BL21(DE3)* transformed with the IMPL plasmids was facilitated by the coexpression of GroES and GroEL. After cell lysis, the GST region of the proteins was bound to a glutathione-sepharose column in the presence of phosphate, *myo*-inositol, and Trition X-100, and was eluted with 50 mM Tris-Cl, pH 8.0 buffer containing 10 mM glutathione. The eluted fractions of IMPLs were estimated to be greater than 95% pure as observed by 12% SDS-PAGE, yielding a total of approximately 10 µg of protein

(Figure 9). Based on the migration on SDS-PAGE, the molecular mass of the fusion proteins is estimated to be 65 kD for IMPL1 and 60 kD for IMPL2. Both IMPL1 and IMPL2 migrated slightly slower than expected given their predicted molecular masses of 55.5 and 55.4 kD, respectively. The eluted fractions were combined and dialyzed in the presence of buffer with 1 mM dithiothreitol to maintain activity for use in biochemical assays.

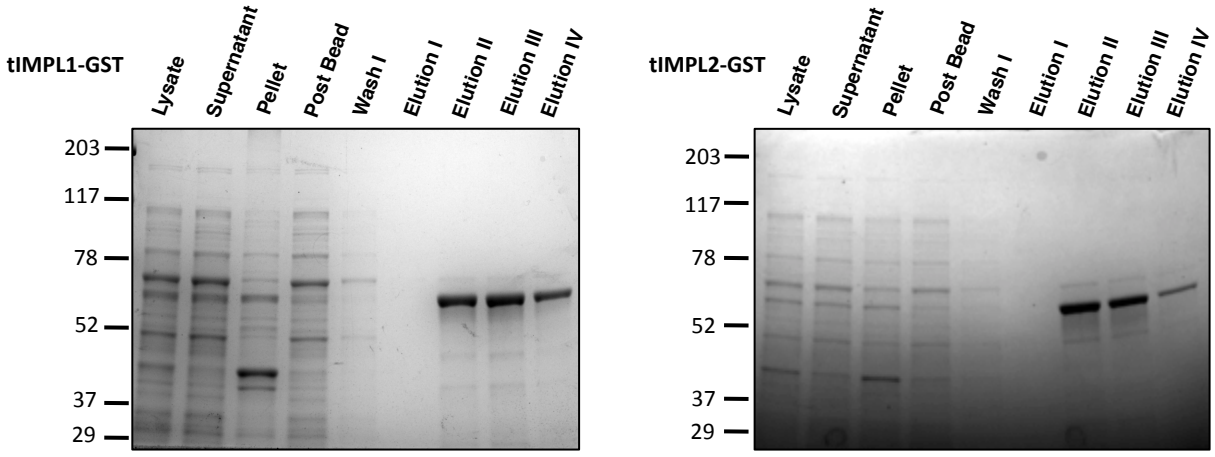

Figure 9. Purification of IMPL1-GST and IMPL2-GST Recombinant Proteins.

After cell lysis and centrifugation, the GST fusions, present in supernatant, were bound to a glutathione-sepharose column and after three washes the proteins were eluted with 50 mM Tris-Cl, pH 8.0 buffer containing 10 mM glutathione in four different fractions. 10% SDS-PAGE was used and stained with Coomassie Blue.

It has been shown that Mg^{2+} is necessary for maximal activity of other IMP enzymes (Gumber et al., 1984; Islas-Flores and Villanueva, 2007; Laing et al., 2004) and AtIMP functions optimally at a $MgCl_2$ concentration of 4 mM and a pH of 7.5 (Torabinejad et al., 2009). The concentration of Mg^{2+} in the chloroplast has been measured to be approximately 0.5 mM and to increase to approximately 2 mM in the stroma upon illumination (Ishijima et al., 2003). There is also alkalization that is induced in the stroma by light, changing by about one pH unit from the neutral state that is normally present in the darkness (Heldt et al., 1973). Therefore for the reaction conditions for testing IMPL proteins a pH of 7.5 and 2 mM $MgCl_2$ were chosen to nearly mimic the chloroplast environmental conditions during daylight.

Arabidopsis IMP has been reported as a bifunctional enzyme hydrolyzing L-Gal 1-P and D-Ins 3-P (Conklin et al., 2000; Laing et al., 2004; Torabinejad et al., 2009). In order to examine the substrate preferences of IMPL enzymes and their possible role in inositol synthesis in plants, we analyzed their abilities to utilize several related substrates (Table 1). For IMPL1, D-Ins 1-P and D-Gal 1-P were determined as potential substrates (Table 1). D-Ins 1-P can be derived from D-Ins(1,4,5)P_3 second messenger breakdown, in contrast to D-Ins 3-P, which is an intermediate in *de novo* inositol synthesis. Interestingly, D-Gal 1-P is hydrolyzed by IMPL1 (Table 1), which is similar to the specificity of the human IMP which hydrolyzes D-Gal 1-P as effectively as D-Ins 1-P (Parthasarathy et al., 1997). β-Glycerophosphate is also a good substrate (39.7% of the D-Ins 1-P rate of reaction). Under these reaction conditions, D-Ins 3-P, D-Ins 2-P, L-Gal 1-P, Adenosine 2'-monophosphate and D-Glc 1-P serve less well as substrates. In addition, Glycerol 3-phosphate, D-Glc 6-P, D-Mannitol 1-P, D-Sorbitol 1-P, D-Fruc 1-P and Fru 1,6-bisP, NADP, NADPH and PAP are not hydrolyzed by IMPL1. IMPL1 is also not able to hydrolyze the poly-phosphorylated inositol compounds (Table 1). Together, these data suggest that IMPL1 has distinct substrate specificity as compared to either IMPL2 or IMP, and might be involved in hydrolysis of D-Ins 1-P and/or D-Gal 1-P.

Table 1. Substrates Tested with IMPL1.

	IMPL1	IMP
Substrate	**Rate %**	**Rate %**
D-*myo*-Inositol 1-monophosphate	100	100
D-Galactose 1-phosphate	105.4	16.6
β-Glycerophosphate (glycerol 2-P)	39.7	52
D-*myo*-Inositol 3-monophosphate	18.8	100
D-*myo*-Inositol 2-monophosphate	17.8	0.94
L-Galactose 1-monophosphate	7.6	166-240
Adenosine 2' –monophosphate	3.6	9.6
α-D-Glucose 1-phosphate	2.8	19.3
D-α-Glycerophosphate (glycerol 3-P)	0.24	4.9
α-D-Glucose 6-phosphate	0	0.25
D-Mannitol 1-phosphate	0	10.5
D-Sorbitol 1-phosphate	0	1.7
D-Fructose 1-phosphate	0	2.3
Fructose 1,6-bisphosphate	0	0.30
NADP	0	NA
NADPH	0	NA
PAP	0	NA
L-Histidinol 1-phosphate	0	NA
Inositol (1,4)P_2	0	NA
Inositol (4,5)P_2	0	NA
Inositol (1,4,5)P_3	0	NA

IMPL1 activity was determined at pH 9 in the presence of 3 mM $MgCl_2$ using the phosphate release assay, 400 ng of IMPL1 enzyme, and 0.4 mM of the indicated substrate (substrate was present in excess amount as compared to the estimated K_m value for D-Ins 1-P). Reaction rates were compared with the rate of activity with 0.4 mM D-Ins 1-P (units). The values for IMP enzyme were published in Torabinejad et al., 2009.

Catalytic properties of enzymes are important factors in determining substrate specificity of an enzyme. In reaction conditions of pH 7.5, 2 mM $MgCl_2$, and 452 ng of IMPL1 recombinant enzyme, the K_m for D-Ins 1-P was 180 ± 3 μM (Figure 10A) and that for D-Gal 1-P was approximated to be 450 ± 60 μM. Substrate inhibition occurred at concentrations greater than 1 mM of D-Ins 1-P. The k_{cat} value for IMPL1 with D-Ins 1-P is 0.6 ± 0.1 s^{-1} and 2.4 ± 1.3 s^{-1} with D-Gal 1-P. Further, the ratio of k_{cat} to K_m provides a perspective on the catalytic efficiency of an enzyme with a specific substrate, and I calculated the k_{cat}/K_m with D-Ins 1-P to be 3.3 ± 0.1 x 10^3 M^{-1} s^{-1} and 5.3 ± 0.5 x 10^3 M^{-1} s^{-1} with D-Gal 1-P (Table 2). The data for D-Gal 1-P is only preliminary results and must be optimized and reproduced.

For the IMPL2 enzyme, testing of different substrates validates that IMPL2 has high specificity for L-histidinol 1-P and is not able to hydrolyze either isoforms of Ins 1-P, Gal 1-P, or Fru 1,6-bisP (data not shown). We conclude that the IMPL2 gene encodes an active histidinol-P phosphatase, and is unlikely to function in inositol phosphate hydrolysis. In reaction mixtures of pH 7.5, 2 mM $MgCl_2$ and 101 ng of enzyme, the K_m for Histidinol 1-P is 180 ± 5 μM, the k_{cat} is 1.4 ± 0.2 s^{-1} and the k_{cat}/K_m is 7.9 ± 0.2 x 10^3 $M^{-1}s^{-1}$ (Figure 10B, Table 2). The K_m value is slightly higher than those reported for the few histidinol-P phosphatase enzymes of the DDDD superfamily (bifunctional) and PHP (monofunctional), which have been characterized (Lee et al., 2008b; Rangarajan et al., 2006a). However the k_{cat}/K_m values reported for these enzymes are significantly higher (Lee et al., 2008b; Rangarajan et al., 2006a). The K_m value of 90 μM and k_{cat}/K_m of 4.7 x 10^6 $M^{-1}s^{-1}$ was reported for the hyperthermophilic archaeon, *Thermococcus onnurineus*, histidinol-P phosphatase (Lee et al., 2008a). The *E. coli* histidinol-P phosphatase is reported to have a K_m value of 54 μM and k_{cat}/K_m value of 3.96 x 10^8 $M^{-1}s^{-1}$ (Rangarajan et al., 2006b). The kinetic values of recombinant IMPL2 are different than those reported for prokaryotic enzymes, perhaps due to the fact that eukaryotic enzymes may go through posttranslational modifications that will affect catalytic efficiency.

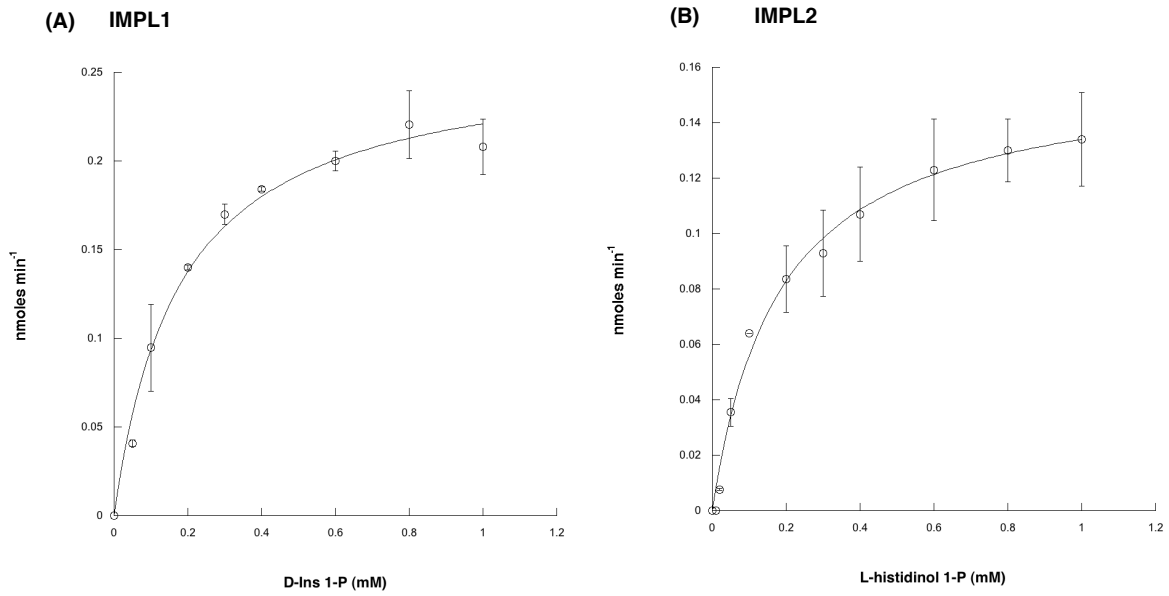

Figure 10. Kinetic Analysis of IMPL1 with D-Ins 1-P and IMPL2 with Histidinol 1-P.

Phosphatase activity was plotted versus varying concentrations of D-Ins 1-P for IMPL1 in **(A)** and Histidinol 1-P for IMPL2 in **(B)** using the standard reaction conditions described in "Materials and Methods". Data (average of 2 independent replicates) were imported into Kaleidagraph (Synergy Software) and fit to a nonlinear curve based on the Michaelis-Menten equation to calculate K_m and $V_{\max}$. The error bars represent standard deviation of the independent replicates.

Table 2. Kinetic Parameters of IMPL1 and IMPL2 Recombinant Proteins.

Enzyme (Substrate)	K_m (μM)	k_{cat} (s^{-1})	k_{cat}/K_m ($s^{-1}M^{-1}$)
IMPL2 (Histidinol 1-P)	180 ± 5	1.3 ± 0.2	7.9 ± 0.2 x 10^3
IMPL1 (D-Ins 1-P)	180 ± 3	0.6 ± 0.1	3.3 ± 0.1 x 10^3
IMPL1 (D-Gal 1-P)	450 ± 60	2.4 ± 1.3	5.3 ± 0.5 x 10^3

The initial rate for IMPL1 and IMPL2 activity was determined at 22°C (50 mM Tris-Cl, pH 7.5, 2 mM $MgCl_2$, and 10% glycerol. The kinetic parameters were obtained from the initial velocity as described in Methods. The concentration of substrates was varied from 0 to 1 mM.

Lithium and calcium ions have an inhibitory effect on other IMPs (Leech et al., 1993; Parthasarathy et al., 1997; Torabinejad et al., 2009) and it was important to determine whether the IMPL enzymes are sensitive to these cations. The LiCl inhibition of AtIMP activity with D-Ins 3-P exhibited a linear noncompetitive inhibition, with a K_i of 6.3 mM (Torabinejad et al., 2009). IMPL1 and IML2 are both inhibited by Li^+ or Ca^{2+} addition (Figure 11). The half-maximal inhibitory concentration (IC_{50}) of IMPL1 with LiCl as an inhibitor in a reaction containing 0.4 mM substrate was 8.7 mM while the IC_{50} for $CaCl_2$ was 0.03 mM. The IC_{50} of IMPL2 with LiCl was estimated to be 0.91 mM and the IC_{50} for $CaCl_2$ was 0.3 mM, thus both IC_{50} values differ almost 10-fold from those of IMPL1. From this data I conclude that the active sites of IMPL1 and IMPL2 differ in their ability to bind both Li^+ and Ca^{2+}. The physiological relevance of inhibition by calcium ions may be an artifact of the *in vitro* reaction conditions, as the concentration of calcium ions in the plant cell is expected to be high. Interestingly, these data also suggest that Li^+ contamination of soil could impact IMPL2 function and His biosynthesis in plants. Indeed, several incidents of lithium toxicity in field-grown citrus with lithium concentrations of 0.06 to 0.1 ppm in the irrigation water has been reported in the state of California (Bradford, 1963).

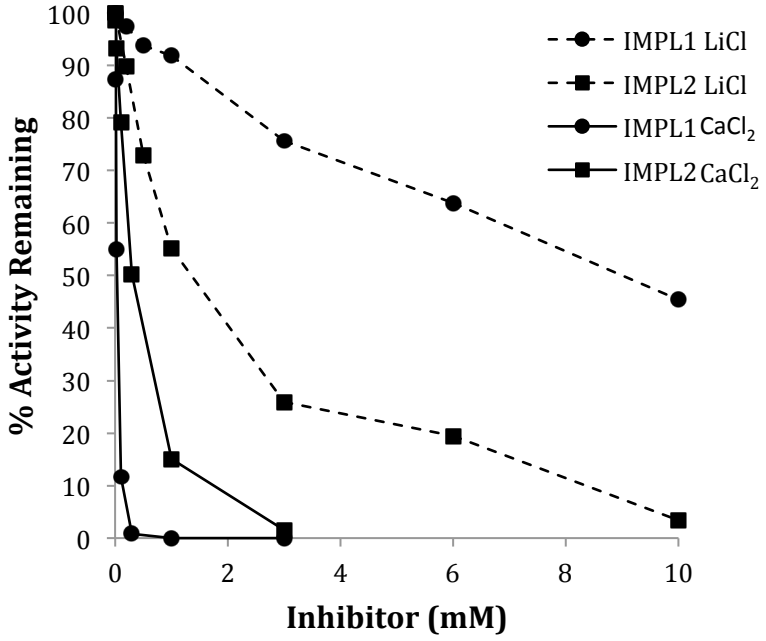

Figure 11. Inhibition of IMPL1 and IMPL2 Activity by either LiCl or $CaCl_2$.

IMPL1 activity was assayed with D-Ins 1-P (circles) and IMPL2 was assayed with histidinol 1-P (squares) in the presence of the indicated concentrations of $CaCl_2$ (solid lines) or LiCl (dashed lines).

IMP and IMPL Gene Expression is Temporally and Spatially Regulated

To determine whether the IMP and IMPL genes are differentially regulated, I performed Real-time PCR to compare relative expression of IMP, IMPL1, and IMPL2 in various tissues (Figure 12). I found that IMP is expressed in all tested tissues except seeds and levels are high in seedlings during early development and also in leaves. IMPL1 has a similar expression pattern as IMP, however it is expressed at slightly lower levels, and it is the only gene expressed in seeds. IMPL2 expression is overall lower than for IMP and IMPL1, and IMPL2 appears to be expressed constitutively in all tissues except seeds. The results are similar to those reported from microarray data provided by Genevestigator database (Zimmermann et al., 2004) (Figure 13). Overall, these data indicate redundancy of IMP and IMPL1 expression in most plant tissues, except for seeds. In addition, IMP is expressed at higher levels in most tissues as compared to IMPL1 and IMPL2, and IMPL2 appears to be constitutively expressed at low levels.

To investigate the spatial pattern of regulation of the IMP and IMPL genes, I generated transgenic plants expressing IMP, IMPL1 and IMPL2 promoters fused to the *uidA* gene, which encodes β-glucuronidase (GUS). Two independent transgenic lines for ProIMP-*uidA* and ProIMPL1-*uidA* constructs were analyzed and consistent patterns were detected (Figure 14).

In ProIMP-*uidA* 3-d-old seedlings, β-glucuronidase (GUS) activity was noted in the entire cotyledon, within the upper hypocotyl, leaf primordia, lateral root primordia, primary root tips, and guard cells (Figure 14A-D). ProIMPL1-*uidA* shows a similar pattern in 3-d-old seedlings however IMPL1 is not expressed in root tissue (Figure 14E and not shown). In 7-d-old seedlings, IMP expression is mostly restricted to the vascular tissue in cotyledons, roots, and leaves, and trichomes also express IMP (Figure 14F-H). At 7-d, IMPL1 expression is weakly maintained in the cotyledons but expression in leaf primordia is stronger (Figure 14I). In 14-d-old plants, IMP expression is similar to 7-d seedlings with vascular expression in most leaves and within roots (Figure 14J-K). At 14-d, IMPL1 expression is highest in young sink leaves, and is restricted to vascular tissue within older, source leaves (Figure 14L). In 19-d-old plants, IMP expression is observed in all cells of young, sink leaves and becomes restricted to vascular tissue within older, source leaves (Figure 14M). The expression of IMP in 19-d-old roots remains the same as in the earlier stages of development (Figure 14K). At 19-d, the IMPL1 expression

pattern is similar to that of IMP, however expression is restricted to the shoot (Figure 14N and not shown). Examination of leaves from soil-grown plants indicates that IMP expression is restricted to the vascular tissue and IMPL1 is expressed throughout the leaf (Figure 14O-P). In flowers, IMP is expressed in the pistil while IMPL1 expression is present in vascular tissue in the sepals (Figure 14Q-R). Both genes are expressed in the mature embryo, however, once again, IMPL1 is restricted to the shoot portion of the embryo (Figure 14S-T). Within siliques, IMP is expressed in the tips and abscission zones of immature siliques (Figure 14U), while IMPL1 is restricted to the stem of the immature silique (Figure 14V). Together, these data indicate that the IMP and IMPL1 genes are developmentally and spatially regulated in a similar fashion. In addition, IMPL1 is restricted to shoot tissues, while IMP is expressed in both shoots and roots.

I have analyzed multiple transgenic plant lines containing three different IMPL2 promoter:*uidA* constructs. The promoter region of IMPL2 is exceptionally small for a eukaryotic gene; therefore I varied the length of base pairs that were taken from the upstream gene. Genomic regions containing putative promoters for IMPL2 for three different lengths of 1628bp, 1085bp or 461bp were amplified from CS60000 genomic DNA. The small promoter of 461bp is the size of the promoter region of IMPL2 and the other promoter lengths extend into the sequence of the upstream gene, annotated as Dehydrin. I have been unsuccessful in obtaining lines that show any expression in tissues that were examined, including seedlings from 1-d to 14-d-old, leaves, flowers, roots of mature plants. Therefore, I conclude it is likely that sequences outside of the promoter are necessary for dictating IMPL2 expression. To address this I constructed plants expressing the entire IMPL2 promoter and genomic sequence fused to the *uidA* gene. Analysis of these transgenic plants is underway.

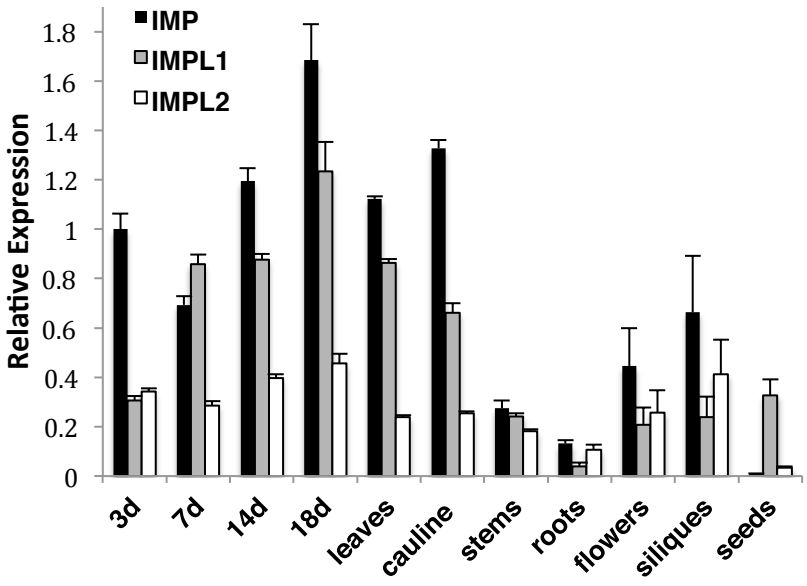

Figure 12. Relative Expression of IMP and IMPL Genes as Determined by Real-time PCR.

IMP, IMPL1, IMPL2 gene expression was measured in 3,7,14-d-old wild type seedlings grown on 0.5x MS plus 1% sucrose-soaked filter paper under 16-h-light conditions, soil-grown 18-d-old whole plants (18d), young rosette leaves (leaves), roots, cauline leaves (cauline), flowers and immature siliques from 35-d-old plants and seeds imbibed in water for 3 d at 4°C. Real-time PCR amplification curves of genes of interest were compared with PEX4 (peroxisomal ubiquitin4) amplification to generate relative expression levels. PEX4 was used as an endogenous control because it is expressed constitutively at all stages of development. Means of triplicate reactions of three biological replicates ± SE are presented.

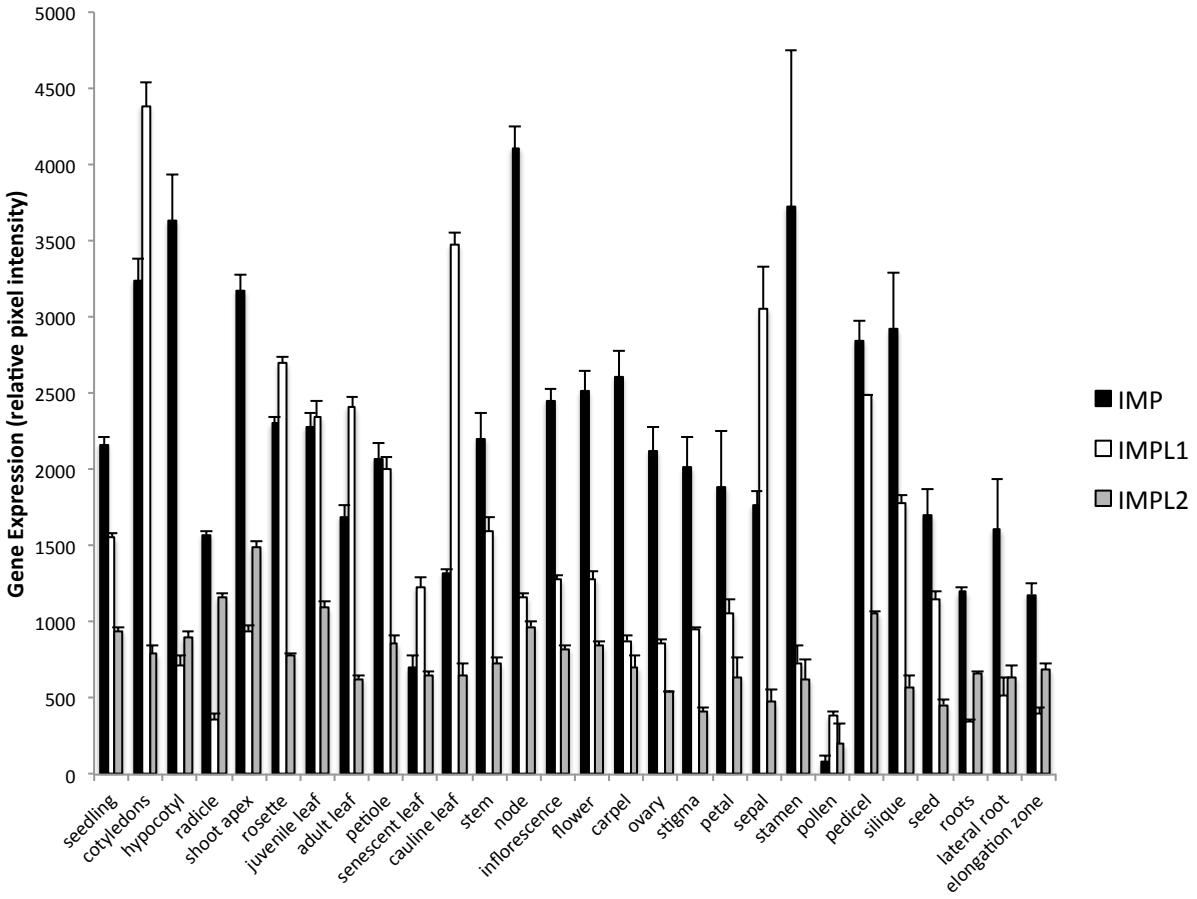

Figure 13. Gene Expression of IMP, IMPL1 and IMPL2.

Genevestigator (https://www.genevestigator.com/gv) microarray data was queried to determine IMP, IMPL1 and IMPL2 expression in various tissues. Data from Genevestigator database was analyzed and plotted. The different tissues are indicated on the x-axis. Values represent the mean ± SD of three replicates.

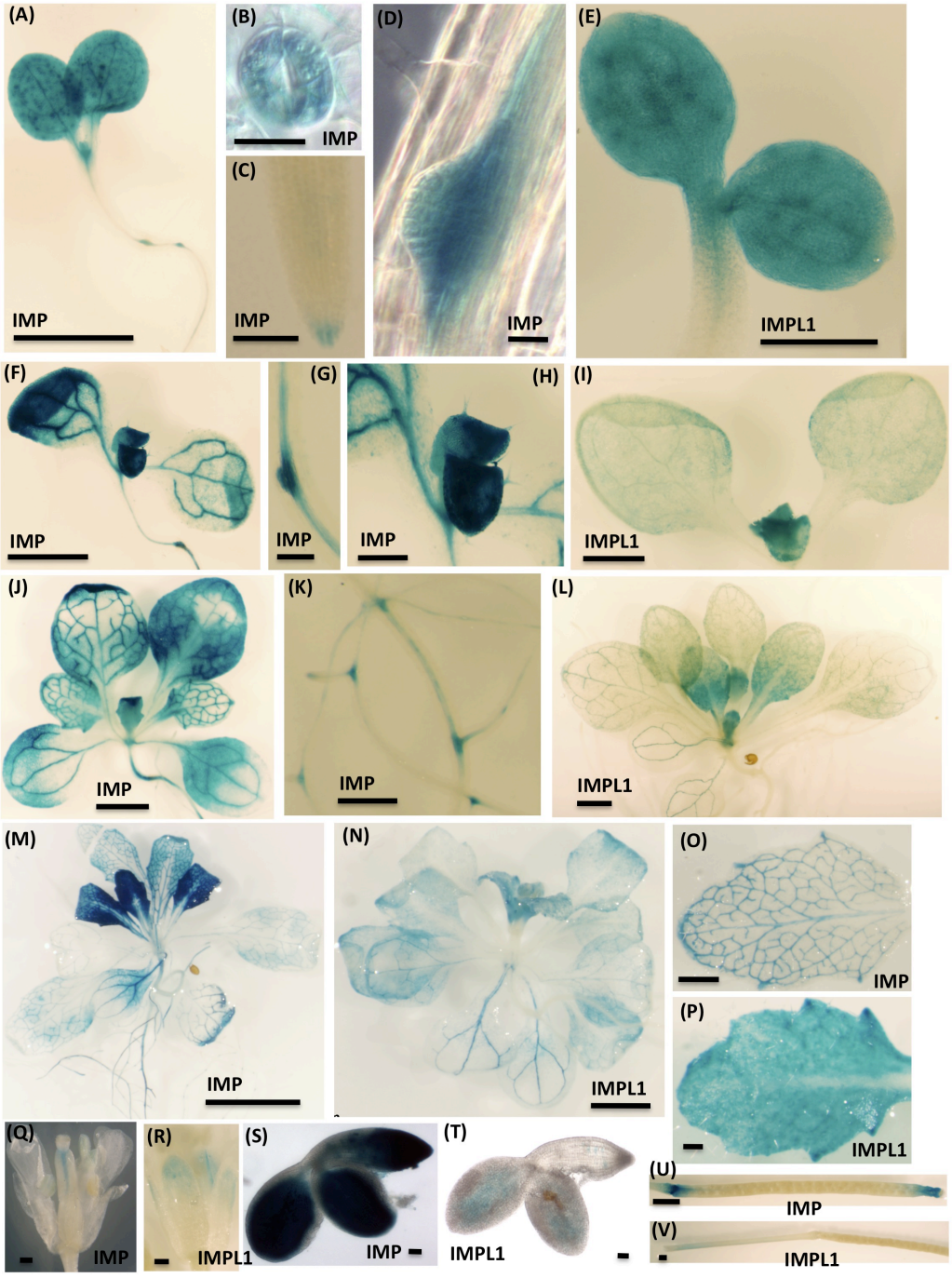

Figure 14. Spatial Expression Patterns of IMP and IMPL1 Genes.

Figure 14. Spatial Expression Patterns of IMP and IMPL1 Genes.

The promoters from IMP and IMPL1 were used to drive GUS expression in transgenic plants.
(A) to **(E)** Three-day-old seedlings grown on 0.5x MS plus 1% sucrose. Bars = 1 mm in **(A)**, 20 μm in **(B)**, **(D)** 200 μm in **(C)**, and 500 μm in **(E)**.
(F) to **(I)** Seven-day-old seedlings grown on 0.5x MS plus 1% sucrose. Bars = 1.3 mm in **(F)**, 200 μm in **(G)**, 377 μm in **(H)**, and 1 mm in **(I)**.
(J) to **(L)** Fourteen-day-old seedling grown on 0.5x MS plus 1% sucrose. Bars = 2 mm in **(J)**, **(L)**, and 500 μm in **(K)**.
(M), **(N)** Nineteen-day-old seedling grown on 0.5x MS plus 1% sucrose. Bars = 5 mm in **(M)** and 2 mm in **(N)**.
(O) to **(V)** Organs from soil-grown plants.
(O), **(P)** Leaves. Bars = 50 μm in **(O)**, and 200 μm in **(P)**.
(Q), **(R)** Flowers. Bars = 500 μm.

To examine accumulation of IMPL1 and IMPL2 proteins in plant extracts, I generated transgenic plants expressing a HA-tagged protein under the control of the native promoter fused to the entire genomic sequence of each gene (Figure 15). The predicted molecular weight for HA-tagged IMPL1 and IMPL2 is 40 and 38 kDa, respectively. However the HA fusion proteins both migrated slightly faster indicating the likelihood that the transit peptide is cleaved upon entrance into the chloroplast resulting in HA fusion proteins with smaller molecular mass than predicted. The protein blots in Figure 15 are preliminary data showing that IMPL1-HA protein is expressed in most tissues except roots and seeds and IMPL2-HA is expressed in all tissues except seeds. Since the protein loading is not equal in all lanes as shown by the Ponseau S staining, only tentative conclusions can be drawn as to the relative amount of protein expressed at each developmental stage. Future protein blot analyses need to be done to ensure equal loading of plant extracts to produce a comparative analysis of protein accumulation throughout plant development. In summation, I can speculate that IMPL1 and IMPL2 are produced in most developmental stages of the plant and most probably are present at constitutive levels.

The IMP Protein is Located in the Cytosol and IMPL Proteins are Located in the Chloroplast

Both IMPL1 and IMPL2 have been localized to the chloroplast in transient expression assays and proteomics analysis of chloroplasts (Petersen et al., 2010; Sun et al., 2009). To investigate the subcellular location of IMP and IMPL proteins in multiple tissues, I constructed transgenic plants expressing IMP:GFP, IMPL1:GFP or IMPL2:GFP under the control of the 35S cauliflower mosaic virus (CaMV) promoter (Figure 16). I analyzed homozygous progeny from two independent lines for each construct with confocal microscopy and found similar patterns from each set of transgenic lines. Western blot analysis was performed to confirm that the fusion proteins were accumulating in plants (Figure 17). For IMP:GFP, GFP fluorescence was predominantly associated with the cytoplasm in 3-d-old light-grown seedling shoots and roots (roots are shown in Figure 16A). To determine whether IMP:GFP is associated with the cell wall, 3-d-old seedlings were treated with 800 mM NaCl to stimulate plasmolysis (Figure 16B). In plasmolyzed

cells, GFP fluorescence retracted away from the cell wall, confirming a cytosolic localization.

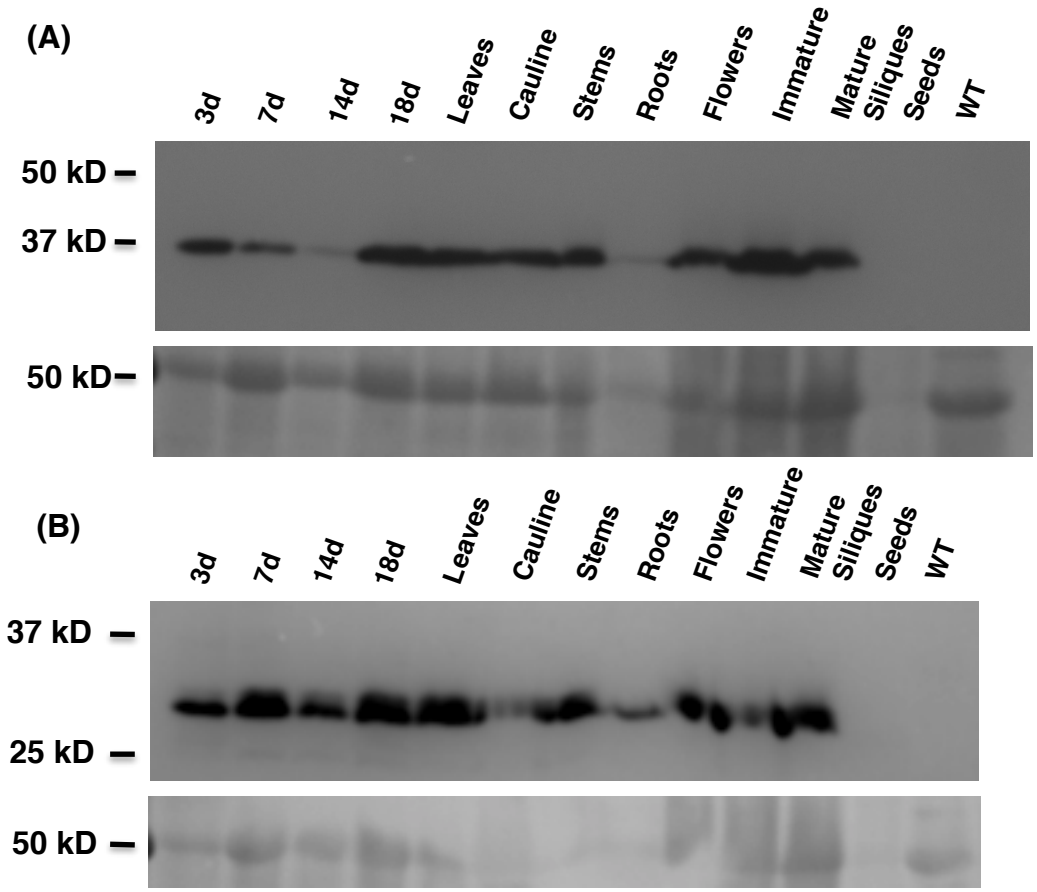

Figure 15. Expression Pattern of IMPL1:HA and IMPL2:HA Proteins.

(A) Denaturing SDS-PAGE and protein gel blot analysis of plant extracts using anti-HA antibody. Different tissues were taken from transgenic plants expressing IMPL1:HA under the control of IMPL1 native promoter. Ponceau S staining of the blot is shown in the bottom panel. **(B)** Denaturing SDS-PAGE and protein gel blot analysis of plant extracts using anti-HA antibody. Different tissues were taken from transgenic plants expressing IMPL2:HA under the control of IMPL2 native promoter. Ponceau S staining of the blot is shown in the bottom panel.

As expected I found that IMPL1:GFP localized to small organelles in root and shoot tissues within seedlings and mature plants (seedling tissues shown in Figure 16F,H). The expression pattern was also detected in mesophyll cell layers in the cotyledons and leaves. Similar data were collected for IMPL2:GFP plants, verifying its likely plastid and chloroplast subcellular presence. To confirm the identity of the small organelles, I completed a co-localization experiment using transgenic plants expressing IMPL2:GFP or IMPL1:GFP proteins with a plastid-mcherry marker containing the signal peptide of the pea Rubisco small subunit (Nelson et al., 2007a). The data demonstrate that both IMPL1 and IMPL2 proteins are directed to plastidic structures. To determine if IMPL1 and IMPL2 proteins accumulate in the same compartment, I performed a co-localization experiment using transgenic plants expressing IMPL1:GFP and IMPL2:RFP fusion proteins (Figure 16C-E). The data strongly supports that both IMPL1 and IMPL2 are present in the same compartment.

IMPL1 and IMPL2 proteins have N-terminal extensions of 77 amino acids that are predicted to function as a transit peptide and are not present in homologous IMP proteins. To determine whether the predicted transit peptide mediates organelle targeting, the 77 amino acid N-terminal extension of IMPL-1 and IMPL-2 were fused to GFP. The resulting constructs, Pro35S:NterIMPL1:GFP and Pro35S:NterIMPL1:GFP were stably transformed into Arabidopsis. The putative IMPL2 signal peptide directed a chloroplast and plastid pattern of GFP expression similar to that seen with IMPL2:GFP localization (Figure 18A). The 77 amino acid putative transit peptide from IMPL1 also was sufficient for localization to chloroplasts and plastids similar to those seen with IMPL1:GFP, however the intensity of expression was significantly reduced (Figure 18B,C). From these data, I conclude that the N-terminal extension of 77 amino acids on both IMPL1 and IMPL2 are sufficient for localization to chloroplasts and plastids.

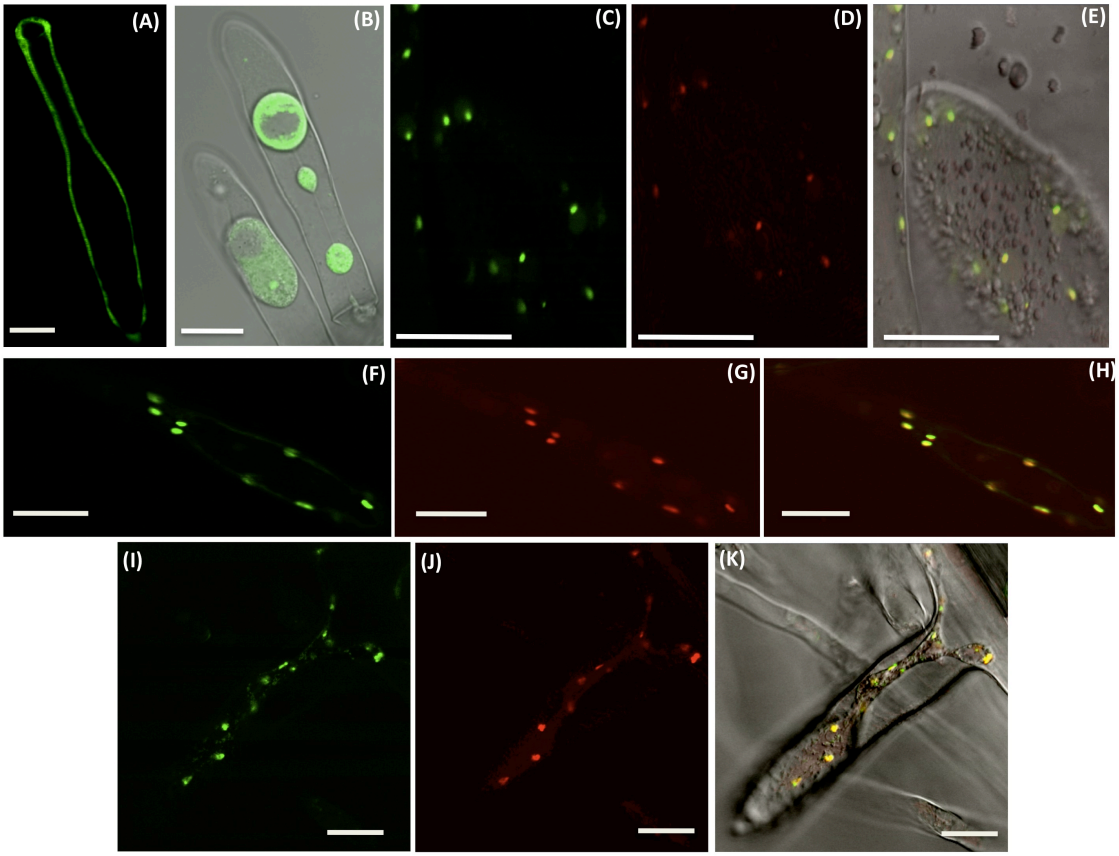

Figure 16. Subcellular Location of IMP, IMPL1, and IMPL2:GFP Proteins.

Single optical sections of transgenic plants expressing IMP:GFP **(A)-(B)**, IMPL1:GFP **(C)**, IMPL2:RFP **(D)**, overlay of IMPL1:GFP/IMPL2:RFP **(E),** IMPL2:GFP **(F)**, Plastid mcherry **(G)**, overlay of IMPL2:GFP/plastid-mcherry **(H)**, IMPL1:GFP **(I)**, Plastid mcherry **(J)**, overlay of IMPL1:GFP/plastid-mcherry **(K)**. All images were taken of root hairs with differential interference contrast (DIC) overlay of plasmolyzed cells **(B)**, DIC overlay of co-localizations **(E)**,**(K)**. Bars = 20 μm.

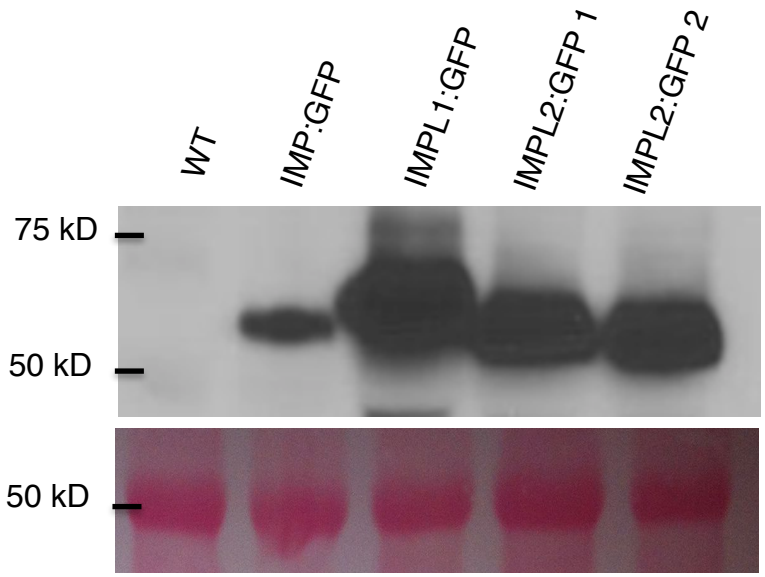

Figure 17. Western Blot Analysis of IMP:GFP, IMPL1:GFP and IMPL2:GFP Fusion Proteins.

Denaturing SDS-PAGE and protein gel blot analysis of plant extracts using anti-GFP antibody. 23-d-old rosettes were taken from transgenic plants expressing IMP:GFP or IMPL1:GFP or IMPL2:GFP under the control of 35S promoter. Ponceau S staining of the blot is shown in the bottom panel and the is due to staining of Rubisco at the expected molecular mass of 55 kD.

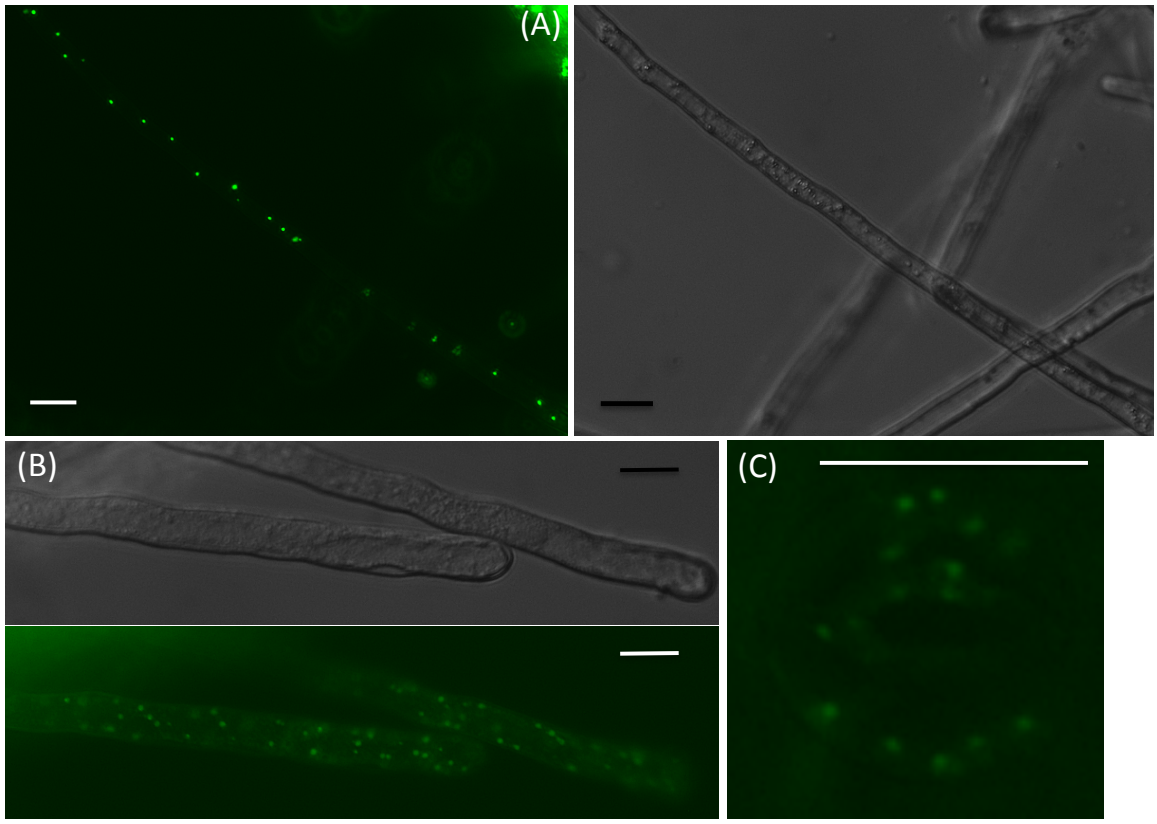

Figure 18. Subcellular Location of IMPL1, and IMPL2 N-terminal Signal Peptide Fused to GFP Protein.

Single optical sections of transgenic plants expressing IMPL2 N-ter:GFP **(A)**, IMPL1 N-ter:GFP **(B)**,**(C)**. All images were taken of root hairs and guard cells with differential interference contrast (DIC). Bars = 20 μm.

Characterization of *impl2* Mutants

To determine how IMPL2 gene impacts His synthesis and plant growth and development, T-DNA insertion mutants were obtained from the SALK T-DNA insertion collection (Alonso et al., 2003). Seeds for *impl2-3* (SAIL_35_A08) and *impl2-4* (SAIL_146_E09) were obtained, and homozygous mutants were verified by diagnostic PCR screening and DNA sequencing, as described in the Methods. The *impl2-3* mutant contains two tandem T-DNA insertions occurring 24 nucleotides from the start of translation (Figure 19A). The *impl2-4* mutant contains two tandem T-DNA insertions 66 nucleotides from the start of translation (Figure 19A). IMPL2 gene expression was verified in the mutants by quantitative Real-time PCR (Figure 19B). Our data indicate no detectable expression of IMPL2 in *impl2-3* and *impl2-4*, indicating that both mutants are defective in expressing a full-length IMPL2 RNA. From this analysis, I conclude that both mutants are suitable for studying the consequences of IMPL2 loss of expression.

Interestingly, when primers downstream of exon one are used, the transcript levels increase by 15-fold in *impl2-3* and 5-fold in *impl2-4* (Figure 19B). This suggests that a truncated transcript that does not contain the transit signal peptide is being produced at high levels in these mutants. Thus there is a possibility that a functional or nonfunctional IMPL2 protein accumulates in the cytosol of these mutants.

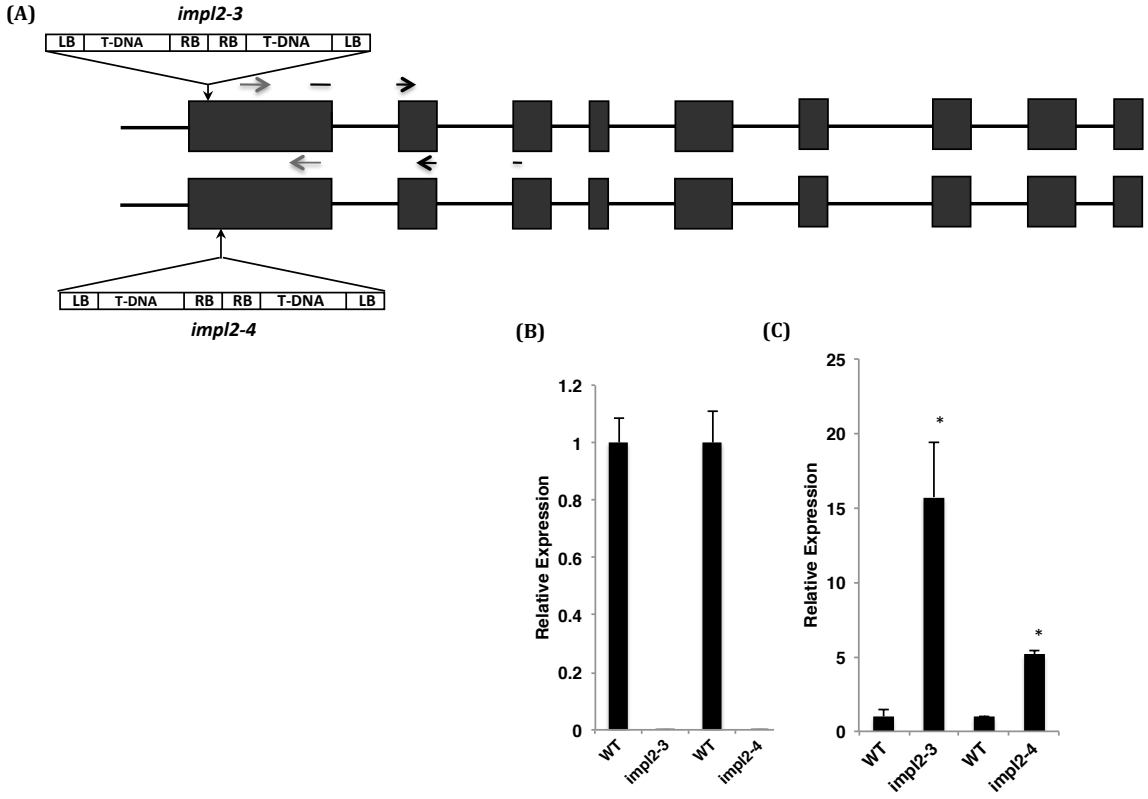

Figure 19. T-DNA Insertions and Mutant Gene Expression.

(A) Schematic of T-DNA insertion sites in the *impl2-3* and *impl2-4* mutants. Exons are shown as dark-gray boxes; the gray arrows indicate primers that are used in **(B)**; black arrows indicate primers that are used in **(C)**.
(B), (C) Expression levels of IMPL2 gene in 21-d-old wild-type and mutant plants. Real-time PCR amplification (see Methods) was compared with PEX4 amplification to generate relative expression levels. Means of triplicate biological reactions ± SE are represented. Asterisks indicate significant difference from the wild-type ($p<0.01$) in a Student's t-test.

To test this hypothesis I generated a polyclonal antisera in rabbits, using purified IMPL2:GST recombinant protein as an immunogen. The IMPL2 antisera is able to detect both IMPL1:GST and IMPL2:GST recombinant proteins as well as IMPL2:HA or IMPL2:GFP fusion proteins in transgenic plant extracts (Figure 20 A,B). In order to increase the sensitivity of the westerns, I purified the antisera by affinity chromatography using IMPL2 recombinant protein covalently bound to Reactigel matrix (Pierce). I also purified chloroplasts using a percoll gradient and precipitated chloroplast proteins (Methods) to further enrich for IMPL2 protein, however I could not detect endogenous IMPL2 protein levels in wild-type purified chloroplasts (Figure 20C). Thus, I cannot draw any conclusions about IMPL2 protein location or levels in the *impl2* mutants.

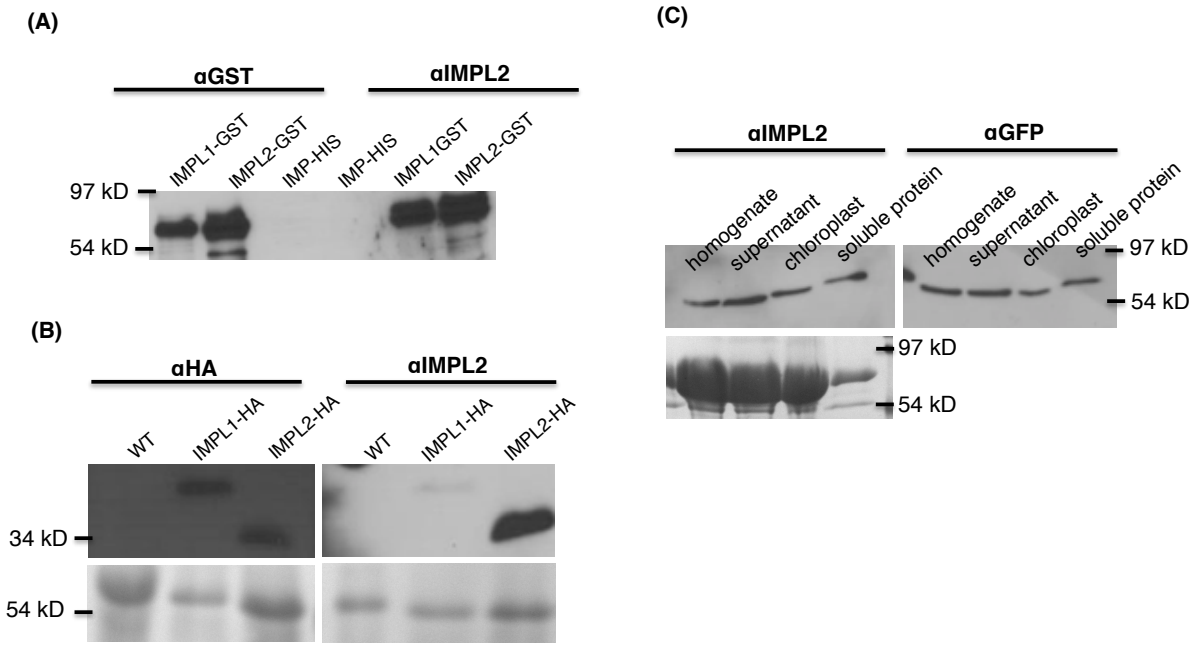

Figure 20. Optimization of IMPL2 Detection Using the Anti-IMPL2 Antibody.

(A) Denaturing SDS-PAGE and protein gel blot analysis using anti-IMPL2 antibody. The antibody detects IMPL1-GST and IMPL2-GST recombinant proteins, however it does not detect IMP-His protein.
(B) Denaturing SDS-PAGE and protein gel blot analysis of plant extracts using anti-HA and anti-IMPL2 antibody. Leaves from 15-d-old transgenic plants expressing either IMPL1:HA or IMPL2:HA under the control of native promoter were taken for analysis. The HA lines were from fist generation T_0 that were segregating for the transgene. The anti-HA antibody detects the fusion protein in both extracts, however anti-IMPL2 antibody only detects IMPL2-HA and no detection is present in IMPL1-HA or WT extracts. **(C)**. The chloroplast purification steps (describe in methods) done from leaves taken from 34-d-old IMPL2:GFP transgenic plants. IMPL2:GFP was detected in all fractions using both the anti-GFP and anti-IMPL2 antibodies. Ponceau S staining of the blot is shown in the bottom panels (Rubisco at the expected size of 55 kD) **(B)** and **(C)**.

The *impl2* Mutants Are Altered in Growth and Development

Examination of *impl2* mutants offers a unique opportunity to assess the importance of the His biosynthetic pathway in plant growth and development. It has been previously reported that the *impl2-3* mutant is embryo-lethal (Petersen et al., 2010), however I was able to obtain homozygous progeny of both *impl2-3* and *impl2-4* that produce viable seeds. I analyzed two other T-DNA insertion mutant lines, *impl2-1* and *impl2-2*, and was not able to recover homozygous progeny, strongly suggesting embryo lethality. Analysis of 30 siliques in wild-type and *impl2-1* revealed that approximately 20% of the seeds were shriveled suggesting embryo lethality in *impl2-1* plants.

The *impl2-3* and *impl2-4* mutant plants are severely compromised in growth and exhibit several main phenotypes, which are quantified in Table 3 and described below (Figure 21A-E). These phenotypes include smaller size, and reduced inflorescences and seed production. To ensure that these phenotypes result from an IMPL2 loss-of-function, I complemented *impl2-3* with the IMPL2:GFP transgene. These complemented plants (*impl2-3*/IMPL2:GFP) exhibited wild-type or near wild-type phenotypes in several different assays (Figure 21A,C). This, along with the finding of two separate mutant alleles (*impl2-3* and *impl2-4*), strongly supports alteration in IMPL2 function as the primary cause for the observed phenotypes.

Although both *impl2* mutant lines show very similar phenotypes, *impl2-3* has been the focus for my experiments. I first analyzed the germination rate of mutant seeds and noted that only 75% of *impl2-3* seeds germinate (Figure 22A). After germination of *impl2-3* mutant seeds, I noted significant delay in seedling development as compared to wild-type seedlings, which continues throughout development. Homozygous *impl2* mutants are overall smaller than wild-type plants (Figure 21A-E), *impl2* mutant roots do not grow, and most seedlings do not produce true leaves and die after a few days (Figure 21E). The seedlings that develop beyond this stage are able to produce true leaves, however the leaves are a pale green color with increased anthocyanin accumulation present in most leaves (Figure 21B), and roots remain stunted. The pale green color of leaves may indicate malfunction in chloroplasts and the production of anthocyanin suggests stress conditions in these mutants. Mutant cotyledons and leaves were observed by microscopy and the overall presence and structure of mutant chloroplasts appeared similar to

those from wild-type plants (data not shown). Throughout development the mutant root system remains stunted and the rosette leaves are irregular in shape and purple or light green in color (Figure 21B). The dramatic difference in size of the plants is evident from the measurements listed in Table 3 as compared to wild-type plants (rosette diameter of wild-type plants are approximately 4 times larger than *impl2-3* plants). These *impl2* plants generate some viable seeds by producing very few siliques (Figure 21D, Table 3). Both the root and the shoot phenotypes of *impl2* mutants can be complemented in the *impl2-3* (Figure 21A) and *impl2-4* (data not shown) background with the IMPL2 gene fused to GFP, again, indicating the functionality of the transgene and confirming that these growth phenotypes are due to the loss of IMPL2 function.

Next, I attempted to chemically rescue the growth phenotype of *impl2* mutants by watering mutants and wild-type plants with either His or a control amino acid, glutamine. The results show that continuous watering with 1 mM His (Figure 21C) but not 1 mM glutamine (data not shown), alleviates much of the severe growth reduction in *impl2* mutants.

To test whether His deficiency is responsible for the altered root structure in *impl2* mutants, I produced age-matched seed populations that had been harvested from plants grown at the same time. Control and mutant age-matched seeds were plated on Murashige and Skoog (MS) medium in the presence of various concentrations of His, Glutamine and inositol and stratified for 3 days at 4°C. The results indicate that *impl2-3* mutants germinate at the same rate in the presence or absence of His (Figure 22A). However, root growth is restored to wild-type levels in the presence of His, while neither glutamine nor inositol improves root growth of these mutant plants (Figure 22C). The optimal range for chemical complementation with exogenous His is 0.02 to 0.04 mM, and larger concentrations such as 0.4 or 0.8 mM of His have an inhibitory effect on root growth of both *impl2* mutant and wild-type plants (Figure 22B). Since the exogenous inositol added to medium was not able to alleviate the stunted root phenotype, I concluded that IMPL2 is not involved in inositol metabolism (Figure 22C).

Table 3. Overview of the *impl2-3* and *impl2-4* mutant phenotype.

	Wild type	*impl2-3*[a]	*impl2-3* +His	*impl2-3* IMPL2:GFP	*impl2-4*[b]
Rosette diameter (cm)	4.87 ± 0.2	1.10 ± 0.1*	4.14 ± 0.2	3.69 ± 0.2	1.6 ± 0.1*
Number of rosette leaves per plant	18.3 ± 0.7	9.4 ± 0.5*	17.1 ± 1.2	17.3 ± 0.9	12.1 ± 0.6*
Average rosette leaf surface (cm^2)	2.03 ± 0.1	0.20 ± 0.02*	2.03 ± 0.1	1.57 ± 0.1	0.28 ± 0.02*
Number of inflorescence stems per plant	6.6 ± 0.5	1.9 ± 0.3*	7.2 ± 0.8	4.6 ± 0.6	1.8 ± 0.2*
Weight of seeds per 6 plants (mg)	226 ± 9	51.7 ± 2*	247 ± 19	190 ± 3	65.3 ± 4.1*

Rosettes and stems were measured 9 weeks after germination. Seeds were harvested, and weighed after they were dried. Data represents the means ± SE; n = 20 for rosettes and stems; n= 4 for seeds. [a,b]Asterisks indicate values found to be significantly (Student's t-test) different from the wild type: *p <0.005

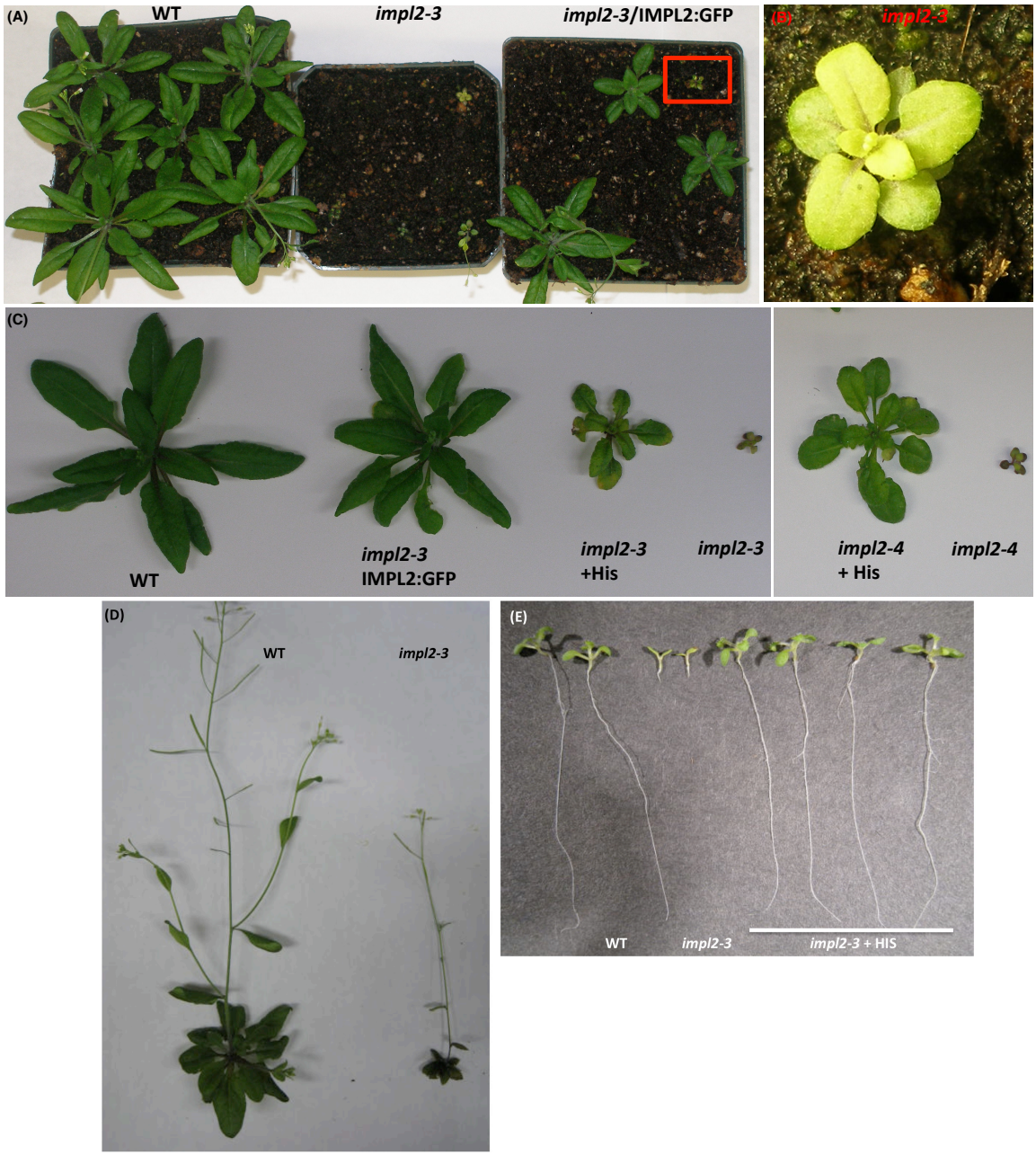

Figure 21. Histidine or IMPL2-GFP Gene Complement the Stunted Stature of *impl2* Mutants.

(A) Segregation of progeny from heterozygous *impl2-3* plants containing a 35S promoter-IMPL2-GFP transgene. **(B)** Image of the *impl2-3* rosette exhibiting small, pale green leaves **(C)** Soil-grown *impl2-3*, *impl2-4*, wild-type (CS60000) and complemented plants. The mutant plants were watered with 1 mM Histidine for the chemical complementation analysis. **(D)** Soil-grown wild-type and *impl2-3* plants reaching flowering stage. **(E)** Photos of 9-d-old wild-type and *impl2-3* seedlings grown on agar plates for root length studies. Root phenotype of *impl2-3* is complemented by the addition of 0.04 mM Histidine (His).

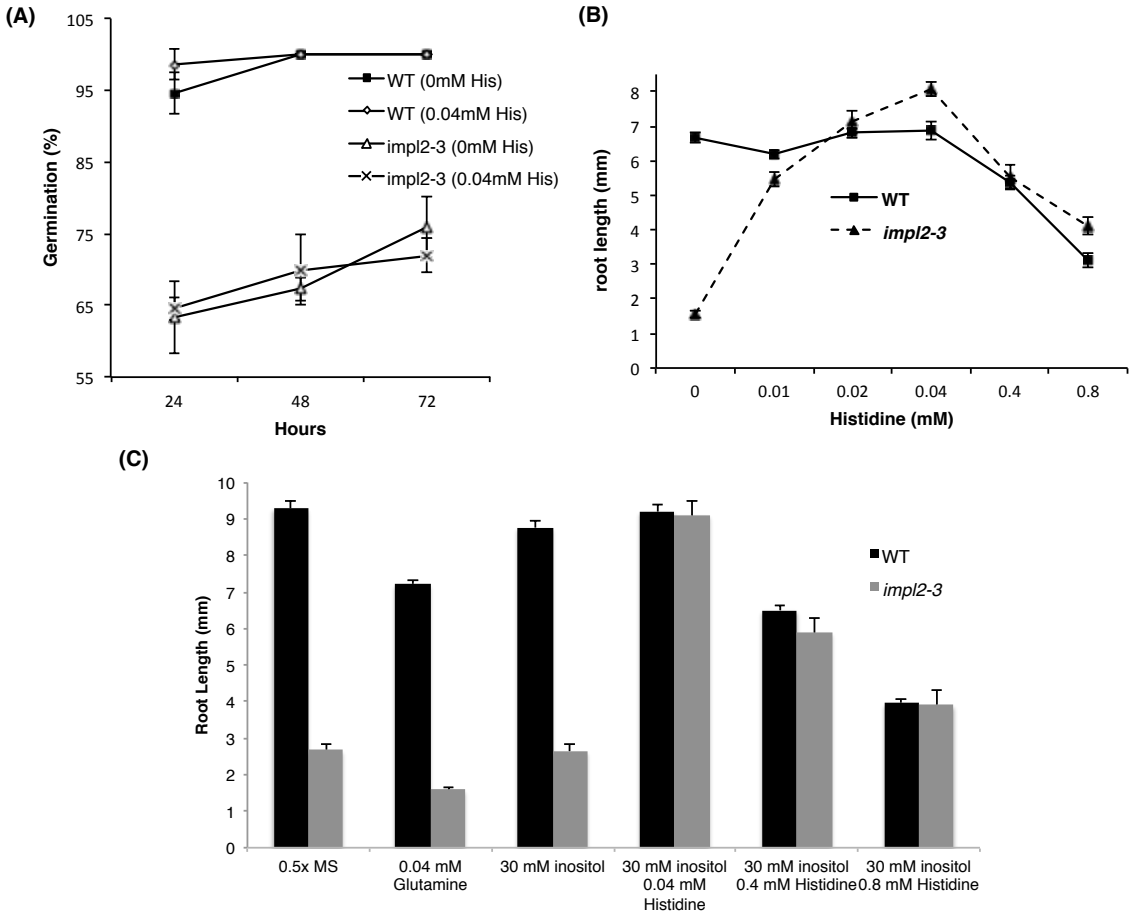

Figure 22. Physiological Responses of *impl2-3* Mutants to Exogenous Histidine and Inositol.

(A) Effects of histidine on germination of the wild-type and *impl2-3* mutants grown on agar plates. **(B)** Dosage Response of 4-d-old wild-type and *impl2-3* mutant seedlings grown for root length studies on agar plates with the indicated histidine concentrations. **(C)** Effects of glutamine, inositol and histidine on root length of wild-type and *impl2-3* mutants grown on agar paltes. Presented are means ± SE of three experiments of n= 50 (germination) and three experiments of n= 30 (root length).

IMPL2 Impacts Histidine Synthesis

To determine if a loss in IMPL2 function impacts His biosynthesis, I used LC-MS-MS to quantify His levels in the wild-type and *impl2-3* mutants (Table 4). The amino acids were extracted using 1:1 chloroform:10 mM HCl (v/v) and norvaline was used as internal standard. Standard curves for His and histidinol were generated using commercially available standards. Peaks within the chromatograms were identified by comparison to the retention times of the standards and detected by MS analysis using a multiple reaction monitoring (MRM) acquisition method (Parameters are listed in Table 5, in Chapter III). The peak areas were quantified from the standard curves and normalized to the amount of tissue and internal standard.

In 7-d-old seedlings, His levels are slightly increased in *impl2-3* mutants as compared to wild-type, and the levels are not rescued to wild-type levels in the complemented plants. The His levels remain elevated as the plant progresses through development reaching the 18-d time point. Interestingly, later in development (31 days), leaves from *impl2-3* mutants show levels of free His equal to that found in wild-type, indicating that the amount of His is not altered in the *impl2* mutants at this time in development.

Next, I measured histidinol, the product of IMPL2 action on histidinol-P. Although I expected that *impl2* mutants would have reduced histidinol levels, *impl2-3* 7-d-old seedlings accumulated 1.66 ± 0.04 μM mg dried weight^{-1} histidinol as compared to the barely detectable wild-type levels of 0.0046 ± 0.0001 μM mg dried weight^{-1} (Table 4). This suggests that lack of histidinol-P hydrolysis in *impl2* mutants results in accumulation of precursors in the His pathway. Further, at 31 days histidinol accumulation in the *impl2* mutant remains the same, while His levels revert back to wild-type levels at this stage. Importantly, in the IMPL2 complemented plants, histidinol levels at both 7 and 23 days are similar to those from wild-type plants (Table 4). This strongly implicates elevation of precursors in the His pathway correlate with the altered growth and development of *impl2* mutants as the complemented plants contain normal levels of histidinol and undergo normal growth and development. However, the His levels in complemented plants remain high as seen in the *impl2* mutants.

A common issue with metabolite extraction of phosphorylated compounds is hydrolysis of

phosphates during sample extraction and derivitization. Consequently, I tested whether the histidinol measured in the assays was due to accumulation of histidinol-P and hydrolysis during sample preparation. To address this possibility, I added 100 µM of purified histidinol-P to wild-type tissue during the extraction procedure along with the addition of internal standard, norvaline. In the wild-type extract where no histidinol-P is added, histidinol levels are barely detectable (0.008 ± 0.014 µM mg dried weight^{-1}), and in the wild-type extract with added 100 µM histidinol-P, histidinol levels are increased by 57-fold to a concentration of 0.48 ± 0.02 µM mg dried weight^{-1} (Figure 23). In order to test whether nonspecific phosphatase activity in the plant extract might be hydrolyzing histidinol-P during extraction, I performed the extraction procedure with 100 µM of pure histidinol-P. When a 1:5 dilution (20 µM) of the extract was analyzed on LC-MS-MS, 15.6 µM of histidinol was recovered. This indicates that the hydrolysis is due to the extraction method and not due to non-specific phosphatase activity towards this substrate in the plant extracts. In conclusion, from this data I speculate that histidinol-P is the His precursor accumulating to high levels in *impl2-3* mutants. This speculation is supported by my *in vitro* data showing that IMPL2 is capable of hydrolyzing histidinol-P.

To test the possibility that the *impl2* phenotype can be rescued by histidinol, I grew *impl2-3* and wild-type seeds in the presence of varying concentrations of histidinol (Figure 24). The root length phenotype of *impl2-3* seedlings was complemented by 0.8 to 1 mM of histidinol and this amount was not toxic to the growth of wild-type seedlings. I speculate that the levels of histidinol found in *impl2* mutants are not high and perhaps these plants suffer from histidinol deficiency. This data further supports that histidinol-P is the intermediate that accumulates in the mutant plants.

Together, my developmental analysis and His metabolite data analyses firmly establish that *impl2* mutants have alterations in the His biosynthetic pathway that lead to severe growth alterations, and underscore the importance of this pathway in plant growth and development.

Table 4. Histidine and Histidinol Levels at Different Developmental Stages.

Tissue	WT (μM mg DW^{-1})	*impl2-3* (μM mg DW^{-1})	*impl2-3* IMPL2:GFP (μM mg DW^{-1})	IMPL2:GFP (μM mg DW^{-1})
histidine 7-d	0.74 ± 0.01	1.33 ± 0.04	1.40 ± 0.02	0.73 ± 0.02
histidine 18-d	1.24 ± 0.02	1.91 ± 0.03	1.84 ± 0.07	1.77 ± 0.08
histidine 31-d	1.76 ± 0.01	1.76 ± 0.01	1.78 ± 0.03	1.76 ± 0.02
histidinol 7-d	0.0046 ± 0.0001	1.66 ± 0.04	0.0051 ± 0.0001	0.0046 ± 0.0001
histidinol 18-d	0.0051 ± 0.0002	2.38 ± 0.05	0.0042 ± 0.0003	0.0042 ± 0.0001
histidinol 31-d	0.0037 ± 0.0001	1.70 ± 0.1	0.0043 ± 0.0002	0.0043 ± 0.0007
histidine +	9.34 ± 0.14	10.7 ± 0.1	NM	NM
histidinol +	2.7 ± 0.1	5.16 ± 0.1	NM	NM

Seedlings and plants were grown on 0.5x MS, pH 5.8 and 1% sucrose. Seedlings of 7-d-old, 18-d-old or whole rosette and roots of 31-d-old wild-type, *impl2-3*, *impl2-3* IMPL2-GFP, and IMPL2-GFP plants were harvested, and histidine and histidinol levels were quantified with LC-MS-MS as described in Methods. $^{+}$ histidine and histidinol levels were measured in 7-d-old seedlings that were grown on 0.8 mM histidinol (NM= not measured).

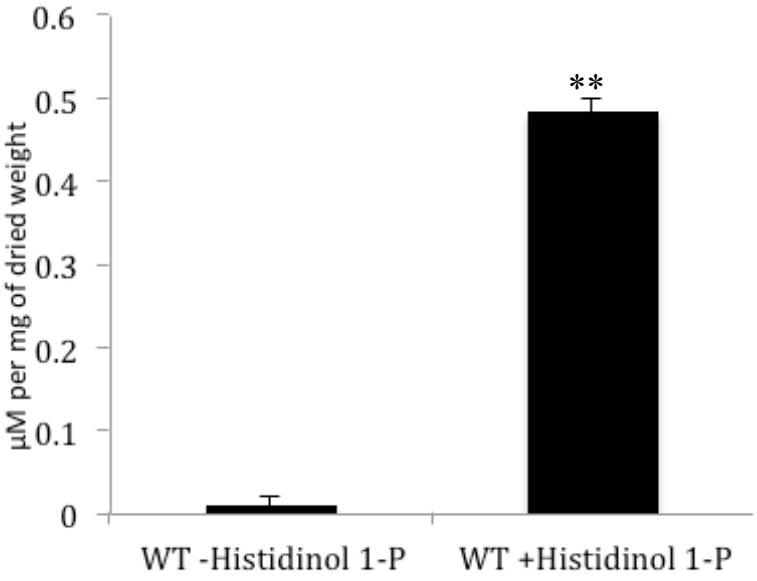

Figure 23. Hydrolysis of L-histidinol-P in Metabolite Extraction Procedure.

Leaves of 23-d-old wild-type plants were harvested and during the extraction procedure 100 µM of histidinol 1-P was added as described in Methods to assess the degree of hydrolysis to histidinol. Standard error is indicated (biological n=3). ** P value < 0.001.

Gene Expression in the Histidine Biosynthesis Pathway is Elevated in *impl2-3*

In order to test whether there is a feedback inhibition regulatory mechanism affecting the His levels in *impl2* mutants, I used Real-time PCR to quantify the level of transcripts from key, regulated genes in the His biosynthesis pathway. HisN1, HisN6A, HisN7 and HisN8 levels were measured in wild-type, *impl2-3*, *impl2-3* IMPL2:GFP and IMPL2:GFP 7-day-old seedlings. The Arabidopsis genome contains two HisN1 genes (HisN1A, HisN1B) that are thought to code for ATP-phosphoribosyltransferase, the first enzyme in the pathway. In this analysis HisN1A was chosen, because HisN1B null mutants are viable and display no obvious phenotype indicating that it is not essential (Muralla et al., 2007). The recombinant HisN1B protein exhibits increased instability and could not be purified (Ohta et al., 2000). This also indicates that HisN1B may have a distinct function that is different from HisN1A gene product. The Arabidopsis genome also contains two genes that code for histidinol-phosphate aminotransferase (HisN6A and HisN6B) which functions upstream of IMPL2 in the pathway. Real-time analysis of these two genes indicated that HisN6A is expressed in all tissues during development while HisN6B transcript levels were not detected (Moore and Purugganan, 2003). In addition, the two genes differ by only two synonymous single nucleotide polymorphisms, but differ drastically in their promoter regions (Ingle, 2011). This could suggest that both genes are differentially regulated; however no evidence for this has been found. The design of my HisN6 primers will capture the levels of both transcripts due to the high homology in the coding sequences. There is only a single copy of the HisN8 gene that codes for histidinol dehydrogenase that functions downstream of IMPL2 and catalyzes the last two steps in the pathway.

The transcript levels were measured in 7-d-old wild-type, mutant, complemented and IMPL2 over-expresser seedlings. In Figure 25, the levels of expression of each gene are shown in relation to the wild-type levels of that same gene. The expression of all three genes is elevated

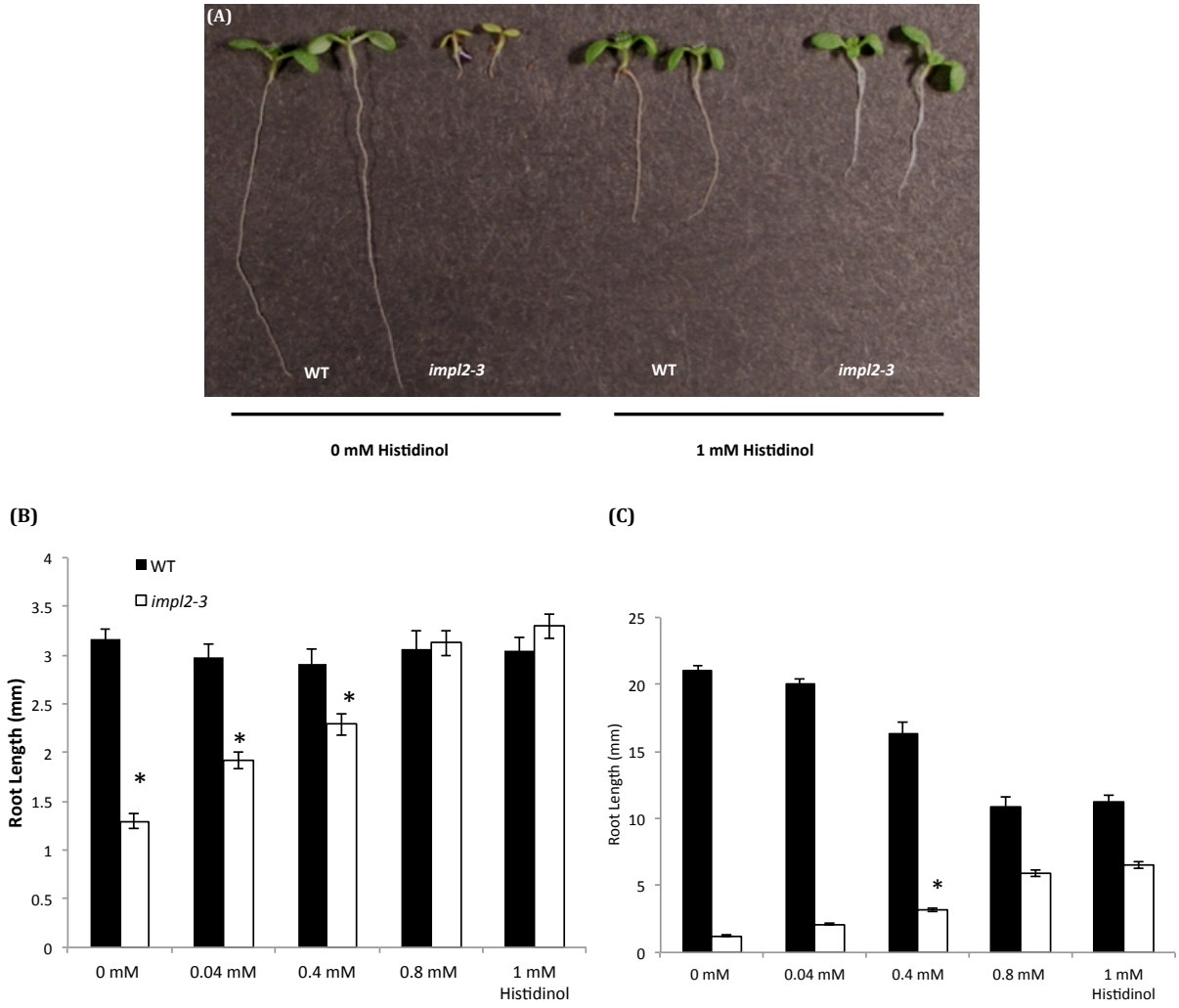

Figure 24. Chemical Complementation of *impl2-3* Mutants with Exogenous Histidinol.

(A) Photos of 8-d-old wild-type and *impl2-3* seedlings grown on agar plates for root length studies. Root phenotype of *impl2-3* is complemented by the addition of 0.8 to 1 mM histidinol. **(B)** Dosage Response of 4-d-old **(C)** 8-d-old wild-type and *impl2-3* mutant seedlings grown for root length studies on agar plates with the indicated histidinol concentrations. Presented are means ± SE of n= 40, *p values below 0.05.

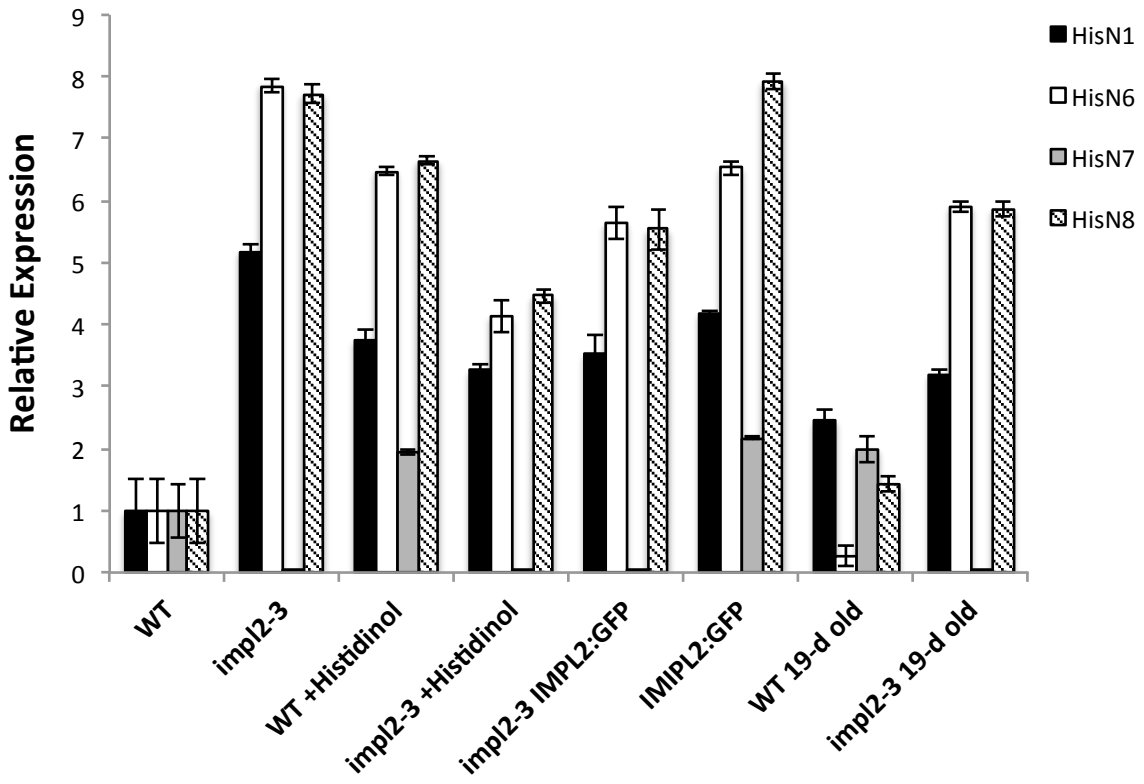

Figure 25. Relative Expression of His Genes as Determined by Real-time PCR.

HisN1, HisN6, HisN7 and NisN8 gene expression was measured in 8,19-d-old wild type, *impl2-3*, *impl2-3* IMPL2:GFP, and IMPL2:GFP seedlings grown on 0.5x MS plus 1% sucrose agar plates under 16-h-light conditions. The measurement from 19-d-old plants is indicated in the x-axis labels, the rest are 8-d-old seedlings. Real-time PCR amplification curves of genes of interest were compared with PEX4 amplification to generate relative expression levels. Means of triplicate reactions of three biological replicates ± SE are presented.

in *impl2* mutants by 5-fold (HisN1), and 8-fold (HisN6 and HisN8). The complementation with IMPL2:GFP partially reverses the increase in expression, however the levels are still higher than wild-type (Figure 25). The expression of genes is also increased in the IMPL2:GFP over-expresser lines, however this induction does not lead to an increase in His levels (Table 4). In addition, the IMPL2:GFP over-expresser lines did not show resistance to NiCl toxicity when they were grown on 25, 50, and 90 μM of NiCl for 7 days, which is expected if these over-expresser plants accumulate higher levels of His (Figure 26A). This data is in accordance with previous findings that only over-expression of ATP-PRT, the first enzyme in the pathway, leads to an increase in His content. Over-expression of cDNAs from the other enzymes did not affect His content (Rees et al., 2009). In addition, the ATP-PRT over-expressing lines, exhibited a higher tolerance to Ni, Co and Zn, which had a negative correlation to plant biomass production. The expression of His pathway genes was also measured in 19-d-old seedlings and results were similar to the ones shown for 7-d-old seedlings.

In order to test whether the alteration in His pathway gene expression in *impl2* mutants is due to perturbations in His pathway intermediates, I grew wild-type and *impl2* mutants on 0.8 mM histidinol for 7 days and analyzed transcript levels. Histidinol treatment elevated HISN1, HisN6 and HisN8 gene expression in wild-type plants, most probably due to excess availability of the intermediate, histidinol. This increase in His pathway gene transcripts was accompanied by a dramatic 9-fold increase in His levels in wild-type as measured by LC-MS-MS (Table 4). Histidinol treatment of *impl2* mutants reduced expression of HISN1, HisN6 and HisN8 gene expression (Figure 25). In addition, the *impl2* seedlings grown on histidinol also exhibit a 10-fold increase in free His levels (Table 4). Interestingly, the transcript levels in wild-type seedlings grown on histidinol are comparable to the levels in the over-expresser line, however the over-expresser lines are not accumulating excess levels of free His.

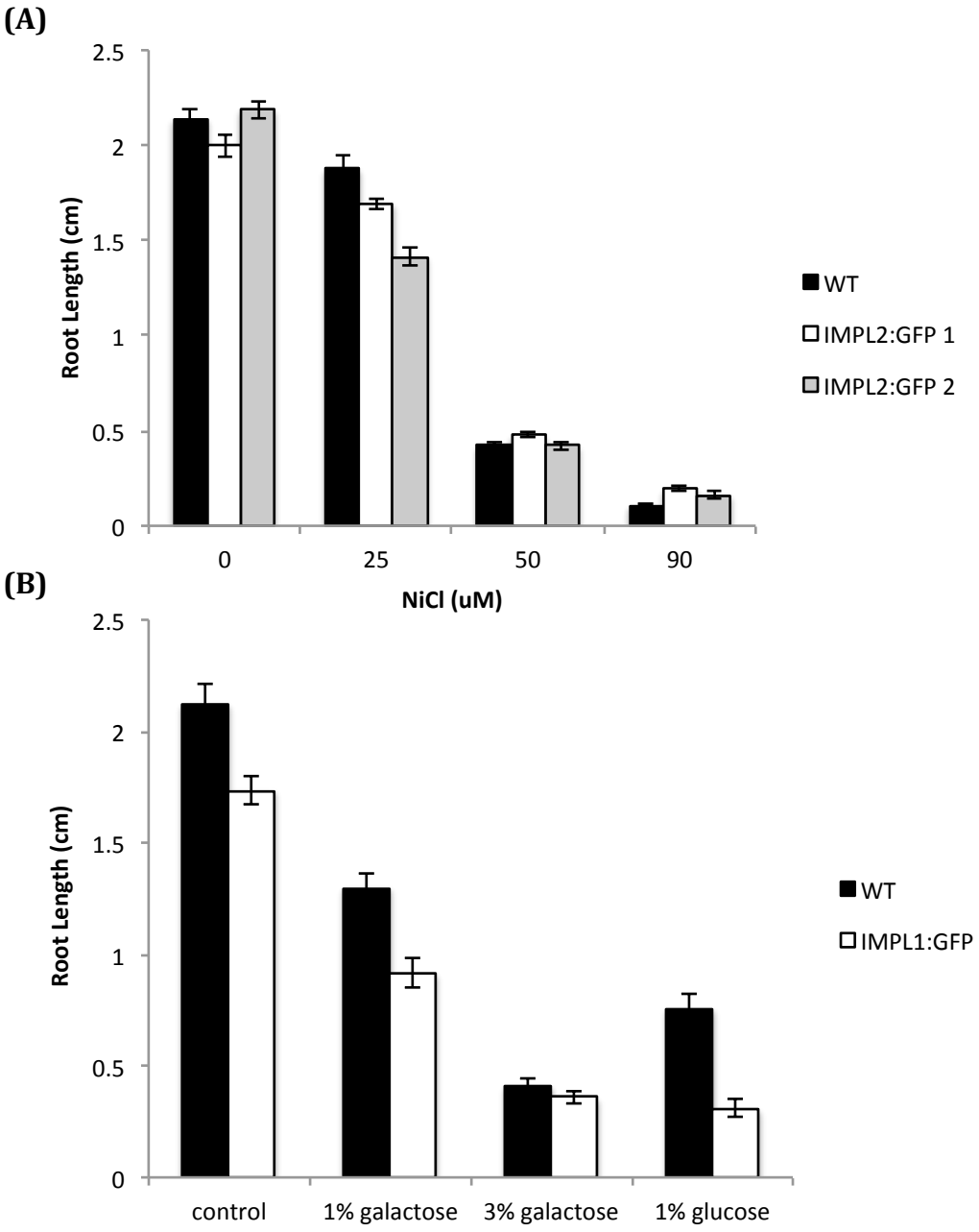

Figure 26. Toxicity Effect of NiCl on WT and IMPL2:GFP and Galactose on WT and IMPL1:GFP Plants.

(A) Dosage Response of 7-d-old wild-type and IMPL2:GFP over-expresser seedlings grown for root length studies on agar plates with the indicated NiCl concentrations. **(B)** Dosage Response of 7-d-old wild-type and IMPL1:GFP over-expresser seedlings grown for root length studies on agar plates with the indicated galactose concentrations. 1% and 3% glucose were used as controls, however none of the seeds germinated in the presence of 3% glucose. Presented are means ± SE of n= 40, *p values below 0.05.

Amino Acid Levels are Altered in *impl2-3* Mutants

It has been speculated that His may be involved in cross-pathway regulation of other amino acid or metabolic pathways. For example, in Arabidopsis, blockage of His synthesis using triazole herbicide led to an increased expression of genes in several amino acid biosynthetic pathways and ultimately the build-up of a number of amino acids, for example alanine, aspartate, glutamate, phenylalanine, proline, threonine, tryptophan, tyrosine and valine (Guyer et al., 1995b). The early His deficiency of *impl2-3* mutants could lead to similar regulatory mechanisms that were shown in plants treated with triazole to inhibit imidazoleglycerol phosphate dehydratase. Sixteen amino acids (methionine, threonine, phenylalanine, lysine, tyrosine, tryptophan, alanine, glycine, valine, leucine, isoleucine, proline, serine, aspartate, glutamate, and glutamine) were measured in *impl2-3* mutant seedlings using Gas Chromatography (Figure 27). Free pools of some but not all amino acids (threonine, phenylalanine, alanine, serine, proline, aspartate, and glutamine) increased between 1.3 to 4-fold in response to His deficiency in mutant plants. In contrast, levels of glycine, valine and isoleucine were decreased between 1.4 to 2-fold in 7-d-old *impl2-3* seedlings. Overall, this data suggests that alterations of His levels can lead to cross-talk regulation of other amino acid synthesis pathways, which may be an important regulatory mechanism for control of free amino acid pools.

IMPL2 Does Not Impact Inositol Levels

Given the bifunctionality of several of the characterized IMPs, I wanted to rule out the possibility that IMPL2 can impact inositol levels by *in vivo* hydrolysis of D-inositol 1(or 3)-phosphate. Consequently, I measured inositol and ascorbic acid (a downstream product that can result from inositol catabolism) levels in *impl2-3* mutants using Gas Chromatography (Figure 28). No difference in inositol levels was observed in *impl2-3* 7-d-old seedlings as compared to wild-type seedlings. However, ascorbic acid levels were slightly increased in these mutants (Figure 28). I speculate that this small ascorbic acid increase results from perceived stress due to the His deficiency. In addition, decreases in glycerate and xylose (Figure 28) were observed that might be due to the dramatic decrease in cell size of these mutant seedlings. Given the lack of activity of recombinant IMPL2-GST with inositol phosphate substrates, and the lack of inositol changes in *impl2* mutants, I conclude that IMPL2 plays little to no role in inositol synthesis or recycling

in the plant cell.

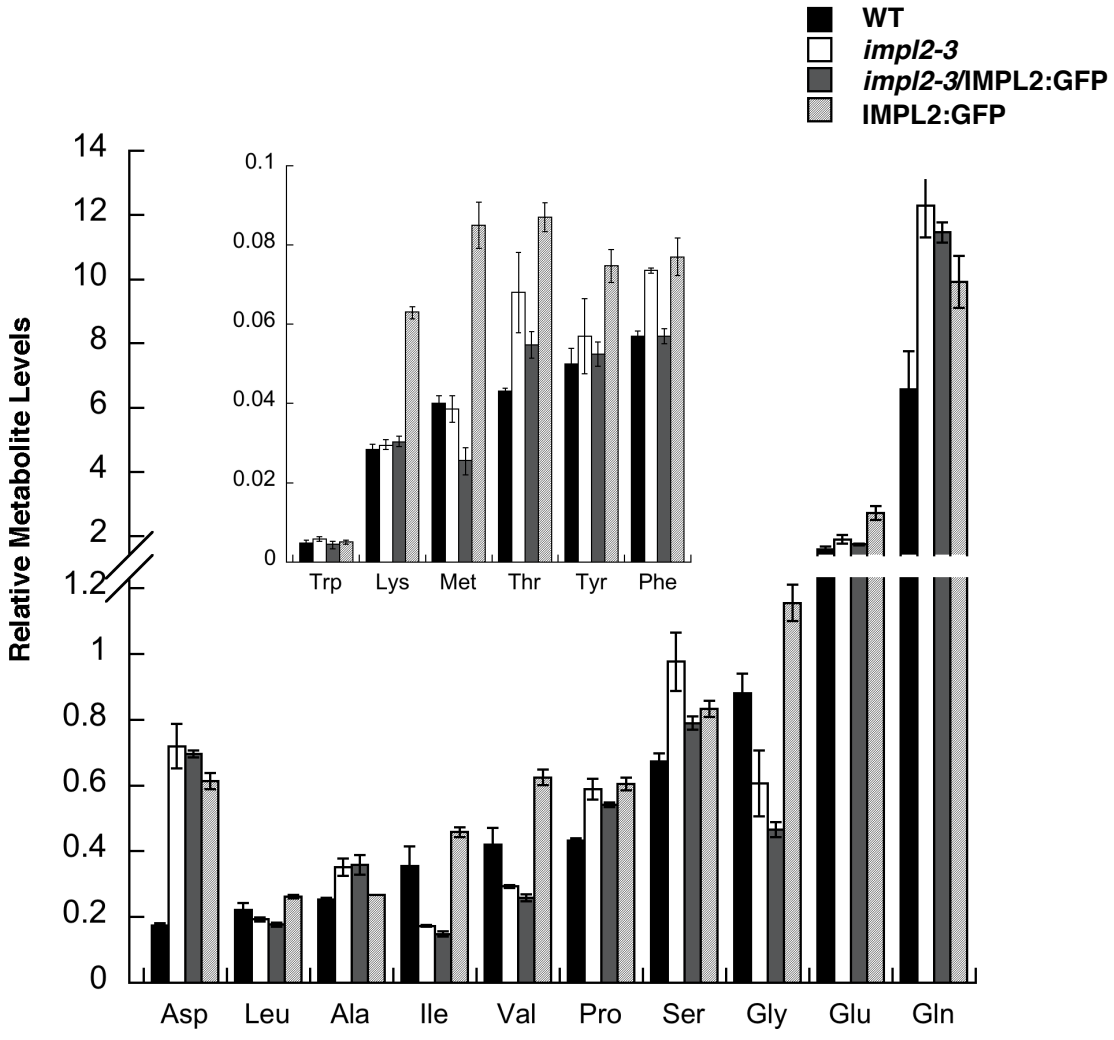

Figure 27. Amino Acid Levels in *impl2-3* Mutants, Complemented Mutants, and IMPL2:GFP plants.

GC-MS was used to measure amino acid levels in 7-d-old seedlings as describe in Methods. Amino acids with relevant abundance were graphed together. Data from three independent biological replicates were averaged. The standard error is indicated.

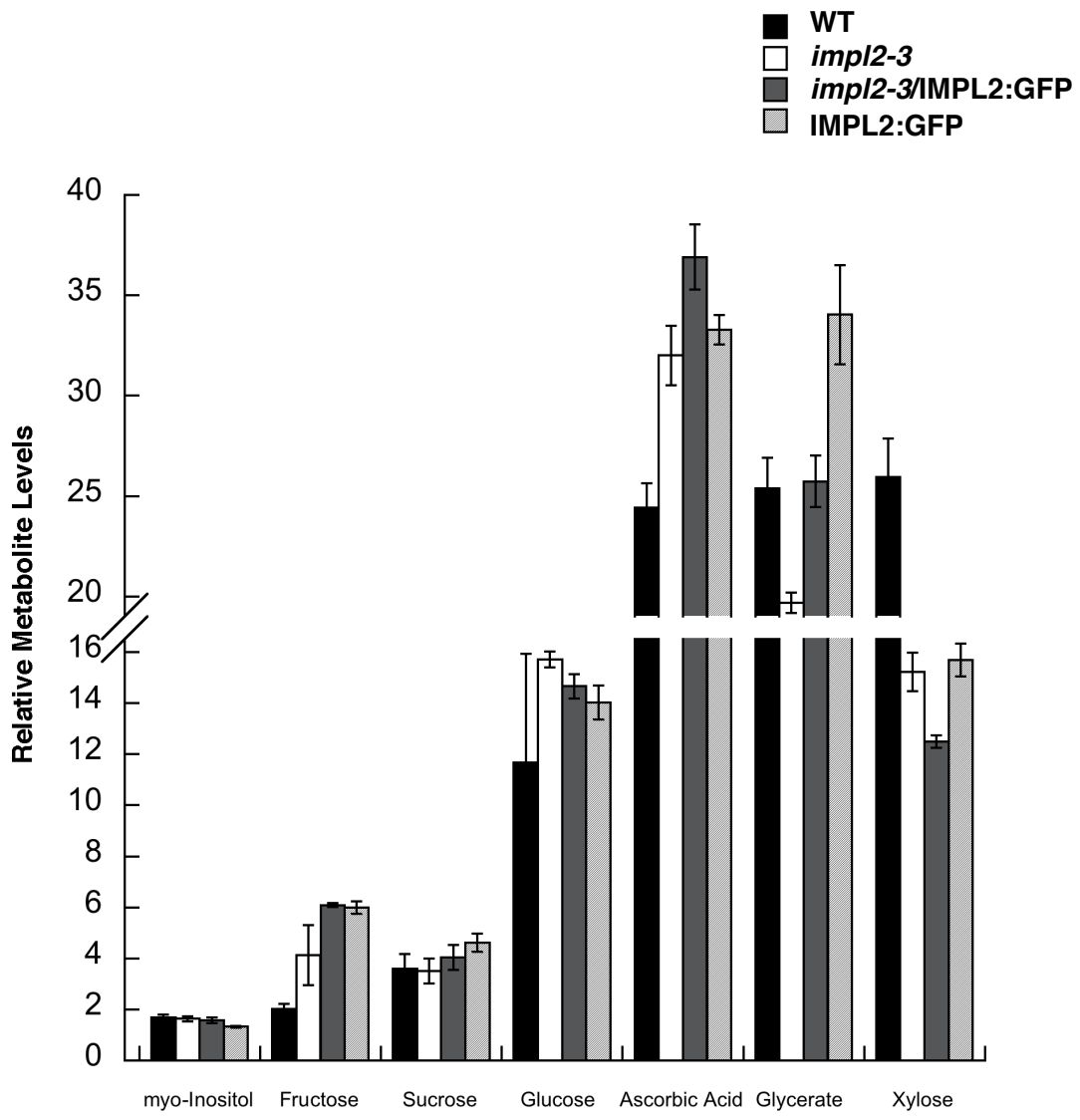

Figure 28. Metabolite Profiling in *impl2-3* Mutants.

Whole tissue of 7-d-old seedlings were extracted as described in Methods and a metabolic profiling using GC-MS was accomplished. Means and SE are presented. Data from three independent biological replicates were averaged.

Metabolite Profiling in IMPL1:GFP Transgenic Plants

In an attempt to generate partial loss-of-function IMPL1 transgenic plants, I obtained an IMPL1 RNAi construct from Open Biosystems; however when Agrobacteria is transformed with this construct it is not able to grow, therefore I was never able to generate transgenic plants. The *Arabidopsis thaliana* amiRNA library has been under development by Dr. Hannon's laboratory at CSHL in collaboration with the Max Planck Institute. Currently, they only have one amiRNA construct available for IMPL1 (Schwab et al., 2006; Schwab et al., 2005).

Due to the lack of additional mutant lines for IMPL1, I used the IMPL1:GFP over-expresser line for an unbiased metabolite profiling analysis performed with GC-MS. The amino acid levels were altered in this line where most amino acids such as glycine, valine, leucine, isoleucine, phenylalanine, serine, tyrosine, threonine, methionine having lower levels than wild-type (Figure 29). In contrast, aspartate and glutamine levels were increased in the IMPL1 over-expressers by 2.5-fold and 1.6-fold, respectively (Figure 29). Since the native function of IMPL1 is still unclear, it is unknown why these amino acid levels are different than in wild-type. However this could indicate that IMPL1 is also functioning as a phosphatase in another amino acid biosynthesis pathway. I have studied the pathways for the other amino acids and I could not find a step that requires a phosphatase that its gene in Arabidopsis is unidentified.

In order to test whether this enzyme might function as an IMP in the chloroplast, inositol, and ascorbic acid levels were measured in the over-expresser lines (Figure 30). There was a slight increase in inositol levels, however statistical analysis revealed this increase as insignificant. However a 1.4-fold increase in ascorbic acid levels are statistically significant as compared to wild-type. These lines also show a slight increase in fructose and glycerate levels, and this may be of importance if IMPL1 native protein has enzymatic preference for fructose 1-phosphate or fructose 1,6-bisphosphate compounds in the chloroplast (Figure 30). While this was not the case with the recombinant protein, IMPL1 was able to dephosphorylate glycerol 2-P and it may be the case that it can also hydrolyze phosphoglycerate compounds.

Due to the fact that recombinant IMPL1 has similar kinetic capabilities towards D-gal 1-P as it does for D-Ins 1-P, I wanted to test whether the IMPL1:GFP over-expresser plants are resistance

to galactose toxicity. Wild-type and IMPL1:GFP plants were grown on 1% and 3% galactose and 1% and 3% glucose as controls and root length was measured in 7-d-old seedlings (Figure 26B). Wild-type and IMPL1:GFP plants were sensitive to high levels of both galactose and glucose and interestingly the over-expresser lines showed higher sensitivity than wild-type. At 3% glucose concentration neither wild-type nor IMPL1:GFP seeds germinated. Together, the preliminary data on IMPL1 suggests that IMPL1 may function as D-Ins 1-P phosphatase in the chloroplast, but most likely it catalyzes some other important reaction in the chloroplast. Generating null or partial loss-of-function mutants for IMPL1 is essential in order to further speculate about the impact of this enzyme on plant growth and development.

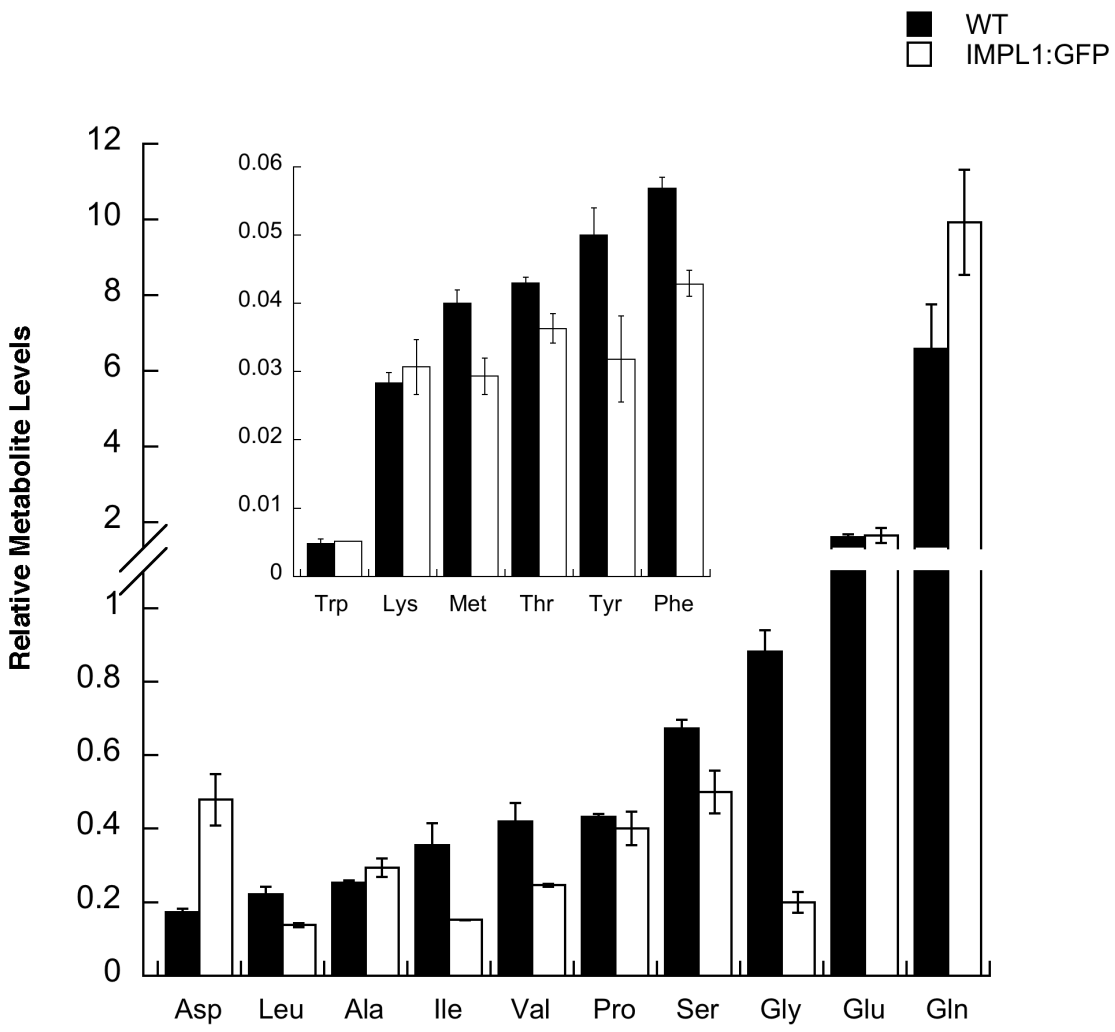

Figure 29. Amino Acid Levels in Wild-type and IMPL1:GFP Plants.

GC-MS was used to measure amino acid levels in 7-d-old seedlings as described in Methods. Amino acids with relevant abundance were graphed together. Data from three independent biological replicates are reported as means ± SE.

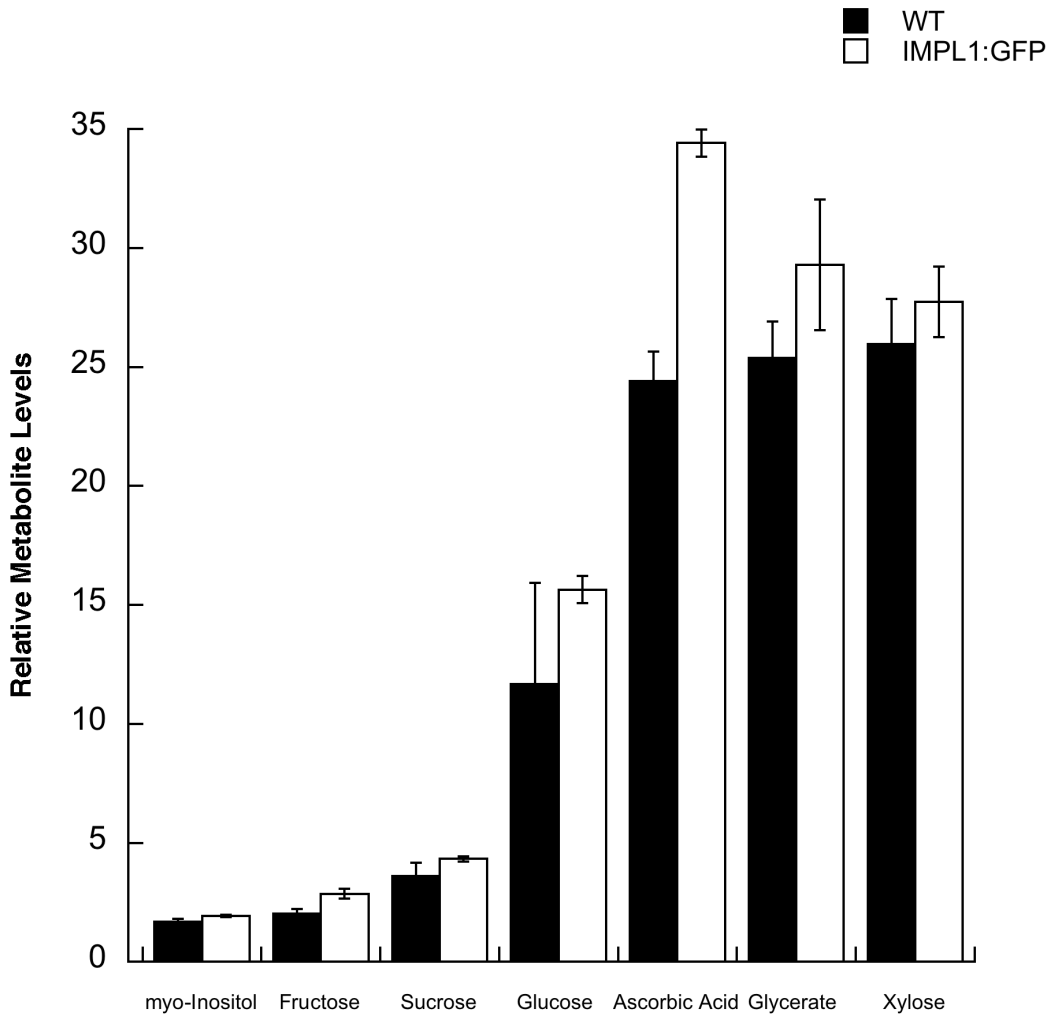

Figure 30. Metabolite Profiling in IMPL1:GFP Overexpression Lines

Whole tissue of 7-d-old seedlings were extracted as described in Methods and a metabolic profiling using GC-MS was accomplished. Means and SE are presented. Data from three independent biological replicates were averaged.

DISSCUSION

The amino acid His is required for plant growth and development. In the late 1990s, the complete pathway for His biosynthesis was elucidated in plants, however the identity of the gene encoding histidinol-P phosphatase was unknown. The probable last missing link in His biosynthesis was identified in the work of Petersen *et al.* (2010), who demonstrated that the IMPL2 gene product is able to rescue the His auxotrophy of a *Streptomyces coelicolor* hisN mutant that lacks histidinol-P phosphatase activity. Furthermore, these authors found that an *impl2*-3 mutant (SAIL_35_A08) is a null mutant that exhibits embryo lethality.

My work on His synthesis has made two fundamental contributions to this field. First, I have shown that the IMPL2 gene encodes an active histidinol-P phosphatase. This is an important contribution as it establishes the biochemical validation of the IMPL2 gene in the His biosynthetic pathway. Secondly, I have used the same *impl2-3* mutant as previously reported (SAIL_35_A08), and have shown that this mutant is capable of producing viable homozygous seed. This allowed me to examine the importance of the IMPL2 gene on plant growth and development. It is important to note that I obtained and characterized two other T-DNA alleles of IMPL2 from the ABRC stock center that I found to be homozygous lethal, thus some IMPL2 null mutants are similar to other classical His biosynthetic mutants in that they are embryo-lethal.

Biochemical Evidence for Histidinol 1-Phosphate Phosphatase Activity

The focus of the Gillaspy lab has been on enzymes functioning in inositol metabolism and signaling, and so the IMP and IMPL gene products have been targets of on-going studies. My collaborators in the lab, Javad Torabinejad and Janet Donahue, previously showed that IMPL1 and IMPL2 partially purified enzymes were unstable, but were able to hydrolyze D-Ins 1-P and L-Gal 1-P *in vitro*, respectively, at very low rates (Torabinejad et al., 2009). They fully characterized IMP activity, and at the time of these studies, the overall understanding implicated IMPL1 and IMPL2 as enzymes involved in the inositol synthesis pathway.

A major goal of my studies was to purify IMPL1 and IMPL2 recombinant proteins and to delineate the substrate specificity of these enzymes. When the genetic data of Peterson et al. strongly suggested that histidinol-P could be the substrate of IMPL2, Dr. Robert White kindly

synthesized this substrate, allowing me to test this substrate. This is an important contribution as no commercial vendor sells histidinol-P, making biochemical examination of histidinol-P phosphatases relatively rare. I found that recombinant AtIMPL2 has a K_m value slightly higher than other monofunctional histidinol-P phosphatases reported previously. In addition, the catalytic efficiency I delineated for AtIMPL2 is much lower than that from histidinol-P phosphatases from unicellular organisms (Lee et al., 2008a; Millay and Houston, 1973). Histidinol-P phosphatase activity was first detected in wheat plant extracts in the 1970s and the K_m value was estimated to be 0.4 mM which is much higher than the K_m value elucidated from my kinetic studies (180 μM). However these authors do indicate that the kinetic analysis revealed that the purified extract contained at least two other phosphatases which may have impacted the derived values (Wiater et al., 1971).

In order to confirm whether IMPL1 also functions as a histidinol-P phosphatase, recombinant IMPL1 protein was tested with histidinol-P, however no activity was detected. This data is in agreement with the genetic complementation of Peterson et al. which showed that IMPL1 is not able to rescue the Actinobacteria *his* auxotroph mutant (Petersen et al., 2010). Thus one key finding from my work is that IMPL2 functions as a histidinol-P phosphatase, but IMPL1 does not. From my kinetic studies, IMPL1 is most likely involved in hydrolyzing D-Ins 1-P and/or D-Gal 1-P. Given the relation between IMP, IMPL1 and IMPL2, the difference in substrate specificity among these highly homologous enzymes suggests that the genes encoding these enzymes have diverged evolutionarily. The evolution of enzymes by divergence impacts how biosynthetic pathways evolve. The "patchwork" hypothesis states that metabolic pathways arise by the recruitment of enzymes with similar activity, and by subsequent modification of their substrate-binding ability (Jensen, 1976). The IMP and IMPL enzymes may support this hypothesis as IMPL2 has most likely altered its substrate binding from an InsP substrate to accommodate a histidinol-P substrate.

Localization and Expression of IMPL1 and IMPL2 Enzymes

His biosynthesis takes place in the chloroplast (Muralla et al., 2007). Thus it is not surprising that IMPL1 and IMPL2 have been localized to the chloroplast, in both transient expression assays (Petersen et al., 2010), and in my work reported here. Through a set of co-localization

experiments I was able to show that both IMPL1 and IMPL2 are located in the same compartment and both also co-localize with a plastid marker. In addition, I was able to show that the initial 77 amino acids at the N-terminus of each protein are sufficient and essential for chloroplastic localization.

Through my transcriptional studies I demonstrated that IMPL2 is expressed throughout plant development in most plant tissues. This data is in agreement with previously reported RNA gel-blot and microarray analyses done on other Arabidopsis HisN genes, suggesting that IMPL2 and the other HisN genes are co-regulated. I was unable to generate transgenic lines expressing IMPL2 promoter:GUS transgenes to study the spatial pattern of expression of IMPL2 within different organs. This type of study could contribute significant knowledge about the demands of His in plant organs and the relationship of His synthesis transport in source and sink tissues. The lack of success of my 3 separate attempts at producing IMPL2 promoter:GUS plants indicates that important control sequences for the IMPL2 promoter are likely located within the exonic and/or intronic regions of the gene.

The Impact of IMPL2 on Histidine Synthesis and Plant Growth

The most common His-starvation phenotype in plants is embryo lethality at the pre-globular stage (Muralla et al., 2007). Therefore, not many homozygous mutant lines are available to study the effects of His on plant development. I report here two different T-DNA alleles for the IMPL2 gene that both exhibit a set of unique phenotypes that are somewhat different from the previously reported His-deficient mutants. I have established that the *impl2-3* and *impl2-4* mutants are not embryo lethal and can produce viable seeds, perhaps due to partial loss-of-function. Two other mutant plants in the His biosynthesis pathway have been described that have exhibited reduced levels of His and were not embryo lethal (Mo et al., 2006a; Noutoshi et al., 2005b). An aerial albino and pale-green seedling phenotype and defective root meristem were evident in *apg10* and *hpa1* mutants, respectively. I have shown that *impl2* mutants have defects in both shoot and root development. To this date no mutation in any of the other His genes have been reported to have both defective root growth and stunted stature in the shoot tissues. Nevertheless, I found that the total, free His levels in *impl2-3* plants are not reduced, and indeed, they are slightly elevated as compared to wild-type plants.

In order to test whether histidinol accumulation was associated with the *impl2* phenotypes I grew *impl2* mutant and wild-type seedlings on different concentrations of histidinol. Higher concentrations of 0.8 to 1 mM histidinol chemically rescued the stunted primary roots of *impl2* mutants, and this concentration did not result in toxicity in wild-type plants. Therefore, I concluded that the defective development in *impl2* mutants is not due to histidinol accumulation.

Importantly, my data suggest that histidinol 1-P accumulates to very high amounts in *impl2-3* mutants. Since, complementation of *impl2-3* with an IMPL2:GFP transgene alleviates the elevated histidinol-P levels but not the His levels, it is possible that the mutant phenotypes are not only due to altered His levels but also due to perturbation in the amounts of intermediates in the His pathway. It is known that His can feedback regulate the expression of the first gene in the His biosynthetic pathway, and my expression analyses indicated that *impl2* mutants contain elevated RNA levels for the HisN1A, N6, and N8 genes. Thus, the probable elevation of histidinol-P in *impl2* mutants can be associated with a dramatic increase in the expression of other HisN genes in the pathway, indicating that alteration in His levels may signal for up-regulation of the His pathway in this mutant.

Previously it has been reported that the promoters of all HisN genes contain the GCN4 promoter element that binds the GCN4 transcription factor that turns on the general control response to amino acid biosynthesis in yeast (Natarajan et al., 2001). Another explanation for the behavior of these mutant lines is that the T-DNA insertion at the beginning of the gene affects the communication of the promoter elements with RNA polymerase and therefore perturbs the regulatory mechanism of the His biosynthesis pathway.

My expression analysis data shows that a full-length transcript with the putative signal peptide is absent from both *impl2* mutant lines, however a truncated transcript that may be capable of directing expression of a cytosolic version of IMPL2 is elevated dramatically. This could indicate that a functional IMPL2 enzyme is produced in *impl2* mutants that lacks the putative chloroplast transit peptide, and is therefore not transported to the correct subcellular compartment. If a cytoplasmic version of IMPL2 is present in *impl2* mutants, it is unclear

whether histidinol-P substrate would ever be available to this enzyme. It is possible that under these conditions, histidinol-P accumulates within the chloroplast and is either transported out slowly, over a period of time, or is hydrolyzed by a non-specific phosphatase within the chloroplast. It is imperative to note that I have looked at the structure of chloroplasts in *impl2* mutants and I was not able to see any difference in the size and structure as compared to those in wild-type plants.

Exploring a Connection Between an Energy Sensor and IMPL2

I began studies to test whether the SnRK1.1 energy sensor could override the defect in *impl2* mutants. The SnRK1.1 energy sensor has been shown to play a critical role in detecting starvation conditions in plants, and in animals it is activated by an intermediate in the purine synthesis pathway (Baena-Gonzalez et al., 2007). I over-expressed a 35S promoter:SnRK1.1:GFP transgene in *impl2* mutants. My preliminary data indicate that SnRK1.1:GFP over-expression may rescue the root and shoot defective phenotypes of *impl2* mutants. SnRK1.1 is a central regulator of carbon source under low nutrient conditions and is an activator of bZIP transcription factors that in turn regulate nitrogen assimilation and amino acid metabolism (Hey et al., 2010; Sugden et al., 1999). Therefore the underlying mechanism for the observed rescue could be due to impaired signaling and regulation of the His biosynthesis that is disrupted due to abnormal accumulation of intermediates in the pathway. Accumulation of histidinol-P in the *impl2-3* mutants will lead to a decrease in His levels that will affect the activity of ATP-PRT through feedback inhibition. It has been shown previously that oat and barley ATP-PRT are sensitive to feedback inhibition by His (Wiater et al., 1971)

In summary, I have shown that IMPL2 functions as a histidinol-P phosphatase *in vitro* and in Arabidopsis, further confirming the identification of the missing step in His biosynthesis pathway by Petersen et al. (2010). My genetic analysis indicates that IMPL2 is a single copy gene that encodes a histidinol-P phosphatase. The fact that IMP or IMPL1 cannot complement the *impl2* mutant shows that IMPL2 has a unique role in plant metabolism.

Function of IMPL1 in the Chloroplast

From my kinetic studies, I can speculate that IMPL1 may be a D-Ins 1-P specific enzyme as it is not active with D-Ins 3-P or L-Gal 1-P. IMPL1 is not similar to IMP in its substrate preference and this could imply that the demands of inositol metabolism in the chloroplast are different than in the cytosol. Perhaps, the *de novo* synthesis pathway of inositol takes place in the cytoplasm where IMP acts upon D-Ins 3-P and inositol is transported to the chloroplast. However, $InsP_3$ may be utilized in the chloroplast for signaling purposes and in this case, IMPL1 could function in the recycling of inositol phosphate signaling metabolites within the chloroplast.

IMPL1 enzyme is also able to catalyze the conversion of D-Gal 1-P to galactose. This activity is shared with the human IMP (Parthasarathy et al., 1997). The physiological relevance for this functionality in plants is unclear. It has been shown that accumulation of D-Gal 1-P inside mammalian and plant cells manifests a toxic affect and the phosphatase activity may be required to break down this compound (Daude et al., 1995; Yamamoto et al., 1988). However, when I grew the IMPL1 over-expresser lines on 1% and 3% galactose, they did not exhibit resistance to D-Gal 1-P.

At the present moment, I cannot speculate any further about the functional role of IMPL1, and generating IMPL1 suppressed or null mutant plants will be indispensible for future functional studies.

CHAPTER III

MATERIALS AND METHODS

Plant Material and Growth Conditions

Arabidopsis thaliana ecotype Columbia plants were maintained in Sunshine Mix #1 soil in a growth room set at 22-24°C. Visible radiation (100 to 140 μmol m^{-2} s^{-1} for 16 h) was provided with fluorescent/incandescent lamps. All soil-grown plants were watered with tap water and twice weekly with added Miracle-Gro Liquid Houseplant Food (8-7-6: 8% total nitrogen, N, 7% available phosphate, P_2O_5, 6% soluble potash, K_2O, 0.1% Iron, Fe; Scotts Miracle-Gro Products, Inc.). Mutant *impl2-3* and *impl2-4* plants were given exogenous His by watering with a 1 mM His solution every other day.

Seedling Root Growth and Seed Germination Assays

Age-matched seeds were used for all assays, which were harvested from plants grown in parallel on the same shelf in a growth chamber. Seeds were harvested on the same day and ripened for 3 weeks at room temperature. For seed germination and root growth assays, seeds were sterilized with 30% Clorox, rinsed, and plated on 0.8% agar plates containing 0.5x MS medium (pH 5.8) and 1% sucrose. As indicated, plates contained His, histidinol, inositol, glutamine, NiCl, galactose and glucose (all from Sigma-Aldrich). Seeds were stratified on plates at 4°C for 3-4 days before germination. A seed was considered as germinated when the radical protruded from the seed coat. Root length was measured on vertical plates. Three plates each of 40 seeds per line were scored in germination assays. Two to three plates with 30 seeds per line were scored for root growth. For germination assays, seeds were plated on medium containing 0 mM or 0.04 mM His and germination was scored over 72 hrs. For root length measurements seeds were plated on 0 mM, 0.01 mM, 0.02 mM, 0.04 mM, 0.4 mM and 0.8 mM His and 0.04 mM Glutamine and 30 mM inositol for controls.

Genomic PCR Analysis of *impl2* Mutants

Mutants were identified from the Sail T-DNA lines (Alonso et al., 2003; Sessions et al., 2002) through the analysis of the SiGnAL database (http://www.signal.salk.edu/cgi-bin/tdnaexpress). Seeds for *impl2-3* (SAIL_146_E09), *impl2-4* (SAIL_35_A08), and the corresponding wild-type plant, CS60000, were obtained from the ABRC at Ohio State University. Genomic DNA from segregating plants was screened by PCR using the primers noted below and then sequenced to verify T-DNA insertion sites. Genomic DNA was isolated from leaves of soil-grown plants using a DNAeasy kit (QIAGEN Inc., Valencia, CA). DNA from segregating plants was screened utilizing the SAIL left border (LB) primer and IMPL2 gene specific primers using annealing temperatures of 53-57°C for amplification (Table 6). For *impl2-3* (SAIL_146_E09), the T-DNA insertions were verified by sequencing both ends of the T-DNA, and were found to consist of two tandem T-DNAs, right border adjoining right border. The insertion site is in Exon 1 after nucleotide #24 from translation start site. Sequencing of the other T-DNA end indicated that several base pairs have been deleted. For *impl2-4*, (SAIL_35_A08), the two tandem T-DNAs, right border adjoining right border, are inserted in Exon 1 at nucleotide #66 from the translation start site.

IMP:GFP, IMPL1:GFP and IMPL2:GFP Construction

IMP/IMPL ORFs without stop codons were amplified by PCR from Arabidopsis CS60000 cDNA with primers noted in Table 6. IMPs were cloned into pENTR/D-TOPO vector (Invitrogen), confirmed by sequencing, and recombined via the Gateway system (Invitrogen) using the manufacturer's protocol into destination vector pK7FWG2 (Karimi et al., 2002). The resulting vectors, IMP:GFP, IMPL1:GFP and IMPL2:GFP contain *Egfp* fused to the 3' end of the cDNAs, under control of the 35S cauliflower mosaic virus promoter, flanked by left border (LB) and right border (RB) and a plant Kanamycin resistance cassette. The constructs were transformed into *Agrobacterium tumefaciens* by cold shock and were used in stable transformation of wild-type plants and *impl2-3* and *impl2-4* mutant plants. Transformation of Arabidopsis was as described (Bechtold et al., 1993).

For IMP:GFP, IMPL1:GFP and IMPL2:GFP, seedlings from two independent homozygous lines were identified on kanamycin screening and GFP production was observed using a Zeiss Axio

imager microscope equipped with fluorescence optics. Also, two independent homozygous complemented lines with detectable GFP expression in the *impl2-3* mutant background with IMPL2:GFP were identified and used in metabolite analyses. Co-localization experiments were performed by stably transforming the IMPL2:GFP homozygous lines with a plastid-mcherry marker that is fused to the signal peptide of Rubisco large subunit (Nelson et al., 2007b). For screening, three day-old seedlings were used for imaging utilizing Axiovision software (Zeiss). Photographs were taken with a Zeiss MC100 camera by using an excitation filter set of 540 to 580 nm for GFP, consisting of a dichroic mirror of 595 nm and a barrier filter of 600 to 660 nm.

The putative signal peptide of IMPL1 (231 bp) and IMPL2 (228 bp) were fused to the N-terminus of eGFP using the previous Gateway cloning method and images were taken as described previously. The genomic DNA sequences of IMPL1 (3954 bp) and IMPL2 (3239 bp) containing the native promoter followed by the exon/intron content was amplified and fused to an HA tag (YPYDVPDYA) using the Gateway technology described above. These HA tagged constructs were recombined into the final destination vector pEarleyGate 301 (Earley et al., 2006) with minor modification. Two homozygous lines were obtained as described above and the accumulation of HA-tagged proteins was confirmed by western blot analysis using HA antibody.

Expression Analyses

RNA was purified using the Qiagen RNeasy kit with DNase treatment from soil grown plants, 3-d-old, and 7-d-old seedlings grown on 0.5x MS/1% sucrose-soaked filter paper under 16 hours of light. Mature seeds, imbibed with water for 3 days at 4°C, were freeze-dried, followed by initial RNA extraction and LiCl precipitation (Vicente-Carbajosa and Carbonero, 2005). cDNA was synthesized from 2 µg of RNA using Bio-Rad iScript cDNA synthesis kit, loaded into 96-well plates containing Sybr Green PCR MasterMix (Applied Biosystems) and primers from IMP, IMPL1, IMPL2 or PEX4 (At5g25760) (Table 6). Reactions in triplicates from three biological replicates were monitored with Applied Biosystems 7300 Real-time PCR instrumentation outfitted with SDS software version 1.3.1. Primers designed to span an intron were optimized: IMP at 60°C, IMPL1 at 60°C, IMPL2 at 60 °C, and PEX4 at 60°C. Calculations involved comparing IMP Ct values with the PEX4 Ct values, because PEX4 (peroxisomal ubiquitin4) was

used as an endogenous control. The normalized values in log form were compared to the wild-type values, and the inverse log was used to determine relative expression levels in IMP genes as compared to wild-type.

Promoter GUS Analysis

Intergenic regions containing promoters for IMP (2000 bp), IMPL1 (2015 bp), IMPL2 (1628bp, 1085bp or 461bp) were amplified from CS60000 genomic DNA by high-fidelity polymerase (Velocity enzyme, BioRad Laboratories, Hercules, CA) with gene-specific primers (IMPpromFor, IMPpromRev, IMPL1promFor, IMPL1promRev, IMPL2promFor, IMPL2promRev, IMPL2shorpromfor, IMPL2longpromfor; Table 6) and cloned into the pENTR/D-TOPO vector (Invitrogen, CA). The resulting clones were recombined into the binary vector pBGWFS7 (Invitrogen, CA) containing a *Egfp:uidA* gene fusion. The gateway recombination was catalyzed by addition of LR clonase according to the manufacture's instructions (Invitrogen, CA). Transgenic plants were generated as described previously. GUS staining of 1- to 19-d-old plants grown on 0.5x MS agar plates with 1% sucrose or of plant tissues from soil-grown plants was as described (Donahue et al. or Styer et al.), and images were taken using Olympus SZX16 microscope with an attached Olympus DP71 camera with DP Controller software (Olympus Corp., Japan).

For the GUS staining procedure, either seedlings or plant tissues from different developmental stages were placed in GUS staining buffer (0.1% Triton X-100, 50 mM phosphate buffer, 0.5 mM $K_4Fe(CN)_6$ x 3 H_2O), 0.5 mM $K_3Fe(CN)_6$, 2 mM 5-bromo-4-chloro-3-indolyl β–D-glucuronide cyclohexamine) and vacuum-infiltrated for 20 min, incubated in the solution overnight at 37°C, and then washed off chlorophyll with 70% ethanol followed by 95% ethanol extractions at 4°C, according to the protocol previously developed (Jefferson, 1987).

Confocal Imaging

GFP fluorescence was detected with a Zeiss LSM510 laser scanning microscope (Carl Zeiss) using excitation with a 488-nm argon laser and a 505- to 550-nm band-pass emission filter. Chlorophyll auto-fluorescence was imaged using excitation with a 543-nm HeNe laser and 560-

nm band-pass emission filter. Slides were examined with a 340 C-Apochromat water immersion objective lens.

Chloroplast Extraction

The chloroplast isolation protocol (VanderVere et al., 1995) was done to improve the sensitivity of IMPL2 protein detection with the IMPL2 antibody. Briefly, plant leaves were cut with a blade and kept on ice until they were emerged in cold homogenization buffer (50 mM HEPES, pH 7.5, 2 mM EDTA, 1 mM $MgCl_2$, 0.3 mM sorbitol) and grinded in a blender. The ground tissue was filtered through Miracloth presoaked with homogenization buffer. The chloroplasts were pelleted by centrifugation at 3500 rpm for 8 min (Sorvall GSA rotor) on a Percoll gradient by layering 40% (v/v) Percoll on 80% Percoll. The chloroplast pellet was layered on top of the Percoll gradient and sediment by centrifugation at 75 rpm for 8 min with the brake off (Sorvall HB4 rotor). The intact chloroplasts were settled in the 40-80 % boundary and were recovered and washed in homogenization buffer. The wash buffer was removed by centrifugation at 3500 rpm for 5 min with the brake on. The chloroplast proteins were precipitated following the methods of Phee *et al.* (Phee et al., 2004). The chloroplasts were lysed in buffer H (10 mM HEPES/KOH, pH 7.9, 4 mM $MgCl_2$, protease inhibitor cocktail (Sigma)) by rocking for 2 hrs at 4°C. The lysate was centrifuged at 10,000 rpm for 20 min. Four volumes of 100% cold acetone were added to the supernatant to precipitate out the soluble chloroplast proteins. The mixture was vortexed and stored at -20°C overnight. The soluble proteins were pelleted by centrifugation at 10,000 rpm for 20 min. BSA protein (10 µg) was added to help visualize the precipitated soluble protein pellets. After the evaporation of acetone, the pellet was solubilized in buffer H and stored at -80°C. The isolated chloroplast proteins were used in western blot analysis in the IMPL2 antibody optimization procedure.

Protein Blot Analyses

Plant tissues were frozen in N_2 (l) and ground into a fine powder using a mortar and pestle. Samples were homogenized in an extraction buffer (50 mM Tris-Cl, pH 7.5, 150 mM NaCl, 5 mM $MgCl_2$, 0.05% Triton X-100, 10% glycerol, 1 mM Dithiothreitol (DTT), and Protease Inhibitor Cocktail for plant extracts, (Sigma-Aldrich)) and centrifuged at 4°C for 2 min at 13.2 k

rpm on a table-top microcentrifuge. The supernatant was kept and quantified by BCA assay (Pierce), and mixed with Laemmle gel loading buffer (100 mM Tris-Cl, pH 6.8, 4% Sodium dodecyl sulfate (SDS), 0.2% bromophenol blue, and 20% glycerol), and boiled for 5 minutes. Proteins were separated on 10% or 12% SDS-PAGE gels and transferred to nitrocellulose using a semi-dry transfer apparatus (Bio-Rad Laboratories, Hercules, CA). The nitrocellulose membranes were incubated in 5% non-fat dry milk in 1x TBST blocking solution for 4 hrs at room temperature. For detection of GFP or HA tags, a 1:5000 dilution of the rabbit anti-GFP (Invitrogen, CA) or anti-HA antibody (Santa Cruz Biotechnology Inc., CA) and for anti-IMPL2, a 1:500 dilution was used. All membranes were probed with a secondary antibody at 1:2500 dilution of goat anti-rabbit horseradish peroxidase-conjugated antibody (Bio-Rad Laboratories, Hercules, CA). All antibody solutions were in 2.5% non-fat dry milk in 1x TBST. Primary antibodies were incubated overnight at 4°C, while secondary antibodies were incubated for 1 hr at room temperature. The nitrocellulose membranes were washed three times for 20 minutes with 1x TBST (50 mM Tris-Cl, pH 7.5, 0.9% [w,v] NaCl, and 0.01 % [v,v] Tween-20) buffer before and after applying secondary antibody. Membranes were illuminated with the Amersham ECL Plus Western Blotting Detection kit (GE Healthcare, UK) and exposed to X-ray film for detecting signal. To ensure equal loading of proteins, Ponceau S staining of the membranes was used.

Gas Chromatography Analysis

Seedlings were grown on filter paper soaked with 0.5x MS, pH 5.8 and 1% sucrose. Extractions and semi-quantitative GC-MS analyses of amino acids and sugar metabolites were performed on three biological replicates as described previously (Collakova et al., 2008; Goyer et al., 2005). Briefly, seedlings and tissues were flash frozen in liquid nitrogen and ground into a powder, lyophilized, weighed (5 mg), disrupted with glass beads and extracted with chloroform: 10 mM HCl 1:1 (v/v). Norvaline and ribitol were added to the aqueous phase as internal standards for amino acid and sugar metabolites, respectively. The samples were vortexed and centrifuged at 13.2 k rpm for 5 minutes. A fifth of the aqueous phase was dried under a stream of nitrogen and derivatives were prepared. Amino acids were derivatized in 50 µl of N-methyl-N-(tert-butyldimethylsilyl)-trifluoroacetamide containing 1% (v/v) tert-butyldimethylchlorosilane (Pierce)/pyridine (1:1 by volume) at 50°C for 1 h. For metabolite profiling, the metabolites were

derivatized in methoxyamine-HCl for 2 hrs at 50°C, and N,O-bis(trimethylsilyl)trifluoroacetamide + 1% trimethylchlorosilane; Alltech) for another 30 min at 50°C. One microliter of derivatized samples was injected with pulsed splitless injector (7683B series injector, Agilent Technologies) and separated on an Agilent 6890 series gas chromatograph equipped with a 30-m DB-5 MS+DG column (0.25mm x 0.25 µm) and analyzed in scan mode using an Agilent 5975C (inert XL MSD with triple-axis detector) series quadrupole mass spectrometer (Agilent Technologies). Agilent enhanced analysis software was used for the analysis of data. Helium was used as the carrier gas with pressure-controlled flow set at 10.3 psi, and a linear velocity of 1.19 ml min^{-1}. The injector port was set at 280°C (300°C for amino acid profiling) with 10.3 psi pressure and a rate flow of 24 ml min^{-1}. The oven gradient was set from 75°C to 320°C at 10°C min^{-1} for metabolite profiling and from 100°C to 300°C at same increments for amino acid profiling. The thermal transfer line to MSD was kept at 250°C. MS was set in a scan mode detecting m/z between 100 to 650 for metabolite profiling and m/z of 50-800 for amino acids.

LC-MS/MS Analysis of Histidine and Histidinol

Approximately 5 mg of lyophilized seedlings and tissue samples were disrupted with glass beads and extracted with chloroform:10 mM HCl 1:1 (v/v) and 40 µM of norvaline was added to the aqueous phase as internal standard. The insoluble chloroform portion was removed by centrifugation. A portion of the (1:5 dilution) supernatant was dried in a speed-vacuum chamber and reconstituted in 200 µl of 65% (0.1% formic acid and water) and 35% acetonitrile. The LC-MS/MS method used for His and histidinol analysis has been described previously and this method with a few modifications was used (Gu et al., 2007). A Tosoh Bioscience, LLC, TSKgel Amide-80 HR, 4.6 x 250 mm, 5 micron column was used. The isocratic gradient 65% A : 35% B at 400 µl per minute for 20 minutes was used. A is LC/MS grade water supplemented with 0.1% formic acid. B is LC/MS grade acetonitrile. Dried samples were dissolved in 200 µl of 65% A: 35% B and 5 µl was injected and gradient was created using an Agilent 1100 Series autosampler and HPLC with attached solvent degasser. Mass spectrometer was an ABSciex 3200 Q Trap. Acquisition method was a multiple reaction monitoring (MRM) method in positive ion mode with both quadrupole 1 and quadrupole 3 operating at unit resolution. Curtain,

nebulizer and turbo gas were 15, 20 and 40, respectively (arbitrary units). Ion spray voltage was 5500, interface heater was on 40°C and source temperature was 320°C. Source used was a Turbo V electrospray source. CAD (collision activated dissociation) gas was set to high (4.5 x 10^{-5} torr). Compound specific voltages and settings are listed in Table 5. Analyst 1.4.2 (ABSciex) was used to collect data, calculate peak areas and generate calibration curves. Areas used for His and histidinol were the sums of the areas for both compound specific MRMs.

Expression of Recombinant Protein

Plasmids containing the genes IMPL1 (at1g31190) and IMPL2 (at4g39120), designated pAtIMPL1H and pAtIMPL2H, respectively, were constructed. Genes were amplified by PCR with primers 5'–ATGGGAAGGTCTCTAATATT-3' (forward) and 5'-TTAAAGCTCTGTATGATAAT-3' (reverse) for IMPL1 and 5'-ATGTTAGCTCAGTCGCACTT-3' (forward) and 5'-TCAATGCCACTCAAGTGACT-3' (reverse) for IMPL2. The template was generated by RT (Omniscript RT kit) of RNA extracted from wild-type plants using the RNAeasy Plant Mini kit (Qiagen) according to the manufacturer's instructions. The resulting PCR product was cloned into plasmid pCRT7/NT-TOPO using the PCR T7 TOPO TA expression kit (Invitrogen).

Plasmids containing the genes IMPL1 (At1g31190) and IMPL2 (at4g39120, truncated at the 5' end, were designated ptIMPL1AE and ptIMPL2AE. The truncation of IMPL1 was accomplished by removing the coding region for the N-terminal 74 amino acids, then replacing the codon for the next amino acid (Gly) with an ATG codon. In a similar fashion, the N-terminal 76 amino acids were removed from IMPL2 by deleting nucleotides and replacing the Glu codon with an ATG codon. The genes were amplified by PCR from pAtIMPL1H and pAtIMPL2H plasmid templates and primer pairs 5'-ATAggatccATGGCTAAAACCACCGGAAC-3' (forward)/ 5'-CGCgaattcTTAAAGCTCTGA- TGATAATC-3' (reverse) and 5'-ATAgattcATGCTTAGCGACACTGAGCTG-3' (forward)/ 5'-GGCgaattcTCAATGCCACTCAAGTG-3' (reverse), respectively (lowercase letters indicate restriction sites). The products were digested with *Bam*HI and *Eco*RI and ligated to digested pGEX2T (GE Healthcare). The plasmids are designed to express truncated proteins fused to a C-terminal glutathione S-transferase. The sequences of the plasmids were verified by sequencing.

Overexpression of IMPL1 and IMPL2 was induced in the host strain pREP4 BL21(DE3)*. A 1.0 L culture with optical density at 600 nm of 0.6, grown in Luria-Bertani medium with 100 µg ml^{-1} ampicillin and 50 µg ml^{-1} kanamycin, was induced with 0.1 mM isopropyl-D-thiogalactopyranoside overnight at room temperature without shaking. Cells were harvested by centrifugation and frozen at 80°C. All subsequent steps were performed at 4°C. Cells were resuspended in 20 ml of lysis buffer (50 mM potassium phosphate, 400 mM NaCl, 100 mM KCl, 10% glycerol) pH 7.8, supplemented with 1 mg ml^{-1} lysozyme, 0.5 mM phenylmethanesulfonyl fluoride, and 1 mM *myo*-inositol. After incubation at 4°C for 35 min, cells were lysed by sonication and Buffer B (1X phosphate-buffered saline, pH 7.3, 1 mM DTT, 0.2% Triton X-100, 56 mM inositol, 5% glycerol) and C (same as Buffer B with 0.1% Triton X-100) were added before centrifugation for 20 min. The clear lysate was incubated for 2 hrs with Pharmacia Glutathione Sephadex (GE Healthcare), washed with 1X phosphate-buffered saline with 0.1% Triton X-100, and then collected in a column. Protein was eluted with 10 mM glutathione in 50 mM Tris-Cl, pH 8.0, and aliquots were frozen at -80°C. Fractions were collected, combined and dialyzed extensively in 50 mM Tri-Cl, pH 7.5, 1 mM $MgCl_2$ and 1 mM DTT. Purified recombinant proteins were frozen in aliquots at -80°C with 10% glycerol. Protein purification and size were estimated by gel fractionation using a 10% SDS-PAGE and pre-stained markers (Bio-Rad).

Preparation of Anti-IMPL2 Antibody

Truncated ptIMPL2AE recombinant protein was washed and dialyzed for use as antigen in antibody production in rabbit (Cocalico Biologicals, Reamstown, PA). The sera from a pre-bleed, a first and a second test bleed were analyzed by Western blot for reactivity to recombinant protein IMPL2:GST, IMPL2:GFP, IMPL2:HA and endogenous IMPL2 protein from plant extracts. The antibody was purified with two different methods. In first method, an affinity column was made by conjugating the ptIMPL2AE recombinant protein, crosslinked onto agarose beads for affinity purification of the antibody using Reactigel (6X) (Pierce). The recombinant protein was extensively dialyzed in coupling buffer (PBS pH 7.2, 100 mM NaCl, 100 mM $NaHCO_3$, pH 9.5) at 4°C. The dialyzed protein was incubated with Reactigel (washed with cold water to removed acetone) for 3 days with gentle rocking at 4°C. The carbodiimidazole moieties

on the beads were quenched by adding 1M Tri-Cl, pH 9, with rocking at room temperature for 2 hours. The beads were washed with l ml 1x PBS 5 times. Using an Gilson Minipuls 2 machine, 1 ml of sera along with 1x PBS was run over column at speed of 2.00 overnight at 4°C. After washes with PBS, the antibody was eluted with 2 ml of 4M $MgCl_2$/1% BSA and dialyzed in PBS overnight at 4°C and stored at -20°C.

In the second method, anti-IMPL2 was purified as described in Harlow and Lane, 1988. Recombinant proteins were transferred to a nitrocellulose membrane for 30 minutes at 15V. The strip of membrane containing only the IMPL2 protein was cut and blocked in 5% non-fat dry milk in 1x TBST (50 mM Tris-HCl, pH 7.5, 0.9% [w,v] NaCl, and 0.01 % [v,v] Tween-20) buffer for 2 hrs at room temperature. The blot was cut into smaller pieces and incubated in 1 ml of anti-sera final bleed and 1 ml of 5% non-fat dry milk in 1x TBST rocking overnight at 4°C. The cut membranes were washed three times for 20 minutes in 1x TBST and incubated with 750 µl of 0.1 M glycine, pH 2.5 for 10 minutes to elute the IMPL2 antibody. Membrane pieces were removed and 75 µl of 1 M Tris, pH 8.5 and 0.1% sodium azide was added, and the antiserum was stored at 4°C. In all protein blot analysis, a 1:500 dilution in 2.5% non-fat dry milk was used for primary antibody probing.

Phosphatase Activity Assays

The L-histidinol 1-phosphate substrate for IMPL2 was synthesized according to previous methods (Fujimoto and Naruse, 1967; Yoshikawa et al., 1967). Phosphatase activity was determined by the inorganic phosphate quantification assay (Lanzetta et al., 1979) with minor modifications. Standard conditions were 50 mM Tris-Cl, pH 7.5, 2 mM $MgCl_2$, 0.4 mM substrate, and 112 ng of purified enzyme in a total reaction volume of 50 µl for IMPL2. Standard conditions were 50 mM Tris, pH 7.5, 2 mM $MgCl_2$, 0.4 mM substrate, and 100 ng, 450 ng of purified enzyme in a total reaction volume of 50 µl for IMPL1 for D-Ins 1P and D-Gal 1P substrates, respectively. For substrate testing and Li^+ and Ca^{2+} inhibition kinetics, 400 ng of IMPL1 was used in 50 mM CAPS, pH 9, 3 mM $MgCl_2$ reaction conditions. For the inhibition studies, 200 ng of IMPL2 was used in 50 mM Tris, pH 7.5, 5 mM $MgCl_2$ reaction conditions. Reactions were performed at room temperature (25°C) for 10 min, after which 800 µl of color

reagent malachite green/ ammonium molybdate solution was added to terminate the reaction. The A_{660} was determined by spectrophotometer. Control reactions without enzyme or without substrate were used to determine background phosphate levels, which were subtracted from experimental values. Enzyme-specific activity units are in μmol of phosphate. Protein concentrations were determined as described by Bradford (1976) with bovine serum albumin as the standard. Data from kinetic experiments were analyzed with Kaleidograph software (version Mac; Synergy Software). Data were fit to the Michaelis-Menten equation $v= V_{max} [S]/ (K_m + [S])$.

Table 5. LC-MS/MS Acquisition Method Parameters.

	Q1 mass (amu)	Q3 mass (amu)	Dwell time (volts)	declustering potential (DP) (volts)	entrance potential (EP) (volts)	collision energy (CE) (volts)	collision cell exit potential (CXP) (volts)	RT (min)
Histidine	156	93	150	26	5	31	4	10.8
Histidine	156	110	150	21	2.5	17	4	10.8
norvaline	118.2	72	150	16	7	13	4	8.8
Histidinol	142.2	124.3	150	21	4	17	4	13.5
Histidinol	142.2	81.1	150	21	4	23	4	13.5

The method for the LC-MS/MS analysis is provided in Chapter III. Materials and Methods.

Table 6. Primers Used for PCR and Quantitative Real-time PCR.

SAIL LB - GCGTGGACCGCTTGCTGCAACT
*l2-3*for - CAGCTCATGGACGAGTTTGGTAAC
*l2-3*rev – CTCACATAGCATGAGAAGGGAG
L1Nterfor - CACC ATG GGA AGG TCT CTA ATA TTC
L1Nterrev - TTT AGC GCC GAT TCT GGG ATA TC
L2Nterfor - CACC ATG TTA GCT CAG TCG CAC
L2Nterrev - CGA AGG AGA CTC GTT GCT TAT G
promL1for - CACC AAC AGG AAC TTT GGA GTC C
promL1rev - TGT TGG TGT CGC CGG AGA ATT TTC
promshortL2for - CACCAAGCTTCCATACGGATG
prommedL2for - CACC TCT CAC GGA CGC ACA CGG
promlongL2for - CACC ATT TCG CCG TGC TCT GTA CTT TGA C
promL2rev - TTT GCT ATG AGT GGG AAG TTC ACG G
HAL1for - CACC AAC AGG AAC TTT GGA GTC C
HAL1rev - AAGCTCTGTATGATAATCTTCCGG
HAL2for - CACC TCT CAC GGA CGC ACA CGG
HAL2rev - ATGCCACTCAAGTGACTCC
promIMPfor - CACC GAG AAG GAG TTG GAT CAC
promIMPrev- TTT CGA GAG AAG ACG AAA AG
L1gfpfor - CACCATGGGAAGGTCTCTAATA

L1gfprev - AAGCTCTGTATGATAATCTTCCGG
L2gfpfor - CACCATGTTAGCTCAGTCGCAC
L2gfprev - ATGCCACTCAAGTGACTCC
IMPgfpfor - CACCATGGCGGACAATGATTCTC
IMPgfprev – TGCCCCTGTAAGCCGCAAC
PEX4for - CTTAACTGCGACTCAGGGAATCTTCTAAG
PEX4rev - TCATCCTTTCTTAGGCATAGCGGC
IMPqRTfor - CAC AAA GGC CAG GTG GAT TTG GTG
IMPqRTrev - CTA TGAA CTT GTG ATT GGG AAA GAG C
L1qRTfor - AAA CCG GCG CTG AGG TGG TTA TGG
L1qRTrev - GCC TCG CTT GCT TTA TCA GTA TC
L2qRTfor - CCGTGAACTTCCCACTCATAGC
L2qRTrev - AGAAGGATTTGCAGACCGCAAC
HisN1qRTfor - GCAATCGATCTTCTCAAGGAC
HisN1qRTrev - ACCAGACTTCAGTGTTTGGTAAC
HisN6AqRTfor - ACCCTTTGAGGTATTGTCTGC
HisN6AqRTrev - GCTTCAAAAACCTCTGGAGGAGG
HisN8qRTfor - ACGCTCCTCGGAAAGGATACG
HisN8qRTrev - ATGCGAGGGCGTGACTCAAAC
L1GSTfor - ATGGGAAGGTCTCTAATATT
L1GSTrev - TTAAAGCTCTGTATGATAAT

L2GSTfor - ATGTTAGCTCAGTCGCACTT
L2GSTrev - TCAATGCCACTCAAGTGACT
tL1GSTfor - ATAggatccATGGCTAAAACCACCGGAAC
tL1GSTrev - CGCgaattcTTAAAGCTCTGA- TGATAATC
tL2GSTfor - ATAgattcATGCTTAGCGACACTGAGCTG
tL2GSTrev – GGCgaattcTCAATGCCACTCAAGTG

CHAPTER IV

SUMMARY AND FUTURE DIRECTIONS

Inositol has many diverse functions within the plant cell; hence the study of its synthetic pathway has been of interest. In order to maintain proper function, the plant cell conserves a free pool of inositol through the *de novo* synthesis pathway and the recycling of phosphoinositide signaling molecules (Gillaspy, 2011). In the past decade, multigene families encoding MIPS and IMP enzymes have been identified in Arabidopsis and microarray data and expression studies have shown the possibility of specialized roles for individual enzyme isoforms. Arabidopsis has one canonical IMP gene and two IMP-like (IMPL) genes that encode proteins closely related to Arabidopsis IMP (29 and 34 % amino acid sequence identity, respectively). A substantial amount of work has been performed on plant IMP enzymes, which has demonstrated that IMP is a bifunctional enzyme that is involved in both inositol and ascorbic acid biosynthesis pathways (Conklin et al., 2000; Torabinejad et al., 2009). To gain more understanding of the function of IMPL enzymes in Arabidopsis, I performed the following studies: examined the transcript levels of IMP, IMPL1 and IMPL2 genes and studied the spatial and temporal pattern of expression of IMP and IMPL1 genes, determined the subcellular location of IMP and IMPLs, kinetically characterized IMPL1 and IMPL2 enzymes, identified and studied the alteration in an IMPL2 loss-of-function mutant.

My most significant contribution is that I have shown that plastid- and chloroplast-localized IMPL2 functions as a histidinol-P phosphatase in the next to last step in the His biosynthesis pathway. I have shown that recombinant IMPL2 protein hydrolyzes histidinol-P, but not any of the inositol phosphate compounds tested. Interestingly, although IMPL1 is similar to IMPL2 at the amino acid level, my biochemical studies on IMPL1 showed that IMPL1 does not contain histidinol-P phosphatase activity. *In vitro*, IMPL1 displays substrate preference for D-Ins 1-P, which is the breakdown product of the $InsP_3$ signaling molecule. As IMPL1 is also located in the chloroplast, it is intriguing to speculate that IMPL1 is involved in the recycling of InsPs within this organelle. This remains unclear at the moment, as the role of $InsP_3$ signaling in chloroplasts has not been studied to date.

An important aspect of my work has been the characterization of a novel *impl2* mutant line that exhibits phenotypes that have not been described in previously isolated His mutants. I was able to show that exogenous His and a closely related compound, histidinol, rescue the phenotypes of the *impl2* mutant, confirming the role of IMPL2 in His biosynthesis. These *impl2* mutants do not contain a significant decline in His levels as expected, and in fact contain slightly higher than wild-type levels of His. My metabolite analyses indicate the likelihood that a histidinol-P increase is occurring in these mutants and may be the determining factor in causing the phenotypes noted. The two other nonlethal His deficient mutants from Arabidopsis, *apg10* and *hpa1*, also do not have a drastic reduction in His levels. Thus for all three of these mutants the mechanism behind the defective plant growth and development may be more complex than expected (Mo et al., 2006a; Noutoshi et al., 2005b).

In order to further delineate how His synthesis impacts plant growth and development, I would study the intermediate metabolite levels in the His pathway and the connection between His precursors and purine synthesis. My rationale for this is that despite the impact of *apg10*, *hpa1* and *impl2-3* on plant development, these three different mutants do not contain greatly altered His levels as compared to wild-type as expected. This strongly suggests that a similar or closely related regulatory mechanism is impaired in all three mutant plants. Although the regulation of the His operon has been extensively studied in microorganisms, the regulatory mechanisms involved in His synthesis is not known in plants (Stepansky and Leustek, 2006). These three mutant plants are excellent models to use to further investigate the role of the end product His and His pathway intermediates, some of which are required for the purine synthesis pathway.

REFERENCES

Alifano, P., Fani, R., Lio, P., Lazcano, A., Bazzicalupo, M., Carlomagno, M.S., and Bruni, C.B. (1996). Histidine biosynthetic pathway and genes: structure, regulation, and evolution. Microbiol Rev *60*, 44-69.

Alonso, J.M., Stepanova, A.N., Leisse, T.J., Kim, C.J., Chen, H., Shinn, P., Stevenson, D.K., Zimmerman, J., Barajas, P., Cheuk, R.*, et al.* (2003). Genome-wide insertional mutagenesis of Arabidopsis thaliana. Science *301*, 653-657.

Ames, B.N., Garry, B., and Herzenberg, L.A. (1960). The genetic control of the enzymes of histidine biosynthesis in Salmonella typhimurium. J Gen Microbiol *22*, 369-378.

Ames, B.N., Martin, R.G., and Garry, B.J. (1961). The first step of histidine biosynthesis. J Biol Chem *236*, 2019-2026.

Astle, M.V., Horan, K.A., Ooms, L.M., and Mitchell, C.A. (2007). The inositol polyphosphate 5-phosphatases: traffic controllers, waistline watchers and tumour suppressors? Biochem Soc Symp, 161-181.

Baena-Gonzalez, E., Rolland, F., Thevelein, J.M., and Sheen, J. (2007). A central integrator of transcription networks in plant stress and energy signalling. Nature *448*, 938-942.

Bechtold, N., Ellis, J., and Pelletier, G. (1993). In planta Agrobacterium mediated gene transfer by infiltration of adult *Arabidopsis thaliana* plants. Comptes Rendus De L'academic Des Sciences Serie Iii Sciences De La Vie *316*, 1194-1199.

Berdy, S., Kudla, J., Gruissem, W., and Gillaspy, G. (2001). Molecular characterization of *At*5PTase1, an inositol phosphatase capable of terminating IP_3 signaling. Plant Physiol *126*, 801-810.

Berridge, M.J. (1993). Inositol trisphosphate and calcium signaling. Nature *361*, 315-325.

Bradford, G.R. (1963). Lithium Survey fo California's Water Resources. Soil Science *96*, 77-81.

Busa, W., and Gimlich, R. (1989). Lithium-induced teratogenesis in frog embryos prevented by a polyphosphoinositide cycle intermediate or a diacylglycerol analog. Dev Biol *132*, 315-324.

Chang, S.F., Ng, D., Baird, L., and Georgopoulos, C. (1991). Analysis of an Escherichia coli dnaB temperature-sensitive insertion mutation and its cold-sensitive extragenic suppressor. J Biol Chem *266*, 3654-3660.

Chen, I.W., and Charalampous, C.F. (1966). Biochemical studies on D-Inositol 1-phosphate as an intermediate in the biosynthesis of inositol from glucose-6-phosphate, and characteristics of two reactions in this biosynthesis. J Biol Chem *241*, 2194-2199.

Collakova, E., Goyer, A., Naponelli, V., Krassovskaya, I., Gregory, J.F., 3rd, Hanson, A.D., and Shachar-Hill, Y. (2008). Arabidopsis 10-formyl tetrahydrofolate deformylases are essential for photorespiration. Plant Cell *20*, 1818-1832.

Conklin, P.L., Saracco, S.A., Norris, S.R., and Last, R.L. (2000). Identification of ascorbic acid-deficient Arabidopsis thaliana mutants. Genetics *154*, 847-856.

Daude, N., Gallaher, T.K., Zeschnigk, M., Starzinski-Powitz, A., Petry, K.G., Haworth, I.S., and Reichardt, J.K. (1995). Molecular cloning, characterization, and mapping of a full-length cDNA encoding human UDP-galactose 4'-epimerase. Biochem Mol Med *56*, 1-7.

Delorme, C., Ehrlich, S.D., and Renault, P. (1992). Histidine biosynthesis genes in Lactococcus lactis subsp. lactis. J Bacteriol *174*, 6571-6579.

Dunn, T.M., Lynch, D.V., Michaelson, L.V., and Napier, J.A. (2004). A post-genomic approach to understanding sphingolipid metabolism in Arabidopsis thaliana. Ann Bot (Lond) *93*, 483-497.

Earley, K.W., Haag, J.R., Pontes, O., Opper, K., Juehne, T., Song, K., and Pikaard, C.S. (2006). Gateway-compatible vectors for plant functional genomics and proteomics. Plant J *45*, 616-629.
Eisenberg, F.J. (1967). D-myoinositol 1-phosphate as product of cyclization of glucose 6-phosphate and substrate for a specific phosphatase in rat testis. J Biol Chem *242*, 1375-1382.
El Malki, F., Frankard, V., and Jacobs, M. (1998). Molecular cloning and expression of a cDNA sequence encoding histidinol phosphate aminotransferase from Nicotiana tabacum. Plant Mol Biol *37*, 1013-1022.
Erneux, C., Govaerts, C., Communi, D., and Pesesse, X. (1998). The diversity and possible functions of the inositol 5-polyphosphatases. Biochim Biophys Acta *1436*, 185-199.
Fani, R., Brilli, M., Fondi, M., and Lio, P. (2007). The role of gene fusions in the evolution of metabolic pathways: the histidine biosynthesis case. BMC Evol Biol *7 Suppl 2*, S4.
Fujimori, K., and Ohta, D. (1998). Isolation and characterization of a histidine biosynthetic gene in Arabidopsis encoding a polypeptide with two separate domains for phosphoribosyl-ATP pyrophosphohydrolase and phosphoribosyl-AMP cyclohydrolase. Plant physiology *118*, 275-283.
Fujimoto, Y., and Naruse, M. (1967). [Synthesis of nucleotides. 3. Selective phosphorylation of ribonucleoside with phosphorus oxychloride]. Yakugaku Zasshi *87*, 270-274.
Gillaspy, G.E. (2011). The cellular language of myo-inositol signaling. New Phytol *192*, 823-839.
Gillaspy, G.E., Keddie, J.S., Oda, K., and Gruissem, W. (1995). Plant inositol monophosphatase is a lithium-sensitive enzyme encoded by a multigene family. Plant Cell *7*, 2175-2185.
Goyer, A., Collakova, E., Diaz de la Garza, R., Quinlivan, E.P., Williamson, J., Gregory, J.F., 3rd, Shachar-Hill, Y., and Hanson, A.D. (2005). 5-Formyltetrahydrofolate is an inhibitory but well tolerated metabolite in Arabidopsis leaves. J Biol Chem *280*, 26137-26142.
Gu, L., Jones, A.D., and Last, R.L. (2007). LC-MS/MS assay for protein amino acids and metabolically related compounds for large-scale screening of metabolic phenotypes. Anal Chem *79*, 8067-8075.
Gumber, S.C., Loewus, M.W., and Loewus, F.A. (1984). Further Studies on myo-Inositol-1-phosphatase from the Pollen of Lilium longiflorum Thunb. Plant Physiol *76*, 40-44.
Guyer, D., Patton, D., and Ward, E. (1995a). Evidence for cross-pathway regulation of metabolic gene expression in plants. Proc Natl Acad Sci U S A *92*, 4997-5000.
Guyer, D., Patton, D., and Ward, E. (1995b). Evidence for cross-pathway regulation of metabolic gene expression in plants. Proc Natl Acad Sci U S A *92*, 4997-5000.
Gy, I., Gasciolli, V., Lauressergues, D., Morel, J.B., Gombert, J., Proux, F., Proux, C., Vaucheret, H., and Mallory, A.C. (2007). Arabidopsis FIERY1, XRN2, and XRN3 are endogenous RNA silencing suppressors. Plant Cell *19*, 3451-3461.
Hallcher, L.M., and Sherman, W.R. (1980). The effects of lithium ion and other agents on the activity of *myo*-inositol 1-phosphatase from bovine brain. J Biol Chem *255*, 10896-10901.
Heckman, D.S., Geiser, D.M., Eidell, B.R., Stauffer, R.L., Kardos, N.L., and Hedges, S.B. (2001). Molecular evidence for the early colonization of land by fungi and plants. Science *293*, 1129-1133.
Heldt, W.H., Werdan, K., Milovancev, M., and Geller, G. (1973). Alkalization of the chloroplast stroma caused by light-dependent proton flux into the thylakoid space. Biochim Biophys Acta *314*, 224-241.
Hey, S.J., Byrne, E., and Halford, N.G. (2010). The interface between metabolic and stress signalling. Ann Bot *105*, 197-203.

Hinshelwood, S., and Stoker, N.G. (1992). Cloning of mycobacterial histidine synthesis genes by complementation of a Mycobacterium smegmatis auxotroph. Mol Microbiol *6*, 2887-2895.
Inada, T., and Nakamura, Y. (1995). Lethal double-stranded RNA processing activity of ribonuclease III in the absence of suhB protein of Escherichia coli. Biochimie *77*, 294-302.
Inada, T., and Nakamura, Y. (1996). Autogenous control of the suhB gene expression of Escherichia coli. Biochimie *78*, 209-212.
Ingle, R.A. (2011). Histidine biosynthesis. Arabidopsis Book *9*, e0141.
Ingle, R.A., Mugford, S.T., Rees, J.D., Campbell, M.M., and Smith, J.A. (2005). Constitutively high expression of the histidine biosynthetic pathway contributes to nickel tolerance in hyperaccumulator plants. Plant Cell *17*, 2089-2106.
Ishijima, S., Uchibori, A., Takagi, H., Maki, R., and Ohnishi, M. (2003). Light-induced increase in free Mg2+ concentration in spinach chloroplasts: measurement of free Mg2+ by using a fluorescent probe and necessity of stromal alkalinization. Arch Biochem Biophys *412*, 126-132.
Islas-Flores, I., and Villanueva, M.A. (2007). Inositol-1 (or 4)-monophosphatase from Glycine max embryo axes is a phosphatase with broad substrate specificity that includes phytate dephosphorylation. Biochim Biophys Acta *1770*, 543-550.
Jackson, E.N., and Yanofsky, C. (1973). Thr region between the operator and first structural gene of the tryptophan operon of Escherichia coli may have a regulatory function. J Mol Biol *76*, 89-101.
Jefferson, R.A. (1987). Assaying chimereic genes in plants: The GUS fusion system. Plant Mol Biol Rep *5*, 387-405.
Jensen, R.A. (1976). Enzyme recruitment in evolution of new function. Annu Rev Microbiol *30*, 409-425.
Kao, K.R., Masiu, R.P., and Elinson, R. (1986). Respecification of pattern in *Xenopus laevis* embryos-A novel effect of lithium. Nature *322*, 371-373.
Karimi, M., Inze, D., and Depicker, A. (2002). GATEWAY vectors for Agrobacterium-mediated plant transformation. Trends Plant Sci *7*, 193-195.
Laing, W.A., Bulley, S., Wright, M., Cooney, J., Jensen, D., Barraclough, D., and MacRae, E. (2004). A highly specific L-galactose-1-phosphate phosphatase on the path to ascorbate biosynthesis. Proc Natl Acad Sci U S A *101*, 16976-16981.
Lanzetta, P.A., Alvarez, L.J., Reinach, P.S., and Candia, O.A. (1979). An improved assay for nanomole amounts of inorganic phosphate. Anal Biochem *100*, 95-97.
le Coq, D., Fillinger, S., and Aymerich, S. (1999). Histidinol phosphate phosphatase, catalyzing the penultimate step of the histidine biosynthesis pathway, is encoded by ytvP (hisJ) in Bacillus subtilis. J Bacteriol *181*, 3277-3280.
Lee, H.S., Cho, Y., Lee, J.H., and Kang, S.G. (2008a). Novel monofunctional histidinol-phosphate phosphatase of the DDDD superfamily of phosphohydrolases. J Bacteriol *190*, 2629-2632.
Lee, H.S., Cho, Y., Lee, J.H., and Kang, S.G. (2008b). Novel monofunctional histidinol-phosphate phosphatase of the DDDD superfamily of phosphohydrolases. J Bacteriol *190*, 2629-2632.
Leech, A.P., Baker, G.R., Shute, J.K., Cohen, M.A., and Gani, D. (1993). Chemical and kinetic mechanism of the inositol monophosphatase reaction and its inhibition by Li+. Eur J Biochem *212*, 693-704.
Lescot, M., Dehais, P., Thijs, G., Marchal, K., Moreau, Y., Van de Peer, Y., Rouze, P., and Rombauts, S. (2002). PlantCARE, a database of plant cis-acting regulatory elements and a portal to tools for in silico analysis of promoter sequences. Nucleic Acids Res *30*, 325-327.

Limauro, D., Avitabile, A., Cappellano, C., Puglia, A.M., and Bruni, C.B. (1990). Cloning and characterization of the histidine biosynthetic gene cluster of Streptomyces coelicolor A3(2). Gene *90*, 31-41.

Loertscher, R., and Lavery, P. (2002). The role of glycosyl phosphatidyl inositol (GPI)-anchored cell surface proteins in T-cell activation. Transpl Immunol *9*, 93-96.

Loewus, F.A., and Murthy, P.P.N. (2000). *Myo*-Inositol Metabolism in Plants. Plant Sci *150*, 1-19.

Majerus, P.W., Kisseleva, M.V., and Norris, F.A. (1999). The role of phosphatases in inositol signaling reactions. J Biol Chem *274*, 10669-10672.

Marineo, S., Cusimano, M.G., Limauro, D., Coticchio, G., and Puglia, A.M. (2008). The histidinol phosphate phosphatase involved in histidine biosynthetic pathway is encoded by SCO5208 (hisN) in Streptomyces coelicolor A3(2). Curr Microbiol *56*, 6-13.

Maslanski, J.A., Leshko, L., and Busa, W.B. (1992). Lithium-sensitive production of inositol phosphates during amphibian embryonic mesoderm induction. Science *256*, 243-245.

Matsuhisa, A., Suzuki, N., Noda, T., and Shiba, K. (1995). Inositol monophosphatase activity from the Escherichia coli suhB gene product. J Bacteriol *177*, 200-205.

Millay, R.H., Jr., and Houston, L.L. (1973). Purification and properties of yeast histidinol phosphate phosphatase. Biochemistry *12*, 2591-2596.

Mo, X., Zhu, Q., Li, X., Li, J., Zeng, Q., Rong, H., Zhang, H., and Wu, P. (2006a). The hpa1 mutant of Arabidopsis reveals a crucial role of histidine homeostasis in root meristem maintenance. Plant physiology *141*, 1425-1435.

Mo, X., Zhu, Q., Li, X., Li, J., Zeng, Q., Rong, H., Zhang, H., and Wu, P. (2006b). The hpa1 mutant of Arabidopsis reveals a crucial role of histidine homeostasis in root meristem maintenance. Plant Physiol *141*, 1425-1435.

Moore, G.J., Bebchuk, J.M., Parrish, J.K., Faulk, M.W., Arfken, C.L., Strahl-Bevacqua, J., and Manji, H.K. (1999). Temporal dissociation between lithium-induced changes in frontal lobe myo-inositol and clinical response in manic-depressive illness. Am J Psychiatry *156*, 1902-1908.

Moore, R.C., and Purugganan, M.D. (2003). The early stages of duplicate gene evolution. Proc Natl Acad Sci U S A *100*, 15682-15687.

Mori, I., Fonne-Pfister, R., Matsunaga, S., Tada, S., Kimura, Y., Iwasaki, G., Mano, J., Hatano, M., Nakano, T., Koizumi, S.*, et al.* (1995). A Novel Class of Herbicides (Specific Inhibitors of Imidazoleglycerol Phosphate Dehydratase). Plant Physiol *107*, 719-723.

Mormann, S., Lomker, A., Ruckert, C., Gaigalat, L., Tauch, A., Puhler, A., and Kalinowski, J. (2006). Random mutagenesis in Corynebacterium glutamicum ATCC 13032 using an IS6100-based transposon vector identified the last unknown gene in the histidine biosynthesis pathway. BMC Genomics *7*, 205.

Muralla, R., Sweeney, C., Stepansky, A., Leustek, T., and Meinke, D. (2007). Genetic dissection of histidine biosynthesis in Arabidopsis. Plant Physiol *144*, 890-903.

Murguia, J.R., Belles, J.M., and Serrano, R. (1996). The yeast HAL2 nucleotidase is an in vivo target of salt toxicity. J Biol Chem *271*, 29029-29033.

Natarajan, K., Jackson, B.M., Zhou, H., Winston, F., and Hinnebusch, A.G. (1999). Transcriptional activation by Gcn4p involves independent interactions with the SWI/SNF complex and the SRB/mediator. Mol Cell *4*, 657-664.

Natarajan, K., Meyer, M.R., Jackson, B.M., Slade, D., Roberts, C., Hinnebusch, A.G., and Marton, M.J. (2001). Transcriptional profiling shows that Gcn4p is a master regulator of gene expression during amino acid starvation in yeast. Mol Cell Biol *21*, 4347-4368.

Nelson, B.K., Cai, X., and Nebenfuhr, A. (2007a). A multicolored set of in vivo organelle markers for co-localization studies in Arabidopsis and other plants. Plant J *51*, 1126-1136.
Nelson, B.K., Cai, X., and Nebenfuhr, A. (2007b). A multicolored set of in vivo organelle markers for co-localization studies in Arabidopsis and other plants. Plant J *51*, 1126-1136.
Nelson, D.E., Rammesmayer, G., and Bohnert, H.J. (1998). Regulation of cell-specific inositol metabolism and transport in plant salinity tolerance. Plant Cell *10*, 753-764.
Neuwald, A.F., Krishnan, B.R., Brikun, I., Kulakauskas, S., Suziedelis, K., Tomcsanyi, T., Leyh, T.S., and Berg, D.E. (1992). cysQ, a gene needed for cysteine synthesis in Escherichia coli K-12 only during aerobic growth. J Bacteriol *174*, 415-425.
Neuwald, A.F., York, J.D., and Majerus, P.W. (1991). Diverse proteins homologous to inositol monophosphatase. FEBS Lett *294*, 16-18.
Noutoshi, Y., Ito, T., and Shinozaki, K. (2005a). ALBINO AND PALE GREEN 10 encodes BBMII isomerase involved in histidine biosynthesis in Arabidopsis thaliana. Plant Cell Physiol *46*, 1165-1172.
Noutoshi, Y., Ito, T., and Shinozaki, K. (2005b). ALBINO AND PALE GREEN 10 encodes BBMII isomerase involved in histidine biosynthesis in Arabidopsis thaliana. Plant Cell Physiol *46*, 1165-1172.
Odorizzi, G., Babst, M., and Emr, S.D. (2000). Phosphoinositide signaling and the regulation of membrane trafficking in yeast. Trends Biochem Sci *25*, 229-235.
Ohta, D., Fujimori, K., Mizutani, M., Nakayama, Y., Kunpaisal-Hashimoto, R., Munzer, S., and Kozaki, A. (2000). Molecular cloning and characterization of ATP-phosphoribosyl transferase from Arabidopsis, a key enzyme in the histidine biosynthetic pathway. Plant physiology *122*, 907-914.
Parthasarathy, R., Parthasarathy, L., and Vadnal, R. (1997). Brain inositol monophosphatase identified as a galactose 1-phosphatase. Brain Res *778*, 99-106.
Payrastre, B., Missy, K., Giuriato, S., Bodin, S., Plantavid, M., and Gratacap, M. (2001). Phosphoinositides: key players in cell signalling, in time and space. Cell Signal *13*, 377-387.
Petersen, L.N., Marineo, S., Mandala, S., Davids, F., Sewell, B.T., and Ingle, R.A. (2010). The missing link in plant histidine biosynthesis: Arabidopsis myoinositol monophosphatase-like2 encodes a functional histidinol-phosphate phosphatase. Plant physiology *152*, 1186-1196.
Phee, B.K., Cho, J.H., Park, S., Jung, J.H., Lee, Y.H., Jeon, J.S., Bhoo, S.H., and Hahn, T.R. (2004). Proteomic analysis of the response of Arabidopsis chloroplast proteins to high light stress. Proteomics *4*, 3560-3568.
Quintero, F.J., Garciadeblas, B., and Rodriguez-Navarro, A. (1996). The SAL1 gene of Arabidopsis, encoding an enzyme with 3'(2'),5'-bisphosphate nucleotidase and inositol polyphosphatase 1-phosphatase activities, increases salt tolerane in yeast. Plant Cell *8*, 529-537.
Rangarajan, E.S., Proteau, A., Wagner, J., Hung, M.N., Matte, A., and Cygler, M. (2006a). Structural snapshots of Escherichia coli histidinol phosphate phosphatase along the reaction pathway. J Biol Chem *281*, 37930-37941.
Rangarajan, E.S., Proteau, A., Wagner, J., Hung, M.N., Matte, A., and Cygler, M. (2006b). Structural snapshots of Escherichia coli histidinol phosphate phosphatase along the reaction pathway. J Biol Chem *281*, 37930-37941.
Rees, J.D., Ingle, R.A., and Smith, J.A. (2009). Relative contributions of nine genes in the pathway of histidine biosynthesis to the control of free histidine concentrations in Arabidopsis thaliana. Plant Biotechnol J *7*, 499-511.
Roth, J.R., and Ames, B.N. (1966). Histidine regulatory mutants in Salmonella typhimurium II. Histidine regulatory mutants having altered histidyl-tRNA synthetase. J Mol Biol *22*, 325-333.

Roth, J.R., Silbert, D.F., Fink, G.R., Voll, M.J., Anton, D., Hartman, P.E., and Ames, B.N. (1966). Transfer RNA and the control of the histidine operon. Cold Spring Harb Symp Quant Biol *31*, 383-392.

Saiardi, A., Resnick, A.C., Snowman, A.M., Wendland, B., and Snyder, S.H. (2005). Inositol pyrophosphates regulate cell death and telomere length through phosphoinositide 3-kinase-related protein kinases. Proc Natl Acad Sci U S A *102*, 1911-1914.

Schwab, R., Ossowski, S., Riester, M., Warthmann, N., and Weigel, D. (2006). Highly specific gene silencing by artificial microRNAs in Arabidopsis. Plant Cell *18*, 1121-1133.

Schwab, R., Palatnik, J.F., Riester, M., Schommer, C., Schmid, M., and Weigel, D. (2005). Specific effects of microRNAs on the plant transcriptome. Dev Cell *8*, 517-527.

Seeds, A.M., and York, J.D. (2007). Inositol polyphosphate kinases: regulators of nuclear function. Biochem Soc Symp, 183-197.

Sessions, A., Burke, E., Presting, G., Aux, G., McElver, J., Patton, D., Dietrich, B., Ho, P., Bacwaden, J., Ko, C.*, et al.* (2002). A high-throughput Arabidopsis reverse genetics system. Plant Cell *14*, 2985-2994.

Shaldubina, A., Ju, S., Vaden, D.L., Ding, D., Belmaker, R.H., and Greenberg, M.L. (2002). Epi-inositol regulates expression of the yeast INO1 gene encoding inositol-1-P synthase. Mol Psychiatry *7*, 174-180.

Sheard, L.B., Tan, X., Mao, H., Withers, J., Ben-Nissan, G., Hinds, T.R., Kobayashi, Y., Hsu, F.F., Sharon, M., Browse, J.*, et al.* (2010). Jasmonate perception by inositol-phosphate-potentiated COI1-JAZ co-receptor. Nature *468*, 400-405.

Shen, X., Xiao, H., Ranallo, R., Wu, W.H., and Wu, C. (2003). Modulation of ATP-dependent chromatin-remodeling complexes by inositol polyphosphates. Science *299*, 112-114.

Sims, K.J., Spassieva, S.D., Voit, E.O., and Obeid, L.M. (2004). Yeast sphingolipid metabolism: clues and connections. Biochem Cell Biol *82*, 45-61.

Spiegelberg, B.D., Xiong, J.P., Smith, J.J., Gu, R.F., and York, J.D. (1999). Cloning and characterization of a mammalian lithium-sensitive bisphosphate 3'-nucleotidase inhibited by inositol 1,4-bisphosphate. J Biol Chem *274*, 13619-13628.

Stepansky, A., and Leustek, T. (2006). Histidine biosynthesis in plants. Amino Acids *30*, 127-142.

Sugden, C., Donaghy, P.G., Halford, N.G., and Hardie, D.G. (1999). Two SNF1-related protein kinases from spinach leaf phosphorylate and inactivate 3-hydroxy-3-methylglutaryl-coenzyme A reductase, nitrate reductase, and sucrose phosphate synthase in vitro. Plant physiology *120*, 257-274.

Sun, Q., Zybailov, B., Majeran, W., Friso, G., Olinares, P.D., and van Wijk, K.J. (2009). PPDB, the Plant Proteomics Database at Cornell. Nucleic Acids Res *37*, D969-974.

Suzuki, M., Tanaka, K., Kuwano, M., and Yoshida, K.T. (2007). Expression pattern of inositol phosphate-related enzymes in rice (Oryza sativa L.): implications for the phytic acid biosynthetic pathway. Gene *405*, 55-64.

Tada, S., Volrath, S., Guyer, D., Scheidegger, A., Ryals, J., Ohta, D., and Ward, E. (1994). Isolation and characterization of cDNAs encoding imidazoleglycerolphosphate dehydratase from Arabidopsis thaliana. Plant physiology *105*, 579-583.

Tan, X., Calderon-Villalobos, L.I., Sharon, M., Zheng, C., Robinson, C.V., Estelle, M., and Zheng, N. (2007). Mechanism of auxin perception by the TIR1 ubiquitin ligase. Nature *446*, 640-645.

Tolias, K.F., and Cantley, L.C. (1999). Pathways for phosphoinositide synthesis. Chem Phys Lipids *98*, 69-77.

Torabinejad, J., Donahue, J.L., Gunesekera, B.N., Allen-Daniels, M.J., and Gillaspy, G.E. (2009). VTC4 is a bifunctional enzyme that affects myoinositol and ascorbate biosynthesis in plants. Plant Physiol *150*, 951-961.
Torabinejad, J., and Gillaspy, G.E. (2006). Functional genomics of inositol metabolism. Subcell Biochem *39*, 47-70.
Trewavas, A., and Gilroy, S. (1991). Signal transduction in plant cells. Trends Genet *7*, 356-361.
Vaden, D.L., Ding, D., Peterson, B., and Greenberg, M.L. (2001). Lithium and valproate decrease inositol mass and increase expression of the yeast INO1 and INO2 genes for inositol biosynthesis. J Biol Chem *276*, 15466-15471.
Valluru, R., and Van den Ende, W. (2011). Myo-inositol and beyond--emerging networks under stress. Plant Sci *181*, 387-400.
Van Dijken, P., Bergsma, J.C., Hiemstra, H.S., De Vries, B., Van Der Kaay, J., and Van Haastert, P.J. (1996). Dictyostelium discoideum contains three inositol monophosphatase activities with different substrate specificities and sensitivities to lithium. Biochem J *314*, 491-495.
VanderVere, P.S., Bennett, T.M., Oblong, J.E., and Lamppa, G.K. (1995). A chloroplast processing enzyme involved in precursor maturation shares a zinc-binding motif with a recently recognized family of metalloendopeptidases. Proc Natl Acad Sci U S A *92*, 7177-7181.
Vicente-Carbajosa, J., and Carbonero, P. (2005). Seed maturation: developing an intrusive phase to accomplish a quiescent state. Int J Dev Biol *49*, 645-651.
Wiater, A., Krajewska-Grynkiewicz, K., and Klopotowski, T. (1971). Histidine biosynthesis and its regulation in higher plants. Acta Biochim Pol *18*, 299-307.
Xiong, L., Lee, B., Ishitani, M., Lee, H., Zhang, C., and Zhu, J.K. (2001). FIERY1 encoding an inositol polyphosphate 1-phosphatase is a negative regulator of abscisic acid and stress signaling in Arabidopsis. Genes Dev *15*, 1971-1984.
Yamamoto, R., Inouhe, M., and Masuda, Y. (1988). Galactose inhibition of auxin-induced growth of mono- and dicotyledonous plants. Plant physiology *86*, 1223-1227.
York, J.D., Ponder, J.W., and Majerus, P.W. (1995). Definition of a metal-dependent/Li(+)-inhibited phosphomonoesterase protein family based upon a conserved three-dimensional core structure. Proc Natl Acad Sci U S A *92*, 5149-5153.
Yoshikawa, M., Kato, T., and Takenishi, T. (1967). A novel method for phosphorylation of nucleosides to 5'-nucleotides. Tetrahedron Lett *50*, 5065-5068.
Zimmermann, P., Hirsch-Hoffmann, M., Hennig, L., and Gruissem, W. (2004). GENEVESTIGATOR. Arabidopsis microarray database and analysis toolbox. Plant Physiol *136*, 2621-2632.